Design of Wing Structural Elements with Uncertainty in Materials, Loads and Sizing

Jorge Miguel Pires Liquito

Alferes Aluno EngAer 134636-K

A thesis submitted in conformity with the requirements for the degree of Masters in

Aeronautical Engineering

Jury

President:	MGen/EngAer/020829-K Pedro Miguel de Palhares Veloso da Silva
Supervisor:	Doctor André Calado Marta
Examiner:	Doctor Maria Alexandra dos Santos Gonçalves de Aguiar Gomes

Sintra, December 2012

Acknowledgments

I would like to express my deepest appreciation to all of those who, directly or indirectly, supported and helped me during the realization of this thesis.

First, I would like to express my sincere gratitude to my supervisor, Doctor André Marta, for his constant encouragement, support, invaluable advice, guidance and interest in discussions through the course of this work. That was essential for its development and conclusion.

I also want to thank the Informatics Center of the Portuguese Air Force Academy, in person of Captain Marques da Silva, for his availability and help on providing the computer for the analyses.

On a personal level, I would like to thank my friends for the support and understanding about my absence in the last months. I also leave a word of appreciation to my comrades, those who accompanied me during the course, especially my comrade João Campos. He was very important because we talked a lot about our works and we helped each other by giving advices and opinions.

Finally, I would like to express my deep appreciation to my family, specially to my parents, for all the support and presence throughout my academic and military course.

Resumo

A quantificação de incerteza no projecto de elementos estruturais de asas é o principal objectivo da presente dissertação. As incertezas poderão advir dos materias, carregamentos e geometria. Foi feita a revisão bibliográfica sobre diferentes estudos na área da quantificaçao de incerteza, bem como os métodos de quantificação existentes. Para o estudo, foram utilizados três métodos diferentes: método de amostragem de Monte Carlo, método de amostragem de Hipercubo de Latin e método das perturbações. Primeiramente, os métodos foram implementados e validados para uma estrutura treliçada. De seguida foram aplicados a um caso simples de uma longarina de uma asa. Neste caso, os métodos foram utilizados numa análise analítica e posteriormente usando o método dos elementos finitos, validando assim a utilização de análise numérica. Por fim, foi feita uma análise de uma estrutura de uma asa, onde existem diversas variavéis com incerteza. Os resultados obtidos revelam a importância desta abordagem, pois existem diferenças significativas entre os valores determinísticos e os que contabilizam as incertezas.

Palavras-chave: quantificação de incerteza, Monte Carlo, hipercubo de Latin, método das perturbações, elementos finitos, projecto robusto

Abstract

Uncertainty quantification in the structural design of wing elements is the main objective of this thesis. Uncertainties could be from materials, loads and sizing. A literature review was done related to different studies in this field, as well as the existing methods of quantification. For the study, three different methods were used: Monte Carlo simulation method, Latin hypercube sampling method and perturbation method. First, the methods were implemented and validated using a simple truss as test case. Then, they were applied to a simple case of a wing spar. For this case, the methods implemented were used in an analytic analysis and later in a finite elements method analysis, thus validating the application of the numerical analysis. Finally, an analysis was made of a structure of a wing with several variables with uncertainty. The results reveal the importance of this approach, since there are significant differences between the deterministic calculus and the results with uncertainty quantification.

Keywords: uncertainty quantification, Monte Carlo simulation, Latin hypercube sampling, perturbation method, finite elements, robust design.

Contents

List of Tables

List of Figures

Nomenclature

Greek Symbols

α	Coefficient of thermal expansion.
β^0	Initial deformation vector.
δR	Effective initial deformation vector.
Δ	Settling support.
γ	Covariance.
μ	Mean value.
Φ	Cumulative density.
σ	Standard deviation.
σ^2	Variance.
σ_s	Stress.
ε	Convergence factor.

Roman Symbols

A	Area.
B	System equilibrium matrix.
C	Global compatibility matrix.
C_D	Coefficient of drag.
C_L	Coefficient of lift.
C_P	Coefficient of pressure.
c_r	Length of chord on the root.
$\frac{dw}{dx}$	Rotation
D	Beam cross section.

E Young modulus.

$E[...]$ Expectation operator.

F Force.

f Objective function.

f_X Probability density.

G Concatenated flexibility matrix.

g Constraints.

g^d Design constraints.

g^{rc} Reliability constrains.

h Step size.

I Moment of inertia.

J Deformation coefficient matrix.

k Number of compatibility conditions.

L Length.

l Number of forces.

M Moment.

m Number of displacements.

n Total numbers in the set.

$O(...)$ Error terms.

P Probability.

P_f Probability of failure.

p_z Joint probability density function.

P_{allow} Allowable probability of failure.

P_{bounds} Probability of the bounds.

Poi Poisson coefficient.

Q Load.

q Distributed load.

Q^* Load of the structure.

q_x Perturbation term.

r Number of constraints.

S IFM governing matrix.

T Temperature.

t_f Thickness of the flange.

t_s Thickness of the shell.

t_w Thickness of the web.

u, v, w Cartesian displacement components.

V Shear force.

z Vector of the design variables.

z_L Lower bound of the design variables.

z_U Upper bound of the design variables.

Subscripts

i, j Computational indexes.

x, y Cartesian components.

Superscripts

-1 Inverse.

I First order.

II Second order.

T Transpose.

Glossary

CDF	Computational Fluid Dynamics.
CDF	Cumulative Density Function.
CP	Center of Pressure.
FEM	Finite Element Method.
FORM	First-Order Reliability Method.
FPI	First Probability Integrator.
IFM	Integrated Force Method.
LHS	Latin Hypercube Sampling.
LSS	Latin Supercube Sampling.
MCS	Monte Carlo Simulation.
MDO	Multidisciplinary Design Optimization.
PDF	Probability Density Function.
PM	Perturbation Method.
QMCS	Quasi-Monte Carlo Simulation.
RBDO	Reliability Based-Design Optimization.
RDO	Robust Design Optimization.
SORM	Second-Order Reliability Method.
UQ	Uncertainty Quantification.

Chapter 1

Introduction

1.1 Motivation

My interest in aeronautics began when I started practicing aeromodelling some years ago. It is an interesting activity, which enables us to build and control a small aircraft. A few years later, in the aircraft design class, frequented in the last year of aerospace engineering course at Instituto Superior Técnico (IST), the interest grew bigger. I learned about the main stages of an aircraft conceptual design, but the most important moment was the preliminary aircraft design project, that was done by the students.

Designing wing structures under uncertainty is the subject of this thesis. As a graduating aeronautical engineer of the Portuguese Air Force Academy, the interest in gaining knowledge that may allow the development of skills useful to the Air Force in its future projects is very motivating.

In the beginning, for wing design or other aircraft structures design, things were done like a ”prescription” and the projects were all similar and nothing different was implemented. This is the reason why subsonic civilian aircrafts did not suffered relevant changes during long time. The explanation for this fact was that the model, during long time, was only tested in a wind-tunnel or flown. So, taking risks with innovations could spend resources and time, which implied losses of money if the innovations did not turn well. However, the development of computational simulation has permitted the realization of many studies, without building real prototypes and reach some relevant results. These new resources have allowed the evolution, even greater in aeronautical industry, because they enabled the implementation of new aircraft concepts without taking the chance of wasting resources. Furthermore, they allowed to make some improvements and reach the optimum solution faster.

We can say that uncertainty is in everything, but the biggest problem is to quantify it correctly. This concept is relatively recent in aeronautical field, because until few years ago, it was ignored or considered an error of the project. Uncertainty quantification (UQ) appeared as a viable technique in many fields of aeronautical industry like: structures, aerodynamics, propulsion and others. Its application has proven good results both in terms of computational costs and in terms of accurate results.

Working in UQ was an interesting opportunity, because it is a new and emergent area with strong capabilities. This master thesis is focused in UQ applied to aeronautical structures, more precisely,

wings structural components.

The Portuguese Air Force could acquire some knowledge that could be applied in future projects. At the moment, the Air Force is developing several projects, at the Air Force Academy and in a specific department responsible for engineering studies. Maybe in the future, this work could be useful in one of these projects.

Therefore, this work maybe a contribution not only to the development of a graduate aeronautical engineer, but also to the enrichment of UQ community and, eventually, for the increasing in its use in the aircraft design process for future projects.

1.2 Importance of Uncertainty Quantification

"The uncertainty is as important a part of the result as the estimate itself ... . An estimate without a standard error is practically meaningless." H. Jeffreys (1967) [Higdon et al., 2009].

During the last two decades, extensive studies has been developed in non-deterministic analyses, to provide certification of the performance of single components or entire systems. Probability theory has taken an important role on these researches for many different areas, as well as stochastic analysis techniques. These have been applied to model and propagate the uncertainty through the problem in study [Bae, 2004].

UQ is gaining an important role in computational science, because it allows to evaluate the quality of computational results and apply confidence bounds to output metrics. Its importance in computational modeling has been growing, which enables design and analysis of complex engineering systems. Particularly, when obtaining experimental data is difficult or impossible and the associated costs are higher. By using this methodology, it is possible to achieve the results pretended faster and with lower costs. However, the desired accuracy of the results determine the time needed or the approach to be used in UQ.

The accuracy of the results are strictly related to the model, simplifications and all assumptions. So, some studies were developed to observe how accurate the models were [Hemez and Doebling, 2001]. The necessity to quantify the precision of the results has contributed to the development of many methodologies, but some of those imply a strong computational effort. At the same time, there were many researches aiming to reduce the computational effort or to develop new and more efficient methodologies [Shah, 2011]. This thematic is in constant development together with the evolution in technology and optimization methods.

There were other studies with the goal of model uncertainty and the field in which it has been applied. The environment is an important issue, because it affects how the model need to be idealized and discretized [Refsgaard et al., 2006]. The uncertainty could appear from different sources, for example, the lack of information from the operator or the problem, simplifications and uncertainty in the model or in the inputs [Wojtkiewicz et al., 2001]. Uncertainty in the input parameters has been the topic that had experienced many developments, specifically with models in robust design optimization (RDO) and

reliability based design optimization (RBDO) [Youn et al., 2007], [Patnaik et al., 2009], [Patnaik et al., 2010].

In the process of uncertainty quantification, the last phase is the validation of the model, so there are also many studies regarding this [Alvin et al., 1999]. The validation phase is responsible for the investigation about the accuracy of the mathematical model and if it is capable to reproduce particular physical events or relevant data [Lucas et al., 2008]. Validation depends on the area of the project, for example, in the aerospace projects, the model is only valid if it describes correctly the real situation and results are accurate. However, validation is not easy because often it is not possible to do experimental tests and compare them with the model results.

The application of the UQ methods to a particular structure needs a previous hard work on model interpretation. It is also necessary to characterize and identify possible sources of uncertainty or errors. By doing it, the objective of quantifying their influence on the results accuracy is reached [Alvin et al., 1999].

1.3 Relevance to Aeronautic

The aeronautical industry is in constant development, stimulated by computational evolution, technology growth and high importance of aviation in the society. In the last years, the UQ has been gaining strong importance in aeronautical industry and studies.

In aircraft design, there are a lot of sources that may contain uncertainty. Quantify and characterize them is a hard task because it is impossible to classify them equally. Figure 1.1 shows some variables that could be classified as uncertainty variables in structural design.

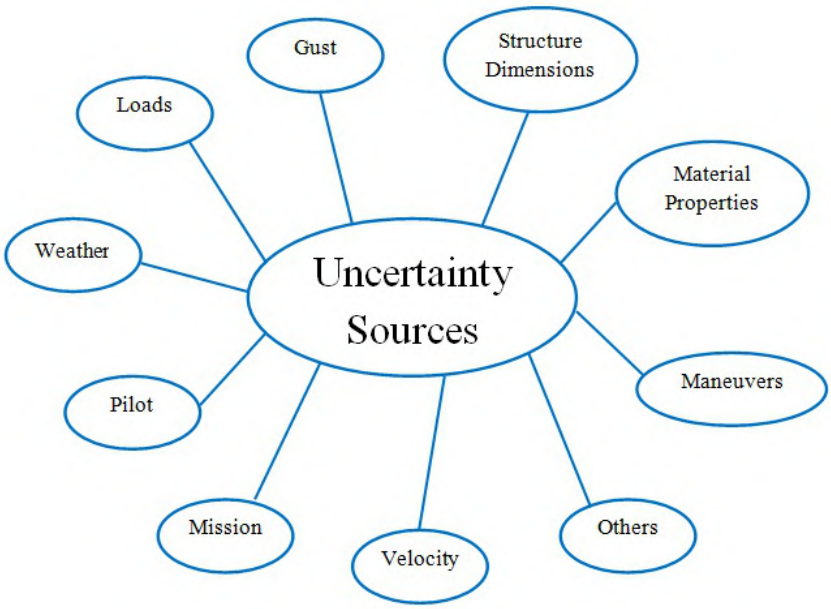

Figure 1.1: Different kinds of uncertainty sources in aeronautical field.

For instance, in real flight, the angle of attack or the free-stream are uncertain because the atmospheric conditions have fluctuations. Also, any uncertainty in material properties or structural dimensions must comply with the design requirements.

Doing a project without considering the uncertainty, present in some of these variables, could result in a compromised structure. Since the majority of these are not static and have fluctuations, it is important to make a project considering these uncertainties.

UQ has been applied in different fields of aeronautics, like aerodynamics, structures, propulsion and others. Computational fluid dynamics (CFD) is one field in which uncertainty is strongly present [Mathelin et al., 2005]. From the beginning, uncertainty in CFD was related to discretization error or turbulence modeling limitations. However, there are some kinds of uncertainty associated with CFD studies. To deal with this issue, it is necessary to take into account all the aspects of uncertainty in the simulations. The first researchers defending this perspective were Mehta, Roache, Coleman and Stern and Oberkampf and Blottner [Mathelin et al., 2005]. The inclusion of uncertainty in CDF simulations has been gaining importance in the last few years. It is also important to define a confidence interval for the simulation-based predictions or design.

Quantifying uncertainty is also present in the design of aircraft components [Díaz et al., 2010]. In this kind of design, deterministic methods has been used, but it is also recognized that there was inherent uncertainty involved in those structures. Methodologies based on UQ produce more accurate results in structural reliability.

UQ has other application in optimization field, precisely in RDO and RBDO. These kinds of optimizations are applied in different aeronautical areas. Bae [Bae, 2004] has done a RBDO using evidence theory applied to wing structures design. This study resulted in an optimum design with a robust performance counting the uncertainties intrinsically. There are studies using the two kinds of optimization [Paiva, 2010] applied to a conceptual aircraft wing design. From this study resulted an optimization tool, which could be used in future for different areas of the aeronautical. The competition in industry for efficient designs and reliable products is pushing the need to consider the UQ methodologies applied to realistic computer models.

1.4 Aircraft Structures

Aircrafts are composed by many different components but, between different aircrafts some are similar, such as wings, fuselage, tail units and control surfaces. These are the essential structures and they depend strongly on the kind of aircraft. The most important parameter in structural design is its function and the environment where it operates. There are different kinds of aircrafts with different missions, so the structures were designed in function of their mission.

Structures are built to support loads. In case of aircrafts, there are two classes of loads [Megson, 2007]: ground loads, resulting from movement or transportation in the ground, or air loads, coming from maneuvers or gusts. Ground loads act over the entire structure and they appear from inertial and gravitational effects. On the other hand, air loads result from the pressure distribution acting on skin

surfaces, they are caused by maneuver, gust or steady flight conditions.

1.4.1 Wing Structures

The purpose of this subsection is exclusively to study about wing structures. They have an important role because they are responsible to generate the lift force. In movement, pressure distribution around the aerodynamic surfaces is created, which translates into the aerodynamic force. However, this force is conditioned by the kind of aerodynamic surface and its incidence. The pressure distribution has two components, one vertical (Lift) and another horizontal (Drag). Its point of application is at the center of pressure (CP), as illustrated in Fig. 1.2. CP varies its position according to the speed and wing angle of attack.

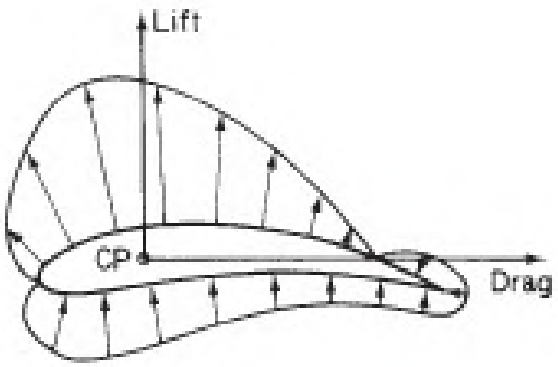

Figure 1.2: Pressure distribution around an airfoil [Megson, 2007].

During many years, wing structures suffered some modifications and these were motivated by the evolution of technology and aircraft mission. Figure 1.3 shows two different kinds of internal structure of a wing, but no matter how complex the internal structure and arrangement is, its function is the same. The majority of aircraft wings are composed by spars, ribs, stringers and skin [Megson, 2007].

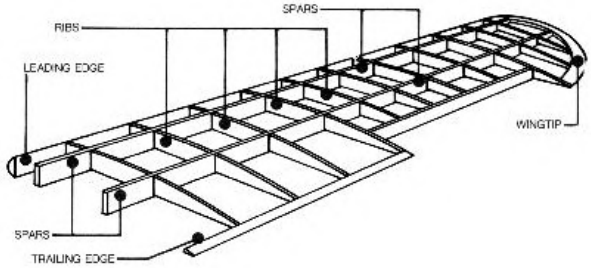

(a) Conventional internal arrangement [TeachEngineering, 2012]

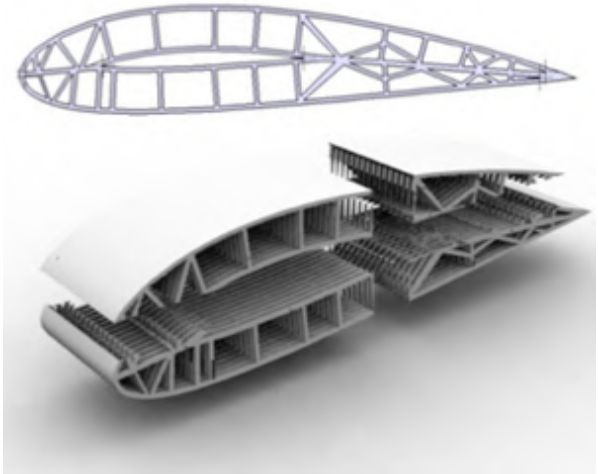

(b) Proposed structure for a wing [Maheshwaraa et al., 2011]

Figure 1.3: Different wing internal arrangements.

The spar is responsible to support bending loads and it is a structural link between wing and fuselage, it is often considered the main structural member of the wing. Its position in the main structure is normal to the flow direction and is extended from the fuselage to the wing tip. Sometimes, it has a certain angle due to the sweep angle of the wing. Normally, the spar has a cantilever shape and there are two spars on the wing. The main spar is near the leading edge, about 25% of the chord, the other one is smaller and is located near the trailing edge. The main spar carries the lift through the fuselage to the other wing, to resist forward and aft movement. The smaller one is tied to the main spar by the ribs or stressed skin (forming a wing-box structure). This configuration provides some rigidity, needed either in flight or on the ground.

The ribs are structural components of the wing and are, often, considered its skeleton. Their function is linking spars, while supporting and shaping the skin with stringers. Ribs are also used as attachment points for control surfaces, flaps, undercarriage and engines. In a traditional wing structure, they have the orientation of the flow.

The stringers are structural components that work together with ribs and are responsible for giving an airfoil shape to the wing. Furthermore, they help to support wing bending and act as stoppers to the propagation of cracks. They support the skin panels and prevent thin-wall buckling under compression or shear loads. Their location is between ribs, parallel to the spar direction and assembled to the skin.

Finally the skin, in conjunction with spars and ribs, compose a wing-box structure. It is composed by panels on the top and bottom of the wing-box, in which they are attached to each other and to the ribs. Its function is to give an aerodynamic shape to the wing.

1.4.2 Wing Materials

The selection of materials for structural wing components has several factors that need to be taken into account. Depending on the area of application, there are some essential characteristics, however, in the aeronautical field, low weight with high strength is probably the most important selection factor. In addition to these, there are other critical properties like stiffness, toughness, resistance to corrosion, fatigue, effects of environmental heating, ease of fabrication, availability, consistency of supply and cost.

There are some main groups of conventional materials used in wing structures such as wood, steel and aluminium alloys. Recently, there are other materials used in the aeronautical field, like titanium alloys and fiber-reinforced composites.

Starting with wood, this material was the first material used in wing structures. In the beginning of aviation, wings had a wooden structure supported by wires and covered by fabric with varnishes [Starke and Staley, 1996]. However, this kind of structure did not support high speeds.

After wood application, it was time to use steel in some structures, because it had a higher strength than wood. However, its elevated density was a big disadvantage since in the aeronautical industry the global weight is very important. Steel has, nowadays, very little usage in main wing structures.

A few years later, some tests were done and was used aluminium alloys [Starke and Staley, 1996]. Aluminium in pure composition is characterized by low strength and extreme flexibility, these proper-

ties are not good for structural applications. However, if it is alloyed with other metals, its mechanical properties will be improved significantly. The most commonly used aluminium alloys are [Borradaile, 2000]:

- Al-Zn alloys - characterized by high strength (Al-7050 and Al-7150);
- Al-Cu alloys - characterized by high fatigue resistance (Al-2024 and Al-2014);
- Al-Li alloys - characterized by high stiffness and lower density (Al-8090).

In aluminium alloys, if one property is increased, other properties will be sacrificed. Beyond chemical composition, their properties could be changed with thermal treatment.

Titanium and titanium alloys are, nowadays, used in wing structures because they present better properties compared to other materials cited previously. The reasons for their application in aircraft industry are [Henriques, 2009]:

- Weight savings;
- Operating temperatures, maintain properties for high range of temperatures;
- Corrosion resistance;
- Composite compatibility.

However, the cost is the biggest disadvantage because, it even tough is not a rare or precious metal, its cost of extraction and production is higher than other metals [Henriques, 2009]. Nevertheless, this material is used frequently in some components in military aircrafts where the objective is the efficiency of the aircraft and not the total cost.

Recently, the use of composite materials has been developing in the aeronautical industry because it is possible to custom produce composite structural elements that exhibit some specified properties [Baker et al., 2004]. However, the biggest disadvantage is the cost of production since they require hand crafting of the material and manual construction processes.

Resuming, all materials are still used but their percentage in the composition are different. Aluminium alloys are still the most used material in wing structures because they have a good trade-off between mechanical properties and cost.

1.5 Thesis Outline

This master thesis is about UQ applied to aeronautical structures, more specifically wing components. It is composed by seven chapters.

The first chapter is the introduction and has a brief explanation about the objective and importance in scientific research. There is also a literature review of the work that has been developed in the UQ topic and its relevance to aerospace engineering, concluding with a review about the wing structures and materials.

The second chapter includes a discussion about UQ, with a literature review about its classification and the process to quantify the uncertainty. After that, some statistical concepts that will be used in the UQ methods are presented. It also has a review about optimization with uncertainty.

The third chapter will expose the UQ methodologies, including a literature review about them and the methods that have been developed.

The fourth chapter presents the problem of a three-bar truss, where the system will be first analyzed deterministically and then using three UQ methods. After the implementation of these methods, the results will be compared and analyzed to check their accuracy using results reported in the literature.

In the fifth chapter, a wing spar will be analyzed and a study similar to the previous chapter will be conducted. However, in this case there will not be other studies to compare, instead it will be developed an interpretation of the real results. It will also be introduced finite elements methods (FEM) with UQ, in order to analyze the same structure and compare the results with analytical analyses.

The next chapter is identical to the previous, but more complex structure will be analyzed: a wing composed by many sources with uncertainty. In this case, it will be only used FEM and UQ methods together to analyze the system.

Finally, in the last chapter, all relevant results obtained during the work developed will be presented, together with some considerations for future work.

Chapter 2

Uncertainty Quantification

This chapter presents the relevant information about UQ. It begins with its definition and then it introduces statistical concepts used by some methodologies. The last section talks about optimization with uncertainty.

2.1 Ranks and Process of Uncertainty Quantification

All systems have, intrinsically, many uncertainties, which can be of different natures. From many researches about UQ, it can be divided in three different technical areas, in which it is necessary to do some research and development efforts [Wojtkiewicz et al., 2001]. These areas are:

- Characterization;
- Propagation;
- Verification and Validation.

In characterization, it is necessary to know the system and its environment very well to characterize the uncertainty. With the uncertainty correctly characterized, it is possible to propagate it through computational models. Finally, it is essential to verify and validate the propagation of the uncertainty through the computational models.

All real systems have systemic and random variations. Systemic variations are those whose behavior is known. Random variations can be from material properties, boundary conditions, initial conditions or excitations imposed on the system. Consequently, the actual behavior of a system depends on all previous variations.

There are different ways to classify uncertainty found in the literature. The classification varies significantly with its application. Uncertainty occurs in many forms but, in simple terms, it can be divided into two classes [Wojtkiewicz et al., 2001] and [Biltgen, 2008]:

- Epistemic vs. Aleatory;
- Reducible vs. Irreducible;

- Parameter vs. Model.

There are other UQ classifications because, depending on the application, these presented above are not applicable sometimes to some problems. Some analysts do not agree with this classification since it is not possible to include all systems in it.

Next, the classifications will be studied more deeply [Biltgen, 2008]. Epistemic uncertainty results from a lack of information or knowledge about some aspects of the modeling process. It can also be denominated as reducible because additional information about the system can reduce its impact in final response. On the other hand, aleatory uncertainty can only be quantified using statistics because it belongs to a random chance. Irreducible uncertainty is another classification for this kind of uncertainty since, even with more information, the uncertainty cannot be reduced.

There is another popular classification of uncertainty: parameter uncertainty and model uncertainty. The first one is also known as natural uncertainty or data uncertainty, and it results from a lack of information in inputs parameters. Model uncertainty also results from a lack of information but, in this case, it is due to not understanding the variable behavior or from some simplifications introduced in the model.

The process to quantify uncertainty can be divided in four steps [Wojtkiewicz et al., 2001]:

1. Identification;
2. Characterization;
3. Propagation;
4. Analysis.

Identification is essential to determine the sources of uncertainty, either from the system or its environment. After that, characterization is a difficult task since it needs experimental tests to obtain substantial data. Without it, both the quantification of uncertainty and the system analysis will be compromised. With the variable correctly identified and characterized, it is possible to propagate the uncertainty through the system and understand how it reacts. This phase is critical because the operator needs to take some decisions in terms of approaches of uncertainty propagation. More precisely, he needs to select the most appropriate methods for the system. Finally, it is necessary to analyze the results, where a critic analysis is imperative. In this phase, risk analysis is performed and the integrity of the system defined.

2.2 Statistical Concepts

Uncertainty can be dealt in different ways but the most used one is the statistical. It is used in many UQ methodologies to treat the results obtained from different methods. Hence, some basic statistical concepts are reviewed here.

2.2.1 Mean, Variance, Standard Deviation and Covariance

In the statistics concepts will be used a random variable (x), this is a variables whose value is subject to variations.

Simple mean (μ) is the arithmetic average of the values, which could be a sample of numbers or a distribution. It is calculated as

$$\mu = \sum_{i=1}^{n} \frac{x_i}{n}, \tag{2.1}$$

where x_i corresponds to a number from the sample and n is equal to the total of numbers in the set. The result indicates the central value of the distribution [Ross, 2004].

Covariance (γ) is a measure which associates two random variables [Murteira et al., 2007],

$$\gamma_{xy} = \frac{1}{n} \sum_{i=1}^{n} (x_i - \mu_x)(y_i - \mu_y). \tag{2.2}$$

For the case when only one variable exists, the previous equation can be simplified to

$$\gamma_x = \sigma_x^2. \tag{2.3}$$

In other words, for one variable, the covariance is equal to the variance.

Variance (σ^2) is a measure of statistical dispersion. It is the mean value of the quadratic deviations relative to the simple mean [Murteira et al., 2007], defined as

$$\sigma^2 = \frac{1}{n} \sum_{i=1}^{n} (x_i - \mu)^2. \tag{2.4}$$

This measure is important because it tells how far the set of numbers or distribution are from the mean value and it is an important parameter to describe a probability distribution (see Sec 2.2.2).

Standard deviation (σ) is the positive square root of the variance [Murteira et al., 2007],

$$\sigma = +\sqrt{\frac{1}{n} \sum_{i=1}^{n} (x_i - \mu)^2}. \tag{2.5}$$

It is another important tool to characterize the probability distribution as its value indicates how far the distribution are from the mean value. Low values of standard deviation indicate that the sample is close to the mean value, high values denote that the sample has a great range and it is far from the mean value. The standard deviation value has the advantage, compared to variance, that it is expressed in the same units as the data, which allows a direct comparison with the mean value.

2.2.2 Probability Distribution

There are two kinds of random variables, which can be classified as discrete or continuous. A discrete random variable is characterized for only taking a finite number, or an infinite number of them

from a defined set of numbers. A continuous random variable can take any value from a range of numbers [Murteira et al., 2007].

Depending on the kind of random variables, there is a probability distribution to characterize them, as such, the probability distribution can be discrete or continuous.

A discrete random variable is denoted by the following probability density function:

$$f_X(x) = \begin{cases} P(X = x) > 0 & \text{if } x \in \text{D} \\ P(X = x) = 0 & \text{if } x \notin \text{D} \end{cases}$$

where D is a set of numbers. If x is out of the set of numbers, its probability will be zero. When x takes a number that belongs to the set of numbers, defined previously, the probability will be between zero and one. A discrete random variable has a particularity that the sum of all probabilities is equal to one [Ross, 2004]. There are different kinds of distributions for a discrete random variable, such as uniform distribution, Bernoulli distribution, binomial distribution, geometric distribution, hypergeometric distribution, Poisson distribution and logarithmic distribution.

In continuous probability distribution, the probability density function (PDF) is not negative, it is defined for all $x \in]-\infty, \infty[$ or a set of real numbers, for example B, as

$$P(X \in B) = \int_B f_X(x)\, \mathrm{d}x. \tag{2.6}$$

The probability of X results from the integration of the PDF over the set of numbers defined. This kind of probability distribution has different types of distribution, examples of this is the uniform distribution, normal distribution, exponential distribution, Gamma distribution and Chi-Square distribution.

During the development of this thesis, it will only be used variables whose distribution is characterized by a normal distribution. It is often used because its properties are good to theoretical and experimental applications and can be applied to many situations. A continuous variable has a normal distribution if its PDF is obtained by [Murteira et al., 2007]

$$f_X(x) = \frac{1}{\sqrt{2\pi\sigma^2}} e^{-\frac{(x-\mu)^2}{2\sigma^2}} \quad (-\infty < x < +\infty), \tag{2.7}$$

where $\mu \in \Re$ and $\sigma^2 > 0$.

Normal distribution could be represented by $X \sim \left(\mu, \sigma^2\right)$ or $X \sim (\mu, \sigma)$, depending if it takes into account variance or standard deviation of the sample.

Figure 2.1 represents the normal distribution where the mean value is zero and the standard deviation is equal to one, $X \sim (0, 1)$. The normal distribution is characterized by a symmetric bell-shape form and its maximum corresponds to the mean value, $f_X(x) = \frac{1}{\sqrt{2\pi\sigma^2}}$. From the PDF graph, it is possible to know the probability associated to a determined value of the response.

Another way to characterize the normal distribution is the Cumulative Distribution Function (CDF), described by

$$\Phi(x) = \frac{1}{\sqrt{2\pi}} \int_{-\infty}^{x} e^{-\frac{t^2}{2}} dt. \tag{2.8}$$

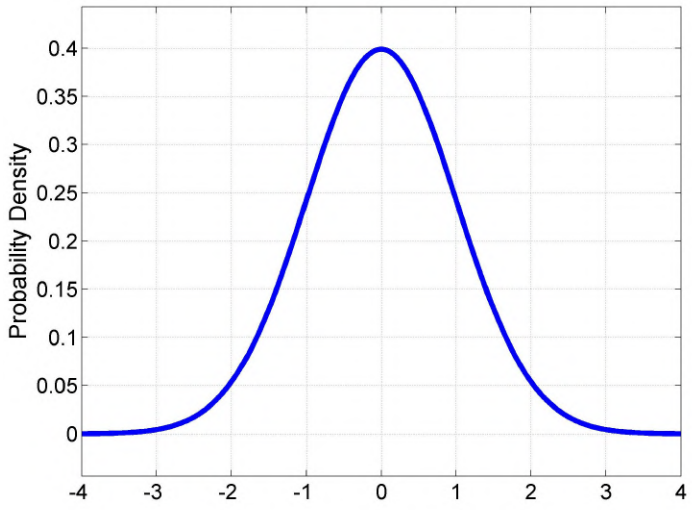

Figure 2.1: Probability density function for the normal distribution.

Figure 2.2 presents a CDF for normal distribution, where $X \sim (0, 1)$.

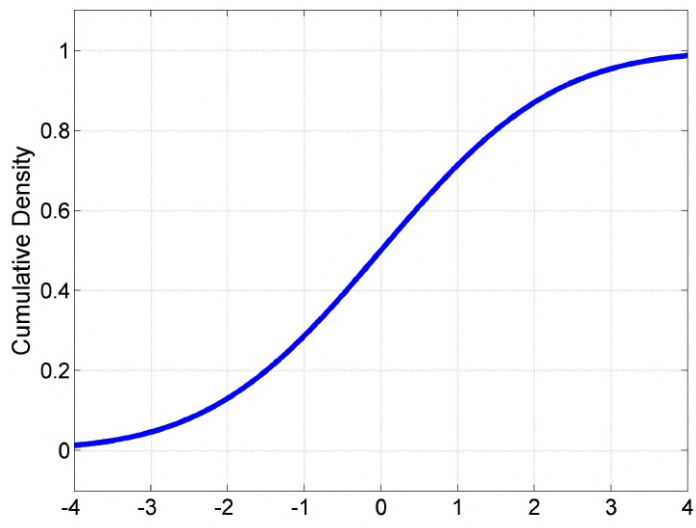

Figure 2.2: Cumulative density function for the normal distribution.

From the CDF graph, it is possible to know the probability associated to the response value to be in the range $]-\infty; x]$.

2.3 Optimization with Uncertainty

The possibility to incorporate uncertainty in design optimization is an important development in the optimization field. However, this kind of optimization implies the introduction of uncertainty quantification methods in the optimization methodology. This optimization can be divided into two main groups: RDO and RBDO. The selection of the kind of optimization depends on the criterion of the designer.

2.3.1 Robust Design Optimization (RDO)

The goal of RDO is to optimize the response of the system in terms of the mean values [Allen and Maute, 2005]. It maximizes the performance of the system by the minimization of the sensitivities to the random variables. This minimization is translated by the reduction of the standard deviation of the system response, along its mean.

A generic deterministic optimization problem can be described as [Padulo et al., 2008]

$$\begin{aligned} \text{minimize} \quad & f(z), \\ \text{with respect to} \quad & z \\ \text{subject to} \quad & g_i(z) \leq 0, \quad i = 1, ..., r, \\ & z_L \leq z \leq z_U \end{aligned} \tag{2.9}$$

where f is the objective function, g_i are the equality and inequality constraints, z is the vector of the design variables, z_L and z_U are the lower and upper bounds of the design variables, respectively.

For the design robustness, the design variables (z) are assumed to be stochastic and, consequently, the objective and the constrains will also be stochastic.

Applying the RDO concept, the optimization problem is reformulated as [Padulo et al., 2008]

$$\begin{aligned} \text{minimize} \quad & f\left(\mu_f(z), \sigma_f^2(z)\right), \\ \text{with respect to} \quad & \mu_f \\ \text{subject to} \quad & g_i\left(\mu_{g_i}(z), \sigma_{g_i}^2(z)\right) \leq 0, \quad i = 1, ..., r, \\ & P(z_L \leq z \leq z_U) \geq P_{bounds} \end{aligned} \tag{2.10}$$

where μ and σ^2 are the mean value and the variance, respectively. f is the objective function, g_i represent the constraints and P is the probability of the interval. f and g_i are function of the mean value and the variance of the distribution. P_{bounds} is the probability of the bounds of the design variables belongs to the interval. This value is prescribed in the beginning by the designer. The mean value (μ_f) and the variance (σ_f^2) of the quantities can be calculated, if the variables are continuous, respectively as

$$\mu_f(z) = \int_{-\infty}^{+\infty} f(t)\, p_z(t)\, dt \tag{2.11}$$

and

$$\sigma_f^2(z) = \int_{-\infty}^{+\infty} [f(t) - \mu_f(x)]^2 p_z(t)\, dt, \tag{2.12}$$

where f represents the interest function and p_z is the joint probability density function of the input variables. When these equations are applied for a few cases, numerical procedures are used, such as Monte Carlo methods and others. However, the numerical approximation implies a trade-off between

computational cost and accuracy.

2.3.2 Reliability Based-Design Optimization (RBDO)

RBDO has a different methodology compared to RDO since it works based on a reliability target [Frangopol and Maute, 2003]. For this target, there are many different parameters which could be taken into account, such as minimum life-cycle cost. It optimizes the structure taking into account the margins of the project. However, it presents some disadvantages, such as serious limitations in terms of convergence or computational efficiency.

The RBDO problem can be posed as [Paiva, 2010]

$$\begin{aligned} \text{minimize} \quad & f(z), \\ \text{with respect to} \quad & z \\ \text{subject to} \quad & g_i^{rc}(z) \leq 0, \quad i = 1, ..., r_{rc}, \\ & g_j^{d}(z) \leq 0, \quad j = 1, ..., r_d, \\ & z_L \leq z \leq z_U \quad . \end{aligned} \tag{2.13}$$

In this case, the constraints are divided into two groups: reliability constrains g_i^{rc} and design constrains g_j^d.

There is another approach to RBDO, where the objective function is defined in terms of the probability, P, of the original function exceed or not the target required [Allen and Maute, 2005],

$$\begin{aligned} \text{minimize} \quad & P\left((f(z) - target) \leq 0\right), \\ \text{with respect to} \quad & z \\ \text{subject to} \quad & g_i^{rc}(z) \leq 0, \quad i = 1, ..., r_{rc}, \\ & g_j^{d}(x) \leq 0, \quad j = 1, ..., r_d, \\ & z_L \leq z \leq z_U \quad . \end{aligned} \tag{2.14}$$

The reliability constraints can be defined as

$$g_i^{rc} = P_{f_i} - P_{allow_i} = P\left(g_i(z) \leq 0\right) - P_{allow_i} \tag{2.15}$$

and

$$P\left(g_i(z) \leq 0\right) = \int_{g_i(z) \leq 0} p_z(t)\, dt, \tag{2.16}$$

where P_{allow_i} is the allowable probability of failure and P_{f_i} is the probability of failure. The probability of failure results from sampling (Monte Carlo or similar methods) or techniques such as First-Order Reliability Method (FORM) or Second-Order Reliability Method (SORM).

Chapter 3

Uncertainty Quantification Methods

Nowadays, technology development has permitted the study of complex engineering models without experimental tests, which have been decreasing because of their high costs. The numerical methods developed take an important function in the analysis of real complex problems because the analyses are quick and inexpensive. This evolution has its barriers since the complexity of the models brings with it the problem of validation of results. All these complex studies have uncertainties from different sources, such as lack of information, assumptions, uncertainties in the input or in the proper model. Consequently, to deal with these uncertainties, some different methods were developed and validated. In the recent past, a hard research was done in this area and several categories of methods were developed to study uncertainty propagation.

The first approach on uncertainty propagation was a conventional sample-based. In this category are included methods like Monte Carlo simulation (MCS) and quasi Monte Carlo simulation (QMCS) with different sequences. There are also the Latin hypercube sampling (LHS) and Latin supercube sampling (LSS) . The last one, it is a combination of two methods, QMCS and LHS. Although this category of methods is relatively easy to implement, it implies a strong computationally effort and a large simulation time for complex studies. Besides, that strong computational effort grows even further if a good accuracy in the results is desired.

Another kind of approach is based on sensitivity analysis. In this methodology, the equations have the propagation of uncertainty and the sensitivities are evaluated during the simulation. These methods can provide accurate results with a reduced computational time. Examples of these methods are the perturbation method (PM) and the fast probability integrator (FPI). These approaches have a complex implementation but the time of simulation is faster than the sample-based methods.

3.1 Monte Carlo Simulation Method

MCS method dates from about 1944 but there are also some isolated and non-developed attempts to implement the method [Hammersley and Handscomb, 1975]. Its name comes from the roulette of the Monte Carlo casino in Monaco, because the sample achievement is equal to take randomly a number

from the roulette. This method has an extensive application in diverse fields, such as physics, mathematics, biology, among others.

MCS is a probabilistic analysis method because it works with random and pseudo-random numbers. This technique is, nowadays, applied to solve many stochastic problems in engineering situations. It is used as a first approach since its application is simple, easy and adaptable for many problems. However, this simplicity implies some problems in computational efforts and simulation time. These problems depend on the accuracy pretended for results and the sample size. As MCS is a methodology whose base is statistics, it is necessary to solve the problem many times to reach the desired accuracy.

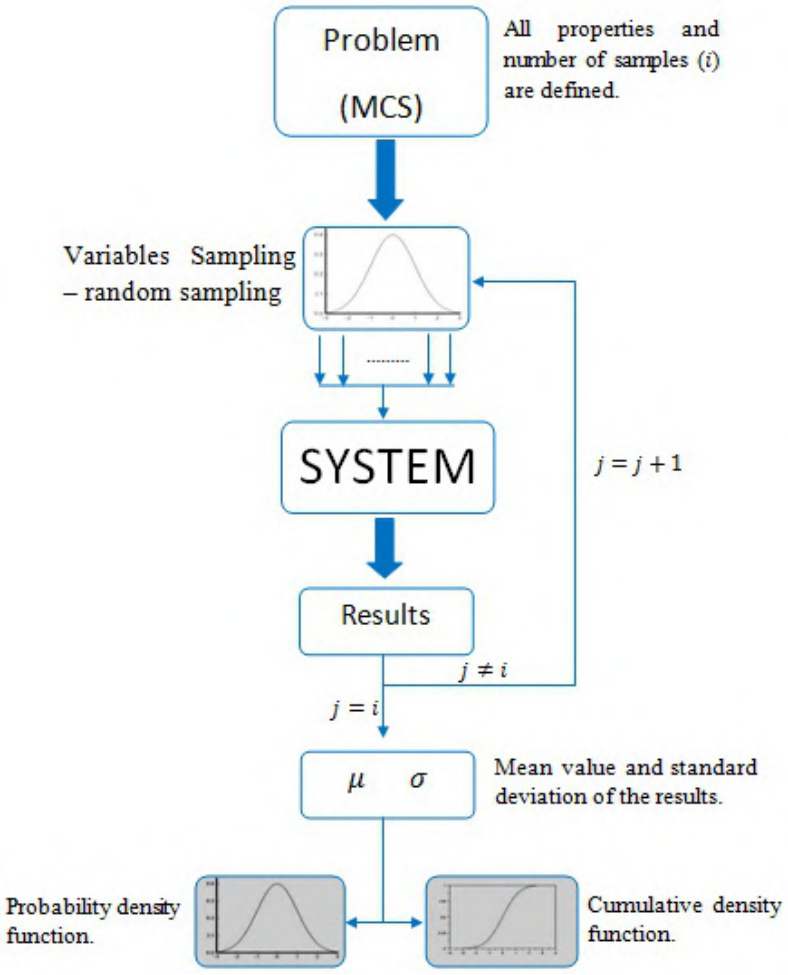

Figure 3.1: Representation of the Monte Carlo simulation method.

Figure 3.1 illustrates how MCS woks. First, it is necessary to define correctly the problem, its variables and number of samples needed to reach the desired accuracy. As it works with samples, it is necessary to choose the number of them carefully because a high number of samples implies a strong computational effort, while a reduced number might not obtain accurate results.

With the problem defined, it is possible to start the analysis. It begins with the sampling of each variable and it is necessary to know their mean value and standard deviation. Each one has one kind of probability distribution and depends on its nature, but for some variables it is difficult to know exactly the probability distribution.

When sets of inputs are randomly or pseudo-randomly defined, the analysis runs and the results are computed for each set.

After repeating this process the specified number of samples, all results obtained in each sample are gathered to determine the mean value and the standard deviation from each output. In the same way as the inputs, the outputs correspond to distributions with a respective mean value and standard deviation. In case the input variables have different probability distributions, determining output distribution is a difficult task. However, for the case when all input variables have a normal distribution, the output distribution will also be a normal distribution.

Having processed the output results, it is possible to plot the CDF and PDF for each output. These illustrations provide insight in problem analysis and model behavior study.

3.2 Quasi-Monte Carlo Simulation Method

QMCS is another sample-based method that works using the same procedure as MCS. However, instead of random or pseudo-random samplings, QMCS uses sequences of quasi-random numbers which are chosen based on equally distributition [Lemieux and L'Ecuyer, 2001].

There are some sequences to generate quasi-random numbers, such as the Haldon sequence [Baghdasaryan et al., 2002], the Hammersley sequence [Hammersley and Handscomb, 1975], the Faure sequence [Wang et al., 2004] and the Sobol sequence [Wang et al., 2004].

This methodology appears to deal with high dimensional problems better than MCS because it needs much less computational time to provide the same accuracy in the results.

3.3 Latin Hypercube Sampling Method

LHS is another approach to MCS and it was proposed to deal with problems when a large number of parameters exist [Olsson and Sandberg, 2002]. MCS has difficulties with situations when a large number of parameters exist because the computational effort increases significantly. Consequently, the accuracy of the results might not be possible to achieve.

This approach is based on a different methodology of sampling as it uses a stratified sampling for a probability distribution [Cronvall, 2007]. With a stratified sampling, it is possible to achieve accurate results with fewer samples, consequently lowering the computational effort. This kind of stratified sampling is known has Latin hypercube sampling and it was developed by McKay, Conover and Beckman (1979) [Wyss and Jorgensen, 1998]. It splits the range of the variable in n non-overlapping intervals, each one having the same probability [Wyss and Jorgensen, 1998]. When the sampling is done, the random values were "forced" to represent each interval according to the input probability distribution, increasing the efficiency of the sample.

In Fig. 3.2, an example of Latin hypercube sampling is presented, in which the distribution was divided in five equal parts, each one having 20% of probability.

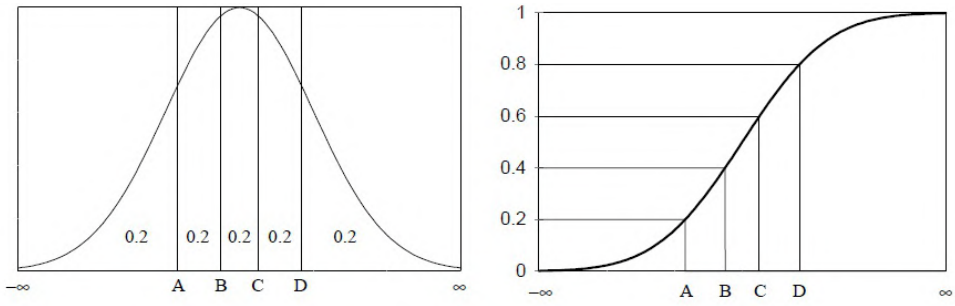

Figure 3.2: Representation of an example of Latin hypercube sampling [Wyss and Jorgensen, 1998].

This method was first applied in a computational example and compared with MCS, in 1979 [McKay et al., 1979].

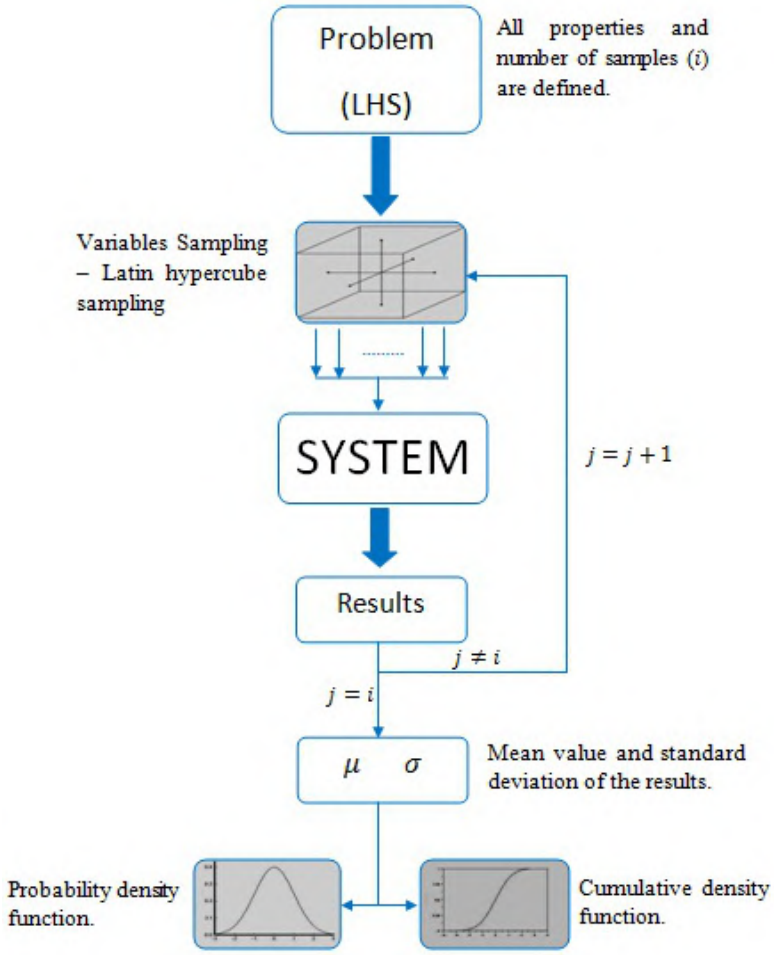

Figure 3.3: Representation of the Latin hypercube sampling method.

Figure 3.3 illustrates how LHS works. Input parameters are represented by a ”cube”, where the number of faces is equal to the number of initial parameters. As it also happens in MCS, in the LHS method, the input variables can have different kinds of probability distributions, depending on their nature.

In each sample, the input variables sets, from Latin hypercube sampling, are introduced in the system. After the analysis, the results from each sample are stored, as in MCS. When the system is ana-

lyzed the number of samples defined, all sample results are gathered to calculate the mean value and the standard deviation for each output. These values characterize the system behavior in the presence of uncertainties.

Output characteristics allow to build outputs probability distributions. If all the input variables have the same probability distribution, the output distribution will have that distribution. In case the input variables have different probability distributions, the determination of the output distribution will be a difficult task to do, similarly to MCS.

LHS is a strong methodology for complex problems with a moderate number of dimensions. To deal with situations with high dimensions, LHS suffered a little modification and a similar method was generated, the LSS. It is a method suited for a very high dimensional simulations that results from the combination of two existent methods, LHS and QMCS. First, LHS is used to group the input variables into subsets and then QMCS is applied to each subset [Owen, 1998].

3.4 Perturbation Method

PM is one approach based on sensitivity analysis. It is a popular technique for solving stochastic partial differential equations and has a large application in stochastic finite elements simulations where the equations describe the system model.

PM has gained more popularity due to the evolution of computational methods to find approximate solutions of differential equations, such as asymptotic approximations, asymptotic expansions, multiple scales and method of homogenization [Holmes, 1998].

Usually, it uses asymptotic expansions with partial differential equations obtained from Taylor expansion [Keese, 2003]. The higher the order of the expansion is, the better the accuracy of results will be. However, higher orders imply more difficulty to obtain the system equations and more computational effort. Commonly, first and second-order derivatives with respect to the primitive random variables are used, but it is necessary to ensure that the covariance of the random variables is small [Wei, 2006].

Results from first-order perturbation method are an estimative of the response so its implementation has a low computational effort and it is applicable for a large range of problems. For second-order, more accurate results are expected, but with a little increase in computational effort compared to the first-order. In second-order, it is necessary that the variance coefficient is less than 20% [Sudret and Kiureghian, 2000].

Figure 3.4 presents a flowchart which explains how PM works. First, it is necessary to define correctly the problem. In this case, it is not necessary to do samplings. After that, the system is analyzed using the variables with a perturbation. Finally, the results are computed using the methodology and the mean value and the standard deviation for each output is obtained.

This method has its disadvantage though. It needs the derivatives of the system equations and these equations take into account the random variables. For complex structures, it is a very difficult task to obtain their derivatives.

For the input variables, it is necessary to know their mean value and covariance, not the standard de-

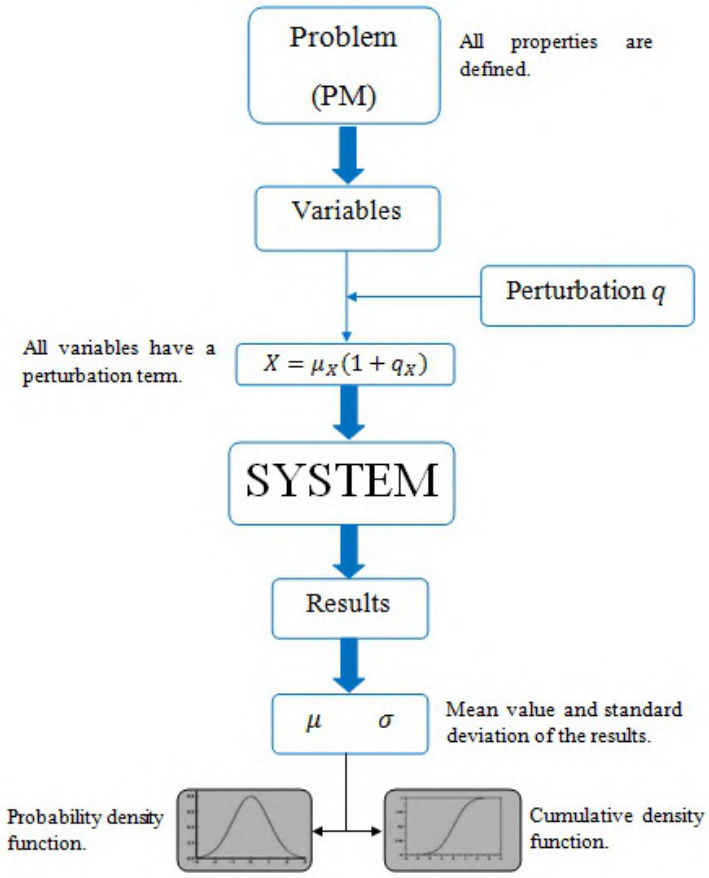

Figure 3.4: Representation of the perturbation method.

viation like in the other methods presented previously. In this method, the input variables are composed by two components, a deterministic part μ_x and a random part or normalized primitive random variable q_x, where the index x represents a generic variable. A normalized variable could be defined as

$$q_x = \frac{x - \mu_x}{\mu_x}, \tag{3.1}$$

where its mean value (μ_{q_x}), variance ($\sigma^2_{q_x}$) and covariance ($\gamma^{ij}_{q\ x}$) are obtained using expectation operator (E[..]).

$$\mu_{q_x} = E[q_x] = E\left[\frac{x - \mu_x}{\mu_x}\right] = \frac{E[x] - E[\mu_x]}{\mu_x} = \frac{\mu_x - \mu_x}{\mu_x} = 0, \tag{3.2}$$

$$\sigma^2_{q_x} = E[(q_x - \mu_{q_x})] = E\left[\left(\frac{x - \mu_x}{\mu_x} - 0\right)^2\right] = \frac{1}{\mu_x^2} E[(x - \mu_x)^2] = \frac{\sigma_x^2}{\mu_x^2} \tag{3.3}$$

and

$$\gamma_{q\ x}^{ij} = E\Big[\left(q_{x_i}-\mu_{q_{x_i}}\right)\left(q_{x_j}-\mu_{q_{x_j}}\right)\Big] = E\left[\left(\frac{x_i-\mu_{xi}}{\mu_{xi}}-0\right)\left(\frac{x_j-\mu_{xj}}{\mu_{xj}}-0\right)\right]$$

$$= \frac{1}{\mu_{x_i}\mu_{x_j}} E\Big[\left(x_i-\mu_{xi}\right)\left(x_j-\mu_{xj}\right)\Big] = \frac{\gamma_x^{ij}}{\mu_{x_i}\mu_{x_j}}. \tag{3.4}$$

To use the Taylor series expansion, it is necessary to assume that the variance of primitive variables is much smaller than the square of its mean. The Taylor expansion for a generic output variable X is defined as

$$\{X\} = \left\{\overline{X}\right\} + \left(\{q\}^T \overline{\mathcal{L}\{X\}}\right) + \frac{1}{2}\left(\{q\}^T \overline{\mathcal{L}\{X\}\mathcal{L}^T}\{q\}\right) + \text{higher order term} \tag{3.5}$$

where

$$\left(\{q\}^T \overline{\mathcal{L}\{\bullet\}}\right) = \sum_i q_i \frac{\partial(\bullet)}{\partial q_i}\bigg|_{\{q\}=\{0\}}$$

and

$$\left(\{q\}^T \overline{\mathcal{L}\{\bullet\}\mathcal{L}^T}\{q\}\right) = \sum_{ij} q_i q_j \frac{\partial^2(\bullet)}{\partial q_i \partial q_j}\bigg|_{\{q\}=\{0\}}.$$

Consequently, the first-order approximation for a generic variable can be reproduced by

$$\{X\} = \left\{\overline{X}\right\} + \sum_{i=1}^{N} \{X_{,i}\}\, q_i, \tag{3.6}$$

where $X_{,i} \equiv \frac{\partial X}{\partial q_i}$.

The mean value ($\mu_X{}^I$) and covariance matrix (γ_X^I) are obtained from Eq. (3.6). The mean value is obtained from

$$\mu_X{}^I = E^I[\{X\}] = E\left[\left\{\overline{X}\right\} + \sum_{i=1}^{N}\{X_{,i}\}\, q_i\right] = \left\{\overline{X}\right\}. \tag{3.7}$$

In Eq. (3.7), it is possible to observe that the mean value for the first-order approximation corresponds to the mean value obtained from a deterministic analysis.

The covariance matrix is also important to characterize the output response. It is calculated as

$$\gamma_X^I\left(\{X\},\{X\}^T\right) = E[\left(\{X\}-E^T[\{X\}]\right)\left(\{X\}-E^T[\{X\}]\right)^T]$$

$$= \sum_{i=1}^{N}\sum_{j=1}^{N}\{X_{,i}\}\{X_{,j}\}^T \gamma_q^{ij}. \tag{3.8}$$

Having the covariance matrix, it is easy to obtain the standard deviation of the system since it is equal to the square root of principal diagonal of covariance matrix.

Looking back to Eq. (3.5), the second-order approximation for a generic variable can be represented by

$$\{X\} = \left\{\overline{X}\right\} + \sum_{i=1}^{N} \{X_{,i}\}\, q_i + \frac{1}{2}\sum_{i=1}^{N}\sum_{j=1}^{N} \{X_{,ij}\}\, q_i q_j, \tag{3.9}$$

where $X_{,ij} \equiv \frac{\partial^2 X}{\partial q_i \partial q_j}$.

The mean value (${\mu_X}^{II}$) and covariance matrix (γ_X^{II}) for second-order approximation are obtained using the same process used to obtain the first-order values, leading to

$${\mu_X}^{II} = E^{II}[\{X\}] = E\left[\left\{\overline{X}\right\} + \sum_{i=1}^{N} \{X_{,i}\}\, q_i + \frac{1}{2}\sum_{i=1}^{N}\sum_{j=1}^{N} \{X_{,ij}\}\, q_i q_j\right] = \left\{\overline{X}\right\} + \frac{1}{2}\sum_{i=1}^{N}\sum_{j=1}^{N} \{X_{,ij}\}\, \gamma_q^{ij} \tag{3.10}$$

and

$$\begin{aligned} \gamma_X^{II}\left(\{X\}, \{X\}^T\right) &= E[\{X\}\{X\}^T] - E[\{X\}]E[\{X\}]^T \\ &= \sum_{i=1}^{N}\sum_{j=1}^{N} \{X_{,i}\}\{X_{,j}\}^T \gamma_q^{ij}. \end{aligned} \tag{3.11}$$

Comparing the equations for first (Eq. (3.7), Eq. (3.8)) and second-order (Eq. (3.10), Eq. (3.11)), it is possible to see that the mean value for second-order has an additional term. In terms of covariance, this quantity is equal for the two approximations.

PM application implies the necessity to have first and second-order derivatives of the system. To obtain them, if possible, system equations are used. For complex systems, it is very hard or even impossible to obtain the system equations analytically, instead, finite difference approximations might have to be used.

Finite differences is an approximation method, often used to determine the numerical solution of partial or ordinary differential equations. All finite differences can be derived from the Taylor series expansion of a function f about a point x [LeVeque, 2005],

$$f(x+h) = f(x) + h\frac{df}{dx} + ... + \frac{1}{n!}h^n\frac{d^n f}{dx^n} + ... = \sum_{i=0}^{\infty}\frac{h^n}{n!}\frac{d^n f}{dx^n}, \tag{3.12}$$

where h represents a step size. On one hand, this needs to be small to reduce the truncation error. On the other hand, too small steps lead to subtraction cancellation errors. As such, the step chosen is very important because the derivative accuracy strongly depends on it.

For first-order derivatives can be computed from different ways, each having an error associated. The error is indicated by O notation and the approximation is obtained by truncating the summation. The order of the error is a measure of the accuracy of the approximation, a higher order implies a better accuracy. Approximations can be *forward difference approximation*, *backward difference approximation* or *centered difference approximation*, each kind of approximation has different possibilities with different error-orders. In the development of PM, *centered difference approximation* for first and second-order derivatives will be used.

Equation (3.13) represents the expression to estimate the first-order derivative [LeVeque, 2005]:

$$\frac{df}{dx} = \frac{f(x+h) - f(x-h)}{2h} + O(h^2). \tag{3.13}$$

For the second-order derivative, Eq. (3.14) [LeVeque, 2005] will be used:,

$$\frac{d^2f}{dx^2} = \frac{-f(x+2h) + 16f(x+h) - 30f(x) + 16f(x-h) - f(x-2h)}{12h^2} + O(h^4). \tag{3.14}$$

Therefore, a second-order error will be used for the first-order derivative, while a forth-order error will be used for the second-order derivative.

3.5 Fast Probability Integrator

The FPI is one of the most recent methods used in uncertainty quantification. This method has not been implemented because there was no time remaining after the implementation of the other methods.

Comparing this methodology with others presented above, FPI has its major advantage in computational speed. This method is more efficient than probabilistic methods for very high or low probabilities because its solution time is independent of the probability level, consequently the simulation time is reduced.

This method can be classified in two types: FORM and SORM [Lee and Hwang, 2008]. For this method, the random variables used in other methods are changed to be an independent standard normal variable with an exact mapping. This transformation is not easy since the variable can become distorted. To deal with this disadvantage, FPI has been in constant development and the aim of the development is the approximation of original distribution to standard normal variables [Cronvall, 2007].

This method can be used for complex problems in which governing equations are difficult to analyze. It uses numerical procedures to solve the multidimensional integral equations to obtain the failure probability or the reliability analyses. FPI allows to evaluate the information about the importance of each random variable and these sensitivity factors are useful in optimization.

Chapter 4

Three-Bar Truss

This chapter presents a generic case that was studied previously using UQ [Patnaik et al., 2010], [Patnaik et al., 2009] and [Wei, 2006]. It begins with a brief explanation of the case to be analyzed, then the methods chosen are implemented in a proper software. Finally, a comparison between the results obtained with the methods implemented and the results from literature are presented.

4.1 Model Description

The model selected to analyze is a three-bar truss, which is a simple structure to initiate the study in this field. The structure is represented in Fig. 4.1 and the units in this study still remain in Imperial system to facilitate the comparison between results. The structure is composed of three bars made of steel, where nodes three and four are fixed, node two is a setting support and node one is subjected to loads and change of temperature.

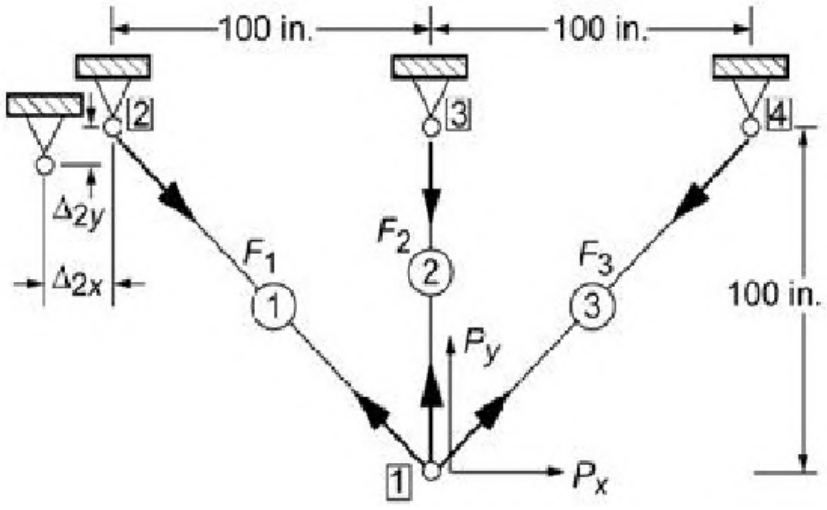

Figure 4.1: Three-bar truss [Patnaik et al., 2010].

The structure has ten random variables in total and these can be grouped in material properties, load and sizing parameters. Each variable is defined by its mean value (μ), standard deviation (σ) and

covariance (γ).

There are some studies about this example [Patnaik et al., 2010], [Patnaik et al., 2009], but the reference that is taken in consideration is [Wei, 2006] because it has available all the information needed for the analyses.

Material properties include the Young modulus (E) and the coefficient of thermal expansion (α). The Young modulus properties are

$$\{\mu_E\} = \{3.00 \times 10^4\} ksi \quad , \quad \{\sigma_E\} = \{3.00 \times 10^3\} ksi \quad \text{and} \quad \{\gamma_E\} = \{9.00 \times 10^6\}.$$

The covariance is obtained by applying Eq. (2.3).

The coefficient of thermal expansion has the follow properties

$$\{\mu_\alpha\} = \{6.6 \times 10^{-6}\} F \quad , \quad \{\sigma_\alpha\} = \{6.6 \times 10^{-7}\} F \quad \text{and} \quad \{\gamma_\alpha\} = \{4.356 \times 10^{-13}\} \, .$$

In the loads group, there are three random variables: the mechanical load (Q), the thermal load (T) and the load due to the setting support (Δ) in node two.

The mechanical load has two contributions, one in the x direction and other in the y direction,

$$\begin{Bmatrix} \mu_{Q_X} \\ \mu_{Q_Y} \end{Bmatrix} = \begin{Bmatrix} 50 \\ -100 \end{Bmatrix} kip \quad , \quad \begin{Bmatrix} \sigma_{Q_X} \\ \sigma_{Q_Y} \end{Bmatrix} = \begin{Bmatrix} 5.00 \\ 5.00 \end{Bmatrix} kip \quad \text{and} \quad [\gamma_Q] = \begin{bmatrix} 25.00 & 6.25 \\ 6.25 & 25.00 \end{bmatrix}.$$

The thermal load is characterized by:

$$\{\mu_T\} = \{100\}^\circ F \quad , \quad \{\sigma_T\} = \{10\}^\circ F \quad \text{and} \quad \{\gamma_T\} = \{100\}.$$

The last contribution from the loads is due to the setting support. This has contributions in the x and y directions,

$$\begin{Bmatrix} \mu_{\Delta X} \\ \mu_{\Delta Y} \end{Bmatrix} = \begin{Bmatrix} 0.10 \\ 0.15 \end{Bmatrix} in \quad , \quad \begin{Bmatrix} \sigma_{\Delta X} \\ \sigma_{\Delta Y} \end{Bmatrix} = \begin{Bmatrix} 0.005 \\ 0.015 \end{Bmatrix} in \quad \text{and} \quad [\gamma_\Delta)] = \begin{bmatrix} 25.00 & 37.5 \\ 37.5 & 225 \end{bmatrix} \times 10^{-6}.$$

Finally, the last group of variables is the sizing design parameters. It is composed by the cross-section areas of each bar,

$$\begin{Bmatrix} \mu_{A_1} \\ \mu_{A_2} \\ \mu_{A_3} \end{Bmatrix} = \begin{Bmatrix} 1.00 \\ 1.00 \\ 2.00 \end{Bmatrix} in^2 \quad , \quad \begin{Bmatrix} \sigma_{A_1} \\ \sigma_{A_2} \\ \sigma_{A_3} \end{Bmatrix} = \begin{Bmatrix} 0.10 \\ 0.10 \\ 0.10 \end{Bmatrix} in^2 \quad \text{and} \quad [\gamma_A] = \begin{bmatrix} 1.00 & 0.50 & 0.25 \\ 0.50 & 1.00 & 0.25 \\ 0.25 & 0.25 & 1.00 \end{bmatrix} \times 10^{-2}.$$

Before the implementation of the UQ methods, it is necessary to do the deterministic analysis of the structure.

4.2 Deterministic Analytical Analysis

For the deterministic analysis, the Integrated Force Method (IFM) was applied. This methodology has been developed and applied in the recent years for many structures analyses. It was proposed by Patnaik [Patnaik et al., 1991], [Patnaik et al., 2009], [Patnaik et al., 2010] and [Wei and Patnaik, 2012].

It is used to study discrete and continuous systems, but for its application is important that all information about the system is available. This methodology is different because it integrates the equilibrium equations and the global compatibility conditions, which allows to obtain accurate results for an indeterminate system. IFM has more advantages compared to the displacement method [Patnaik et al., 1991]. It provides accurate results and requires less computational effort.

The governing equation is discretized in l forces and m displacements unknowns. The number of displacements indicates the number of equilibrium equations. It can be put in matrix form as

$$[B]\{F\} = \{Q\}, \tag{4.1}$$

where $[B]$ is designated as equilibrium matrix and its dimension are $(m \times l)$, $\{Q\}$ is the load components with dimension l and {F} is the force vector with dimension l.

The number of compatibility conditions (k) is obtained from $(n - m)$. In matrix form, these conditions are

$$[C][G]\{F\} = \{\delta R\}, \tag{4.2}$$

where $[C]$ is the compatibility matrix $(k \times l)$, the concatenated flexibility matrix is represented by $[G]$ $(l \times l)$ and $\{\delta R\}$ corresponds to the effective initial deformation (l components).

Finally, the governing equation is obtained by coupling the equilibrium equations (4.1) and the compatibility equations (4.2) as

$$\left[\frac{[B]}{[C][G]}\right] = \left[\frac{\{Q\}}{\{\delta R\}}\right] \qquad or \qquad [S]\{F\} = \{Q^*\}, \tag{4.3}$$

where $[S]$ is the IFM governing matrix $(l \times l)$ and $\{Q^*\}$ represents the load vector of the structure (m components).

The effective initial deformation vector $\{\delta R\}$ and the deformation coefficient matrix $[J]$ are computed using

$$\{\delta R\} = -[C]\{\beta^0\} \tag{4.4}$$

and

$$[J] = mrowsof[S]^{-1}, \tag{4.5}$$

where $\{\beta^0\}$ is the n-component initial deformation vector.

Matrices $[B]$, $[J]$ and $[C]$ are deterministic since their components do not depend on stochastic geometrical parameters. The other matrices $[G]$, $[S]$, $\{L\}$ and $\{\delta R\}$ are stochastic because they depend on stochastic parameters. This method can also be used to analyze structures deterministically, but in this case it is only used mean values without standard deviation values.

The IFM solution procedure consists of five steps [Patnaik et al., 1991]:

1. Assembly of the system equilibrium matrix $[B]$;

2. Generation of the global compatibility matrix $[C]$;

3. Generation of the concatenated flexibility matrix $[G]$;

4. Construction of the load vector $\{Q^*\}$;

5. Solution of the IFM equation.

After determining all the necessary matrices, it is possible to compute the system response. The force applied on the bars (Eq. (4.6)) can be determined, then the displacement on node 1 (Eq. (4.7)) and finally the stress on the bars (Eq. (4.8)).

$$\{F\} = [S]^{-1}\{Q^*\} \tag{4.6}$$

$$\{X\} = [J]\left([G]\{F\} + \{\beta^0\}\right) \tag{4.7}$$

$$\{\sigma_s\} = \{F\}[A]^{-1} \tag{4.8}$$

With these equations, it was possible to compute the deterministic values, being the results from this analysis presented in Tab. 4.1.

Parameter	Deterministic Values
Force $\begin{Bmatrix} F_1 \\ F_2 \\ F_3 \end{Bmatrix}$ [kip]	$\begin{Bmatrix} 62.78 \\ 61.22 \\ -7.93 \end{Bmatrix}$
Stress $\begin{Bmatrix} \sigma_{s_1} \\ \sigma_{s_2} \\ \sigma_{s_3} \end{Bmatrix}$ [ksi]	$\begin{Bmatrix} 62.78 \\ 61.22 \\ -3.97 \end{Bmatrix}$
Displacement $\begin{Bmatrix} u \\ v \end{Bmatrix}$ [in]	$\begin{Bmatrix} 0.20 \\ -0.24 \end{Bmatrix}$

Table 4.1: Deterministic analysis using IFM.

Having the case fully described, it is possible to initiate the implementation of the UQ methods. The methods that will be used in this example will be the MCS, the LHS and the PM as mentioned in the previous chapter. These will be implemented in MATLAB® [The MathWorks Inc., 2009] language and illustative scripts are included in appendix.

4.3 Monte Carlo Simulation Method

Firstly, it is implemented the MCS method. This is a method that has low complexity in terms of implementation but it has high costs in terms of computational time. Its computational effort depends on the number of random variables of the design and the number of samples defined. As the method has not a lot of variables, high number of samples is used, although the simulation time is expected not to be

high. For the random sampling, it was used a MATLAB® function, the *normrnd* function, that needs as input variables the mean value and the standard deviation.

The problem in study has ten random variables. Since the bibliography [Wei, 2006] does not make any reference to the kind of variables probability distribution, the normal probability distribution will be used for every variable in future calculus.

After the simulation, it is possible to obtain the results for different number of samples. To have a way to compare the results, the simulation is done using the same number of samples as mentioned in the report [Patnaik et al., 2009], (12,500 samples). The results and the comparison are summarized in Tab. 4.2.

Parameter	Results		Report Results		Error [%]	
	Mean Value	Std. dev.	Mean Value	Std. dev.	Mean Value	Std. dev.
Force $\begin{Bmatrix} F_1 \\ F_2 \\ F_3 \end{Bmatrix}$ [kip]	$\begin{Bmatrix} 62.76 \\ 61.22 \\ -7.99 \end{Bmatrix}$	$\begin{Bmatrix} 4.71 \\ 5.28 \\ 5.54 \end{Bmatrix}$	$\begin{Bmatrix} 62.77 \\ 61.27 \\ -7.93 \end{Bmatrix}$	$\begin{Bmatrix} 4.39 \\ 5.35 \\ 5.67 \end{Bmatrix}$	$\begin{Bmatrix} 0.02 \\ 0.08 \\ 0.76 \end{Bmatrix}$	$\begin{Bmatrix} 7.29 \\ 1.31 \\ 2.29 \end{Bmatrix}$
Stress $\begin{Bmatrix} \sigma_{s_1} \\ \sigma_{s_2} \\ \sigma_{s_3} \end{Bmatrix}$ [ksi]	$\begin{Bmatrix} 63.22 \\ 61.63 \\ -4.00 \end{Bmatrix}$	$\begin{Bmatrix} 5.97 \\ 5.44 \\ 2.78 \end{Bmatrix}$	$\begin{Bmatrix} 63.16 \\ 61.58 \\ -3.97 \end{Bmatrix}$	$\begin{Bmatrix} 5.89 \\ 5.42 \\ 2.79 \end{Bmatrix}$	$\begin{Bmatrix} 0.09 \\ 0.08 \\ 0.75 \end{Bmatrix}$	$\begin{Bmatrix} 1.36 \\ 0.37 \\ 0.36 \end{Bmatrix}$
Displacement $\begin{Bmatrix} u \\ v \end{Bmatrix}$ [in]	$\begin{Bmatrix} 0.20 \\ -0.24 \end{Bmatrix}$	$\begin{Bmatrix} 0.04 \\ 0.03 \end{Bmatrix}$	$\begin{Bmatrix} 0.20 \\ -0.24 \end{Bmatrix}$	$\begin{Bmatrix} 0.04 \\ 0.03 \end{Bmatrix}$	$\begin{Bmatrix} 0.00 \\ 0.00 \end{Bmatrix}$	$\begin{Bmatrix} 0.00 \\ 0.00 \end{Bmatrix}$

Table 4.2: Probabilistic response using Monte Carlo simulation.

Comparing the results, it is possible to observe that the mean value presents a good match, but the standard deviation exhibits a not so good match. During the simulation, it was observed that the number of samples to reach converged results need to be higher. However, the aim of this comparison is to compare the results obtained from the method implemented and the reference report.

4.4 Latin Hypercube Sampling Method

The second method to analyze the model is the LHS. This method has an increased difficulty in the implementation. However, the computational effort reduces because the kind of sampling is different from the one used in the MCS. For this methodology, the MATLAB® function used was different, being used the *lhsnorm* function instead. It is responsible to do the stratified sampling and it needs as input variables the mean value and the covariance. In the sampling, the standard options were chosen, even though the function allows some options to improve the sampling.

For this case, it was used ten variables with normal probability distribution, like it was done for the MCS but, with the stratified sampling, it was expected that the number of samples to converge would be reduced. In Tab. 4.3 are presented the simulation results and the comparison between results. For the simulation results was used 1,000 samples, like mentioned in the reference report [Patnaik et al., 2009].

Analyzing results, it is possible to observe that the computed results and report results have a very good match. The largest error is observed in standard deviation and the maximum difference is about 7%. For mean values, the difference between results is less then 0.03%. Considering that LHS has its

Parameter	Results		Report Results		Error[%]	
	Mean Value	Std. dev.	Mean Value	Std. dev.	Mean Value	Std. dev.
Force $\begin{Bmatrix} F_1 \\ F_2 \\ F_3 \end{Bmatrix}$ [kip]	$\begin{Bmatrix} 62.75 \\ 61.26 \\ -7.96 \end{Bmatrix}$	$\begin{Bmatrix} 4.70 \\ 5.12 \\ 5.48 \end{Bmatrix}$	$\begin{Bmatrix} 62.76 \\ 61.25 \\ -7.96 \end{Bmatrix}$	$\begin{Bmatrix} 4.39 \\ 5.35 \\ 5.67 \end{Bmatrix}$	$\begin{Bmatrix} 0.02 \\ 0.02 \\ 0.00 \end{Bmatrix}$	$\begin{Bmatrix} 7.06 \\ 4.30 \\ 3.35 \end{Bmatrix}$
Stress $\begin{Bmatrix} \sigma_{s_1} \\ \sigma_{s_2} \\ \sigma_{s_3} \end{Bmatrix}$ [ksi]	$\begin{Bmatrix} 63.17 \\ 61.59 \\ -3.99 \end{Bmatrix}$	$\begin{Bmatrix} 5.90 \\ 5.43 \\ 2.76 \end{Bmatrix}$	$\begin{Bmatrix} 63.15 \\ 61.57 \\ -3.99 \end{Bmatrix}$	$\begin{Bmatrix} 5.77 \\ 5.38 \\ 2.75 \end{Bmatrix}$	$\begin{Bmatrix} 0.03 \\ 0.03 \\ 0.00 \end{Bmatrix}$	$\begin{Bmatrix} 2.25 \\ 0.93 \\ 0.36 \end{Bmatrix}$
Displacement $\begin{Bmatrix} u \\ v \end{Bmatrix}$ [in]	$\begin{Bmatrix} 0.20 \\ -0.24 \end{Bmatrix}$	$\begin{Bmatrix} 0.04 \\ 0.03 \end{Bmatrix}$	$\begin{Bmatrix} 0.20 \\ -0.24 \end{Bmatrix}$	$\begin{Bmatrix} 0.04 \\ 0.03 \end{Bmatrix}$	$\begin{Bmatrix} 0.00 \\ 0.00 \end{Bmatrix}$	$\begin{Bmatrix} 0.00 \\ 0.00 \end{Bmatrix}$

Table 4.3: Probabilistic response using Latin hypercube sampling.

base in statistics, it is normal that in every simulation the final results are not the same every time, which explains the difference in standard deviation. Comparing the simulation time, LHS is significantly faster than MCS and the results are very close.

Concluding, the method implemented is working correctly, which is proved by the accuracy of the results obtained.

4.5 Perturbation Method

Finally, the last method used to analyze the UQ in the structure is the PM. This method, from the methods already implemented, is that one which has the highest complexity in implementation. However, the computation time required to obtain the results is smaller than the other two methods.

In PM, the mean value and the covariance matrix of the response are obtained in two steps. Firstly, the response variable is expanded in a Taylor's series with respect to the primitive random variables and the terms up to the second order are retained (Eq. (3.10), Eq. (3.11)). In this case, the primitive variables are represented in a different configuration, Equation. (4.9) describes the input variables,

$$\begin{aligned} A_1 &= \mu_{A_1}(1+q_{A_1}) \\ A_2 &= \mu_{A_2}(1+q_{A_2}) \\ A_3 &= \mu_{A_3}(1+q_{A_3}) \\ E &= \mu_E(1+q_E) \\ \alpha &= \mu_\alpha(1+q_\alpha) \\ Q_X &= \mu_{Q_X}(1+q_{Q_X}) \\ Q_Y &= \mu_{Q_Y}(1+q_{Q_Y}) \\ T &= \mu_T(1+q_T) \\ \Delta_1 &= \mu_{\Delta_1}(1+q_{\Delta_1}) \\ \Delta_2 &= \mu_{\Delta_1}(1+q_{\Delta_2}) \end{aligned} \quad , \tag{4.9}$$

where μ represents the deterministic part of the variable, more precisely the mean value, and q is the perturbation term.

When all primitive variables are defined, it is possible to do the Taylor expansion, like exemplified

in the perturbation method explanation (Sec. 3.4). With all the expansions, the PM can then be implemented.

Table 4.4 presents the results obtained with this method and also presents the results from report cited previously.

Parameter	Results		Report Results		Error[%]	
	Mean Value	Std. dev.	Mean Value	Std. dev.	Mean Value	Std. dev.
Force $\begin{Bmatrix} F_1 \\ F_2 \\ F_3 \end{Bmatrix}$ [kip]	$\begin{Bmatrix} 62.76 \\ 61.24 \\ -7.95 \end{Bmatrix}$	$\begin{Bmatrix} 4.54 \\ 5.65 \\ 5.81 \end{Bmatrix}$	$\begin{Bmatrix} 62.77 \\ 61.24 \\ -7.95 \end{Bmatrix}$	$\begin{Bmatrix} 4.39 \\ 5.35 \\ 5.67 \end{Bmatrix}$	$\begin{Bmatrix} 0.02 \\ 0.00 \\ 0.00 \end{Bmatrix}$	$\begin{Bmatrix} 3.42 \\ 5.61 \\ 2.47 \end{Bmatrix}$
Stress $\begin{Bmatrix} \sigma_{s_1} \\ \sigma_{s_2} \\ \sigma_{s_3} \end{Bmatrix}$ [ksi]	$\begin{Bmatrix} 63.28 \\ 61.70 \\ -3.98 \end{Bmatrix}$	$\begin{Bmatrix} 6.81 \\ 6.41 \\ 2.41 \end{Bmatrix}$	$\begin{Bmatrix} 63.29 \\ 61.70 \\ -3.98 \end{Bmatrix}$	$\begin{Bmatrix} 6.71 \\ 6.20 \\ 2.34 \end{Bmatrix}$	$\begin{Bmatrix} 0.02 \\ 0.00 \\ 0.00 \end{Bmatrix}$	$\begin{Bmatrix} 1.49 \\ 3.39 \\ 2.99 \end{Bmatrix}$
Displacement $\begin{Bmatrix} u \\ v \end{Bmatrix}$ [in]	$\begin{Bmatrix} 0.20 \\ -0.24 \end{Bmatrix}$	$\begin{Bmatrix} 0.04 \\ 0.03 \end{Bmatrix}$	$\begin{Bmatrix} 0.20 \\ -0.24 \end{Bmatrix}$	$\begin{Bmatrix} 0.04 \\ 0.03 \end{Bmatrix}$	$\begin{Bmatrix} 0.00 \\ 0.00 \end{Bmatrix}$	$\begin{Bmatrix} 0.00 \\ 0.00 \end{Bmatrix}$

Table 4.4: Probabilistic response using perturbation method.

Observing the results, it is possible to see that the results produced present a very good match to the results in the reference report. The biggest difference observed in the results is in standard deviation and it is about 6%, being the smallest less than 0.02%. In terms of computational time, PM is the fastest method and the accuracy of the results are at the same level of the results obtained with the other two methods. However, PM was the methodology that implied more effort in terms of implementation.

In conclusion, the objective about implementation of this method was reached. It is working correctly and the results provide a good accuracy.

4.6 Discussion of Results

After the implementation of the methods selected, it is required to compare the results between them, Tab. 4.5 exhibits a comparison between the results obtained for each method.

Parameter	MCS		LHS		PM	
	Mean Value	Std. dev.	Mean Value	Std. dev.	Mean Value	Std. dev.
Force $\begin{Bmatrix} F_1 \\ F_2 \\ F_3 \end{Bmatrix}$ [kip]	$\begin{Bmatrix} 62.76 \\ 61.22 \\ -7.99 \end{Bmatrix}$	$\begin{Bmatrix} 4.71 \\ 5.28 \\ 5.54 \end{Bmatrix}$	$\begin{Bmatrix} 62.75 \\ 61.26 \\ -7.96 \end{Bmatrix}$	$\begin{Bmatrix} 4.70 \\ 5.12 \\ 5.48 \end{Bmatrix}$	$\begin{Bmatrix} 62.76 \\ 61.24 \\ -7.95 \end{Bmatrix}$	$\begin{Bmatrix} 4.54 \\ 5.65 \\ 5.81 \end{Bmatrix}$
Stress $\begin{Bmatrix} \sigma_{s_1} \\ \sigma_{s_2} \\ \sigma_{s_3} \end{Bmatrix}$ [ksi]	$\begin{Bmatrix} 63.22 \\ 61.63 \\ -4.00 \end{Bmatrix}$	$\begin{Bmatrix} 5.97 \\ 5.44 \\ 2.78 \end{Bmatrix}$	$\begin{Bmatrix} 63.17 \\ 61.59 \\ -3.99 \end{Bmatrix}$	$\begin{Bmatrix} 5.90 \\ 5.43 \\ 2.76 \end{Bmatrix}$	$\begin{Bmatrix} 63.28 \\ 61.70 \\ -3.98 \end{Bmatrix}$	$\begin{Bmatrix} 6.81 \\ 6.41 \\ 2.34 \end{Bmatrix}$
Displacement $\begin{Bmatrix} u \\ v \end{Bmatrix}$ [in]	$\begin{Bmatrix} 0.20 \\ -0.24 \end{Bmatrix}$	$\begin{Bmatrix} 0.04 \\ 0.03 \end{Bmatrix}$	$\begin{Bmatrix} 0.20 \\ -0.24 \end{Bmatrix}$	$\begin{Bmatrix} 0.04 \\ 0.03 \end{Bmatrix}$	$\begin{Bmatrix} 0.20 \\ -0.24 \end{Bmatrix}$	$\begin{Bmatrix} 0.04 \\ 0.03 \end{Bmatrix}$

Table 4.5: Comparison of results from different methods.

Comparing the results, it is possible to conclude that the three different methods present very close results. In terms of mean value, they have an insignificant difference, for standard deviation a very small difference is observed. Thus, it is possible to say that all the methods are working correctly.

With the results obtained, it is possible to compute the PDF and CDF graphs. To facilitate the results analysis, graphs for each output will be drawn, and in each graph the results for the three methods are presented.

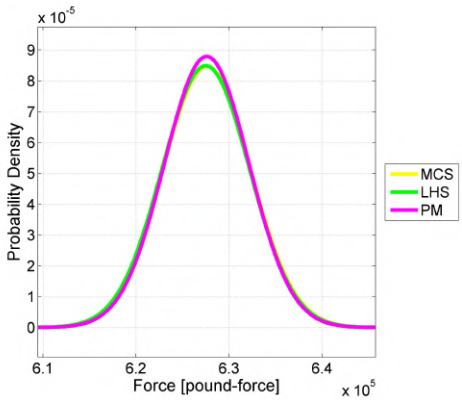

(a) PDF for bar 1

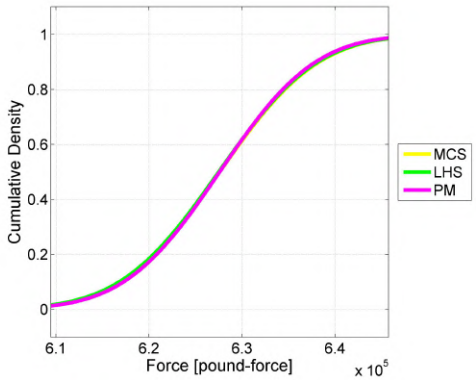

(b) CDF for bar 1

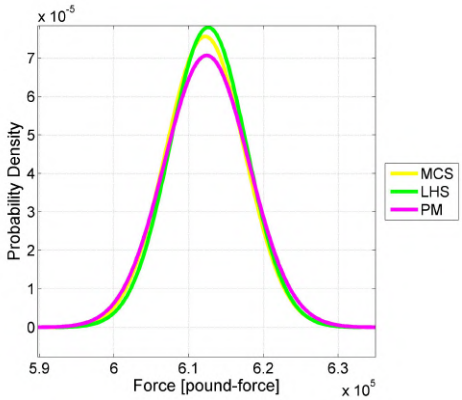

(c) PDF for bar 2

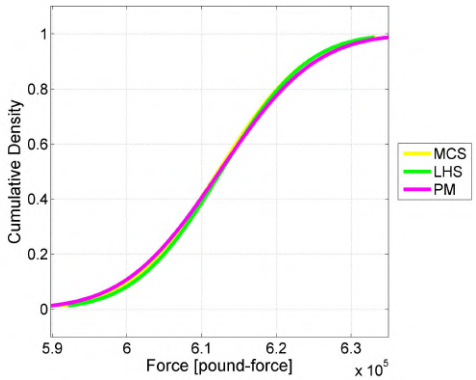

(d) CDF for bar 2

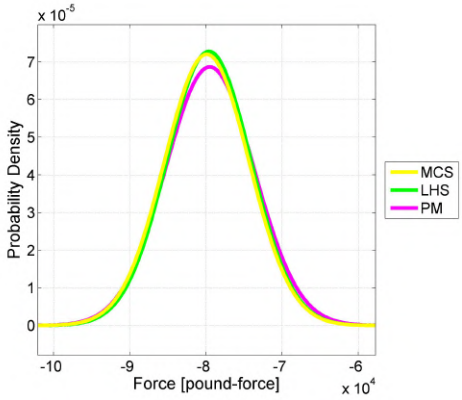

(e) PDF for bar 3

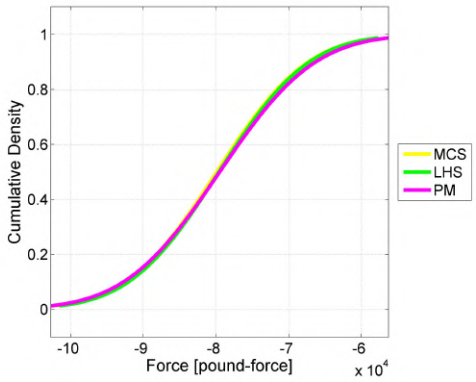

(f) CDF for bar 3

Figure 4.2: PDF and CDF for force.

Making a general comparison using the graphs results shown in Fig. 4.2, Fig. 4.3 and Fig. 4.4, it is possible to observe that the results obtained exhibit a very good match. For displacement, it is only visible PM line because the results for the methods are the same, the other lines are under the PM

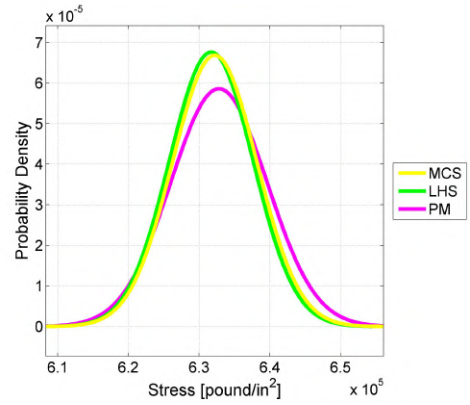

(a) PDF on bar 1

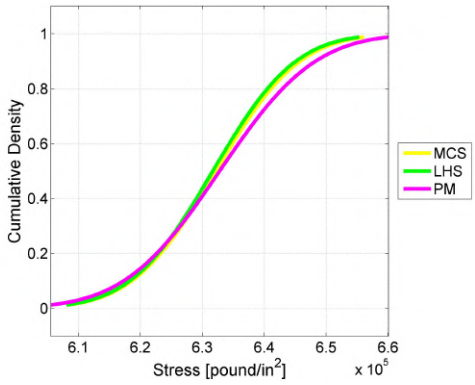

(b) CDF on bar 1

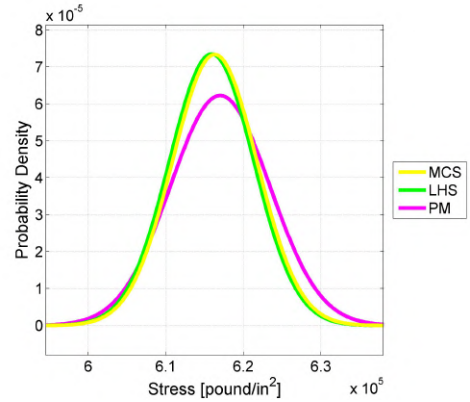

(c) PDF on bar 2

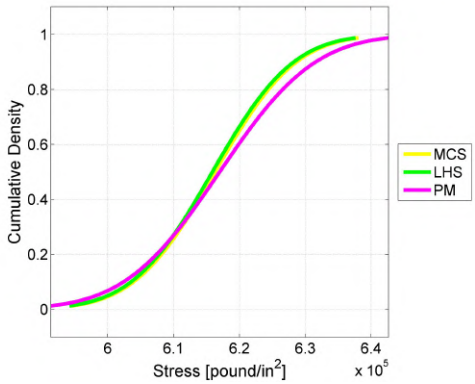

(d) CDF on bar 2

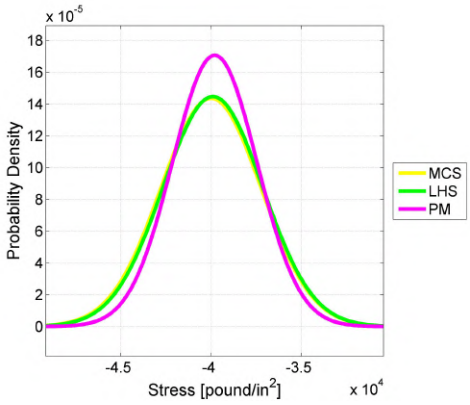

(e) PDF on bar 3

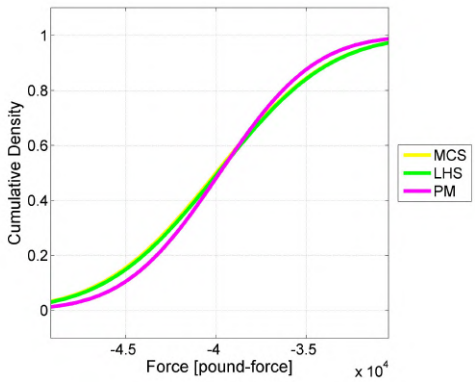

(f) CDF on bar 3

Figure 4.3: PDF and CDF for stress.

line. These graphs are very important for the designer, because they allow to know the behavior of the system and take some important decisions about the design.

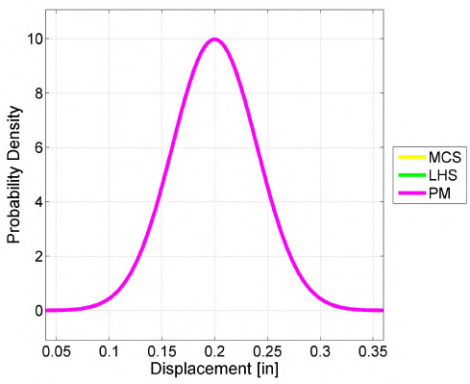

(a) PDF for horizontal displacement

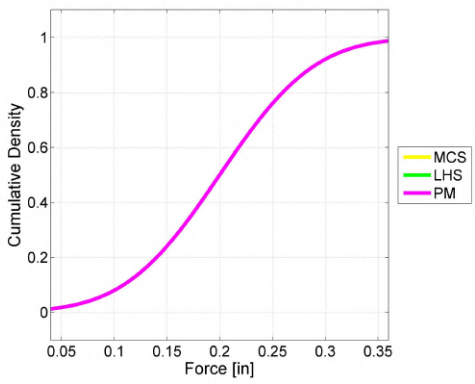

(b) CDF for horizontal displacement

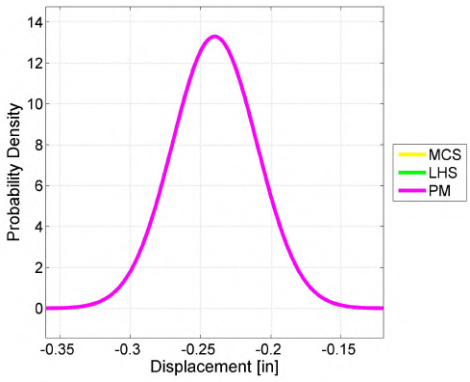

(c) PDF for vertical displacement

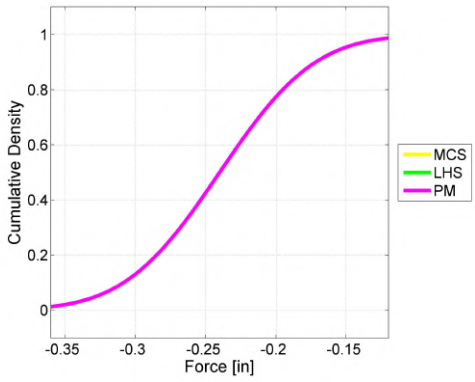

(d) CDF for vertical displacement

Figure 4.4: PDF and CDF for displacement.

Chapter 5

Wing Spar

This chapter presents a study of a wing spar using the knowledge acquired and the methods implemented in the previous chapter. The structure is similar to the three-bar truss and an analytical analysis will also be done using the same UQ methods. The difference is the introduction of FEM software to analyze the same structure with UQ methods. Finally, there will be a comparison between the results obtained from the two kinds of analysis - analytical and numerical. The objective of this chapter is to validate the use of FEM with UQ methods in complex structures, where an analytical analysis is not possible.

5.1 Model Description

The model that will be analyzed in this chapter is a wing spar. The structure is modeled as a straight beam with a constant square cross-section, clamped in one side, simulating the wing root, free at the end, simulating the wing tip, and subjected to a distributed load on its top surface. The system is represented in Fig. 5.1.

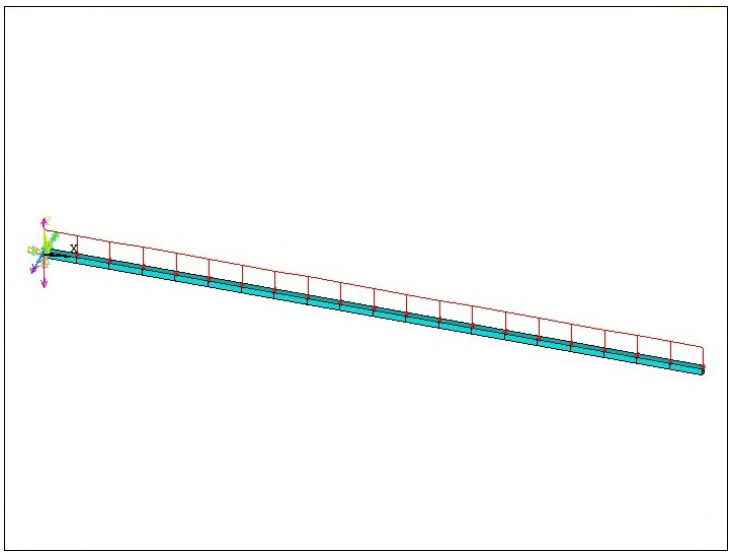

Figure 5.1: Clamped beam.

In this case, there are only four random variables, which are the dimension of the beam cross-section (D), the beam length (L), the mechanical properties, in the form of the Young modulus (E) and the distributed load (q). The material selected for the wing spar was aluminium Al-7050-T7651, which is an alloy with thermal treatment [ASM, 2012], Tab. 5.1 exhibits the mechanical properties of the material.

Parameter	Value
Density [kg/m^3]	2830
Ultimate Tensile Strength [MPa]	552
Tensile Yield Strength [MPa]	490
Modulus of Elasticity [GPa]	71.7
Poison's Ratio	0.33
Shear Modulus [GPa]	26.9
Shear Strength [MPa]	324

Table 5.1: Aluminium - Al-7050-T7651 mechanical properties.

All variables are assumed to have a normal distribution. Each variable is defined by the mean value (μ), the standard deviation (σ) and the covariance (γ).

The beam has a square section and its dimension is

$$\{\mu_D\} = \{1 \times 10^{-2}\}m \quad , \quad \{\sigma_D\} = \{1 \times 10^{-3}\}m \quad \text{and} \quad \{\gamma_D\} = \{1 \times 10^{-6}\}.$$

Another property is related to the beam dimensions, it is the length,

$$\{\mu_L\} = \{1\}m \quad , \quad \{\sigma_L\} = \{1 \times 10^{-1}\}m \quad \text{and} \quad \{\gamma_L\} = \{1 \times 10^{-2}\}.$$

The Young modulus is the mechanical property of the material,

$$\{\mu_E\} = \{71.7 \times 10^{9}\}Pa \quad , \quad \{\sigma_E\} = \{71.7 \times 10^{8}\}Pa \quad \text{and} \quad \{\gamma_E\} = \{5.14 \times 10^{19}\}.$$

Finally, the last random property is the distributed load. Since this load is assumed constant along the beam length, it has only one contribution and it is applied perpendicularly to the beam, on the top face,

$$\{\mu_q\} = \{50\}N/m^2 \quad , \quad \{\sigma_q\} = \{5\}N/m^2 \quad \text{and} \quad \{\gamma_q\} = \{25\}.$$

With this study, the main objective is to observe the maximum displacement at the end of the beam and the maximum stress in the clamped zone of the beam.

5.2 Deterministic Analytical Analysis

This system can be analyzed analytically, starting with the Eq. (5.1) [Beer et al., 2006] for the transverse displacement w of a beam with constant Young modulus E and uniform area moment of the cross-section I, subject to a distributed load q,

$$EI\frac{d^4w}{dx^4} = q, \tag{5.1}$$

where x is the coordinate along the beam length, starting at the root ($x = 0$) and ending at the tip ($x = L$).

Integrating Eq. (5.1) four times, the general equation which describes the transverse displacement is obtained,

$$EIw - \frac{qx^4}{24} + \frac{C_1x^3}{6} + \frac{C_2x^2}{2} + C_3x + C_4 = 0. \tag{5.2}$$

After integration, it is necessary to determine the constants using the boundary conditions of the problem. In this case, there are two kinds: the natural and the essential boundary conditions. The natural boundary conditions are the bending moment and the shear force at the end of the beam, which should vanish,

$$M\big|_{x=L} = EI\frac{d^2w}{dx^2}\bigg|_{x=L} = 0 \tag{5.3}$$

and

$$V\big|_{x=L} = \frac{d}{dx}\left(EI\frac{d^2w}{dx^2}\right)\bigg|_{x=L} = 0. \tag{5.4}$$

The other boundary conditions are the essential, which are composed by the displacement and the rotation in the clamped face of the beam. The clamping implies that these should also vanish,

$$w\big|_{x=0} = 0 \tag{5.5}$$

and

$$\frac{dw}{dx}\bigg|_{x=0} = 0. \tag{5.6}$$

Applying these four boundary conditions, it is possible to obtain the governing equations of the system, which constitutes the basis to analyze the beam behavior.

$$w = \frac{1}{EI}\left(\frac{qx^4}{24} - \frac{qLx^3}{6} + \frac{qL^2x^2}{4}\right) \tag{5.7}$$

$$\frac{dw}{dx} = \frac{1}{EI}\left(\frac{qx^3}{24} - \frac{qLx^2}{2} + \frac{qL^2x}{2}\right) \tag{5.8}$$

$$EI\frac{d^3w}{dx^3} = V = qx - qL \tag{5.9}$$

$$EI\frac{d^2w}{dx^2} = M = \frac{qx^2}{2} - qLx + \frac{qL^2}{2} \tag{5.10}$$

Equations (5.7) and (5.8) describe, respectively, the displacement and the rotation of the beam, while the shear force and bending moment are characterized by Eq. (5.9) and Eq. (5.10), respectively.

As the beam section has a square shape, the moment of inertia in x-plane and y-plane are the same. The stress in the clamped zone includes both tension or compression: the compression is observed in the bottom face, whereas the tension is observed in the top face since the distributed load is downward. For the study, it will be considered the stress in the top face (tension) only. The stress distribution along the beam height, y is described as

$$\sigma_S = \frac{My}{I}, \tag{5.11}$$

where y is the distance between gravity center and the location in study and I is the moment of inertia. The deterministic maximum stress can be estimated by first using (5.10) for $x = 0$ (wing root), to obtain the maximum bending moment, and then using (5.11) for $y = \frac{h}{2}$ (top surface), where h is the beam height.

Using (5.7) for $x = L$ (wing tip), the deterministic maximum displacement can be estimated as

$$w = \frac{qL^4}{8EI}, \tag{5.12}$$

where the moment of inertia is $I = \frac{bh^3}{12}$, being b and h the beam section width and height, respectively.

With the expressions for maximum displacement and maximum stress, it is possible to apply the UQ methods developed to obtain the mean value and the standard deviation of these responses.

5.3 Sampling Convergence Study

MCS and LHS are sampling methods, consequently, it is necessary to do a convergence study to determine the number of samples required to ensure the convergence. This study is very important to obtain the best accuracy with the lowest simulation time. In the convergence study, the convergence factor ϵ used is defined as

$$\epsilon = \left| \frac{d_i - d_{i+1}}{d_{i+1}} \right|, \tag{5.13}$$

where d_i is the previous value and d_{i+1} is the current value. The convergence is ensured when the convergence factor is less or equal to 0.1%, $(\epsilon \leq 0.001)$. For the convergence study, it is only necessary to observe the convergence for one parameter because if the convergence is ensured for one variable, the other it will be also converged. The maximum displacement was chosen as the monitoring parameter.

After the convergence study and observing Fig. 5.2, it is possible to take some important decisions. As they are statistical analyses, it is normal that the convergence graph does not present a consistent convergence line with the increment of samples. It was decided to use about 16,000 samples and about 1,600 samples for the LHS, which resulted in differences between results of about 0.1%.

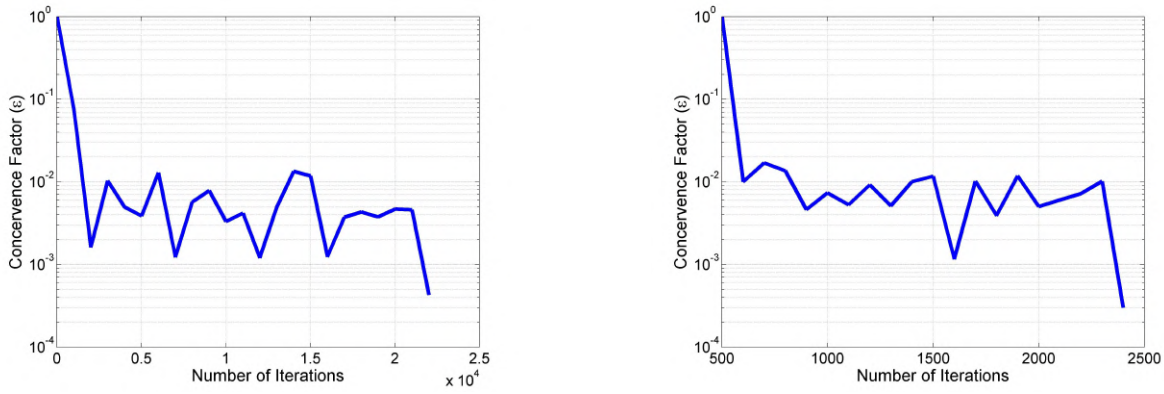

(a) MCS (b) LHS

Figure 5.2: Convergence study for displacement.

5.4 Stochastic Analytical Analysis

Ater the convergence study, it is possible to run the simulation and obtain the results with the accuracy required. Table 5.2 presents the results from MCS, LHS and PM.

Parameter	MCS		LHS		PM	
	Mean Value	Std. dev.	Mean Value	Std. dev.	Mean Value	Std. dev.
Max. Displacement [m]	-0.125	0.082	-0.124	0.079	-0.122	0.061
Max. Stress [N/m^2]	1.621×10^8	6.516×10^7	1.612×10^8	6.491×10^7	1.605×10^8	5.613×10^7

Table 5.2: Stochastic analytical analysis.

Comparing the results obtained from different methods applied using an analytic analysis, it is possible to observe that all methods present similar results. MCS and LHS exhibit very close results and PM provides also good results, but not as close to the results of the other two methods. The standard deviation obtained from PM presents the biggest difference compared with the other standard deviations. The mean value from PM is very close to the other values. In the mean values, the difference is less than 3%, whereas for the standard deviation is about 30%, these values are related to displacement. As a displacement is a small amount and when it is done a comparison, the difference is bigger than the difference observed for maximum stress. For the maximum stress, the difference between PM and the other methods is less then 15% for standard deviation.

5.5 Deterministic Numerical Analysis

In this section, the same wing spar structure will be analyzed, but it will be used FEM and the software selected was ANSYS® [ANSYS, Inc., 2010].

For the model construction, a beam element was used to obtain realistic results, which would mimic the analytical analysis. The element selected for the analysis was the BEAM4 [ANSYS, Inc., 2010], which is a 3-D element whose characteristics and outputs satisfy the requirements for the study. During

the structure definition, the same premises used for the analytical analysis were used because the objective is to obtain the same results with these two kinds of analyses.

To validate the use of FEM, it is necessary to compare the results obtained from analytical and numerical analyses. Table 5.3 presents the deterministic results computed from these two different ways, analytical analysis and FEM analysis.

Parameter	Analytic	FEM
Max. Displacement [m]	-0.105	-0.105
Max. Stress [N/m^2]	1.500×10^8	1.500×10^8

Table 5.3: Finite element method model validation.

Observing these results, it is plausible to say that the model created in ANSYS® produces the same results as the analytical analysis, which means that the FEM model is valid. For the model validation, a convergence was done in terms of the number of elements. For future analyses, it will be used the model with 40 elements which proved to accurately reproduce the expected analytical results.

Figure 5.3 exhibits the deterministic deformation and the stress distribution along the beam. From the stress distribution, it is possible to see that the stress in the clamped zone are equal in magnitude in the top and bottom face, as expected. Also, the maximum displacement occurs at the tip.

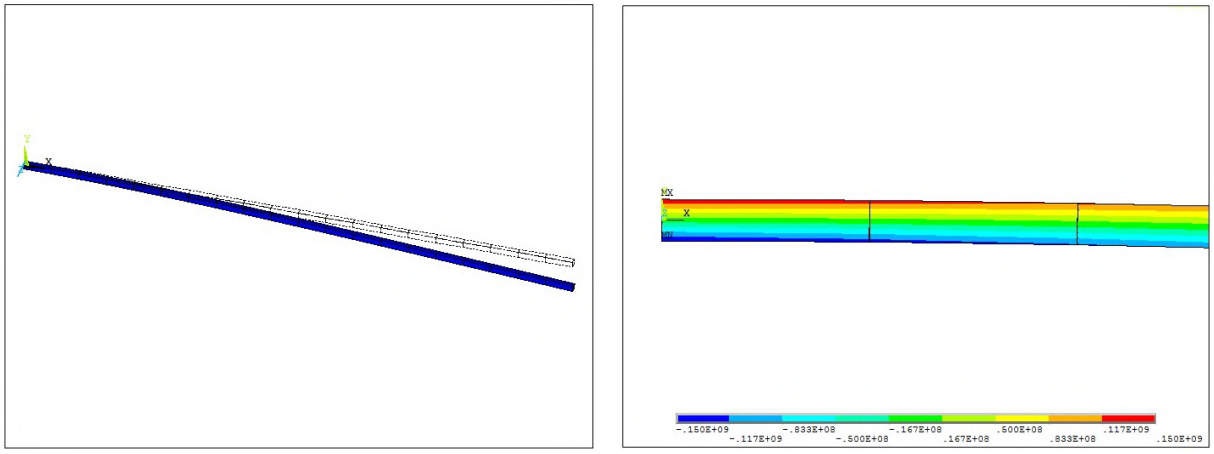

(a) Maximum displacement (b) Maximum stress

Figure 5.3: Deterministic output results.

5.6 Stochastic Numerical Analysis

After model validation, it is possible to study the wing spar with the UQ methods developed in Chap. 4.

In order to study the case using the UQ methods implemented previously, it is necessary to do some modifications because the model will be analyzed in ANSYS® and the results will be treated in MATLAB®.

Figure 5.4 represents the generic flowchart which explain how the methodology works. This flowchart represents all the methods but in each method it is necessary to do some modifications inherent to the

methods in use. First, MATLAB® is responsible for creating files with the required data to describe the structure, which include the structural analysis and the input values with uncertainty. Next, ANSYS® reads these files and uses them to build the model, which it then analyzes and computes its results. The results are written in a file created in ANSYS® script. Finally, MATLAB® does the the post-processing by reading the file with results, treating them and plotting the final results.

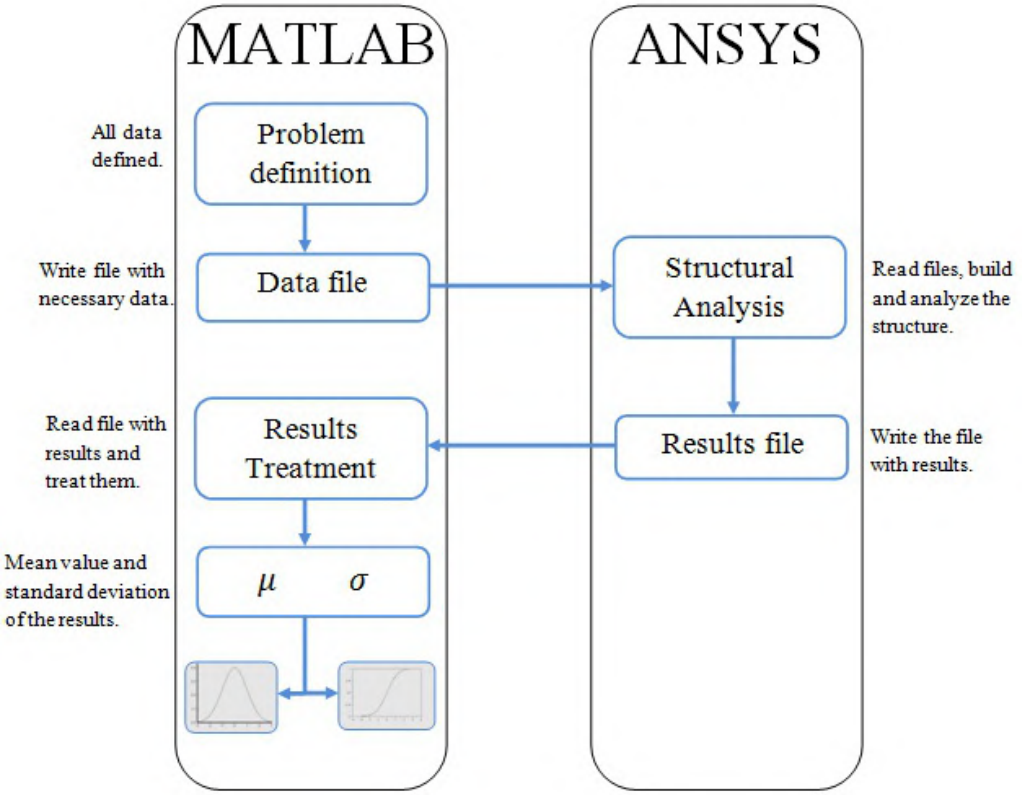

Figure 5.4: UQ methodology using FEM.

In MCS and LHS, the way the methods work is similar, the only difference is in the sampling and the number of samples required to ensure accurate results. In these methods, the phases where the sampling data is written and the structural analysis is done are repeated the number of samples defined in the beginning.

As PM does not work with samples, it implies some differences comparing with the other two methods, however it requires an extra treatment of the results after the structural analysis. As this method works with first and second order derivatives, it is necessary to apply finite differences to estimate them. However, these derivative values are slightly different from the derivatives obtained using the methodology presented in Sec. 3.4. Next, it will be presented a brief explanation about the relation between these two kinds of derivatives.

Considering a generic system, which its behavior is described by

$$Z = x^2 y, \tag{5.14}$$

where x and y are generic variables. Differentiating Eq. (5.14) yields

$$\frac{dZ}{dx} = 2xy \tag{5.15}$$

and

$$\frac{d^2Z}{dx^2} = 2y, \tag{5.16}$$

where the variables x and y correspond to mean value, μ_x and μ_y, respectively. On the other hand, using PM methodology, the variables are equal to

$$x = \mu_x (1 + q_x)$$

and

$$y = \mu_y (1 + q_y).$$

Substituting the variables in Eq.(5.14) and applying the methodology already presented, the expression for the derivatives are

$$\frac{dZ}{dx} = 2{\mu_x}^2\mu_y \tag{5.17}$$

and

$$\frac{d^2Z}{dx^2} = 2{\mu_x}^2\mu_y. \tag{5.18}$$

Comparing the expressions for the first derivative (Eq. (5.15) and Eq. (5.17)), it is possible to observe that they are different. The difference appears because, in PM, it is the perturbation term which is differentiated and not the mean value, like in common differentiation. Now, the task is to find a relation between these two kinds of derivatives to enable the use of finite differences in PM. From this comparison, it is possible to see that the difference is a constant term, equal to the mean value of the variable that was differentiated. For the second-order derivative, the process is the same but the result from the finite differences needs to be multiplied by the constant twice.

Applying these methods, it is possible to obtain the mean value and the standard deviation for the required outputs. Table 5.4 presents the results for FEM analysis with UQ methods.

Parameter	MCS		LHS		PM	
	Mean Value	Std. dev.	Mean Value	Std. dev.	Mean Value	Std. dev.
Max. Displacement [m]	-0.124	0.079	-0.124	0.080	-0.122	0.061
Max. Stress [N/m^2]	1.612×10^8	6.367×10^7	1.615×10^8	6.520×10^7	1.605×10^8	5.612×10^7
Normalized Time	781		72		1	

Table 5.4: Finite element method analysis.

Similarly to the analytical analysis, the same number of samples was used for the FEM analysis: 16,000 samples for MCS and 1,600 for LHS. Like it is referred in the analytical analysis, the computational time for PM is less than the observed in the other methods.

Analyzing the results from Tab. 5.4, it is observed that the results from MCS and LHS are very close. However, the results from PM present a little difference compared to the other two methods, as it also

appears in the analytical analysis. In this case, as PM uses finite differences, there could exist a small error associated, but it does not justify all the difference. This difference also exists in the analytical analysis and is greater for the standard deviation, which is about 30% in maximum displacement and about 13% in maximum stress. For mean values, the differences are less than 2%.

Observing the computational times, PM is the fastest method used and presents good results compared to the other methods. In this particular case of a simple clamped beam, an analytical analysis is the best option because it is faster than FEM and the structure is simple. However, for complex structures, where it is very difficult or even impossible to analytically solve the governing equations, this numerical approach using FEM is the best option and produces accurate results. As drawback, PM needs an additional effort during the implementation.

5.7 Discussion of Results

The aim of this section is to compare the UQ methods used in the two kinds of analyses. Comparing Tab. 5.2 and Tab. 5.4, it is possible to observe that the results for each method are very close, moreover they generally present good accuracy. In terms of results, it is the same to use either analytical system of equations or FEM to study the model behavior.

The biggest difference in these analyses is the computational time. In this case, the structure is simple and an analytical analysis is faster than FEM analysis. The analytical analysis takes approximately, 0.01 seconds whereas FEM takes about 2 seconds. These results were obtained using a laptop computer, with an Intel Pentium 4.0 GHz processor and 4 GB of RAM.

The introduction of ANSYS® in this kind of study allows to analyze complex structures and reach to the results more quickly because, for complex models, it is a very difficult or impossible task to solve the governing equations. Using ANSYS® with UQ methods is a good option when there are complex structures to solve, as seen in Chap. 6

After this study, it is possible to make a comparison between the values obtained from deterministic analysis and UQ analysis. The values from UQ methods suffered a decrease due to the uncertainty in the inputs. For displacement, the difference is about 14% and for maximum stress is 7%. If the uncertainty in the inputs are higher, the percentage of decrease in the output will also increase. The difference observed in the displacement is larger comparing with the difference in the maximum stress. To assess this difference, it was done one more analysis using an extreme number of samples in order to verify a possible variation of results. From this study, it was observed that the results did not vary significantly, so the difference is the displacement is high due to the magnitude order and small value of the variable.

Computing the results, it is possible to build the PDF (Fig. 5.5) and the CDF (Fig. 5.6) for the outputs. These graphs allow to obtain some important data about the structure and its behavior with uncertainties in the input variables. All the graphs show the results obtained for the three different methods.

Observing the maximum displacement PDF distributions, it is possible to see that all the distributions present a low possibility of the displacement to take positive values. This situation happens since the

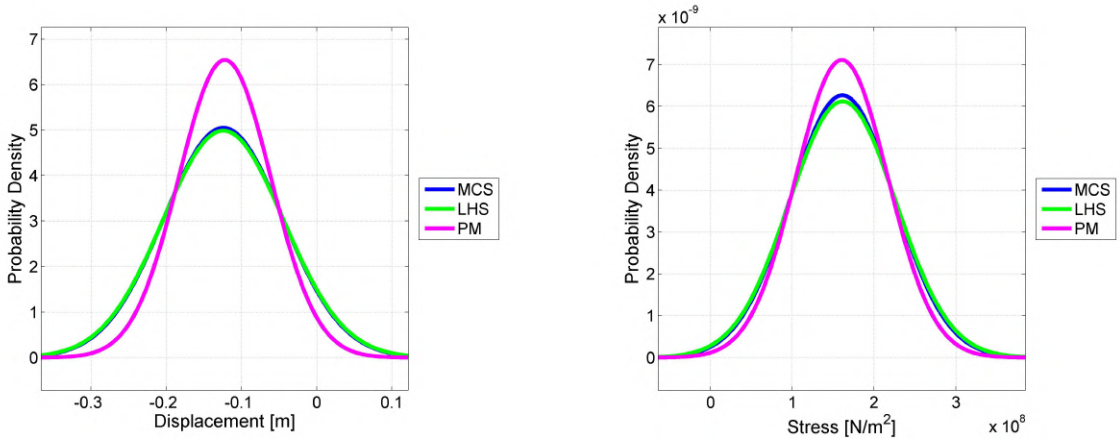

(a) Maximum displacement (b) Maximum stress

Figure 5.5: Probability density functions of outputs.

standard deviation in input variables is a little bit higher. As this case is a academic study and it is a study to validate the use of FEM, the results will be accepted. If the standard deviation of input variables are lower, the standard deviation of the displacement will be also lower. Analyzing the distributions, MCS and LHS have similar results of mean value and standard deviation. PM has accurate results but they are not as close to the other methods, like it was mentioned in the previous section.

For maximum stress, the situation is the same about higher standard deviation in input variables. This situation gives a probability of the maximum stress on the clamped zone to be zero or to change from tension to compression. Once again, comparing the results from MCS and LHS, they are very close, but PM has a difference compared to the other methods. However, in this case, the difference between them is lower than the difference observed for the displacement. This happens because the order of magnitude of the results is significantly different. It is also possible to verify graphically that, even for extreme situations, the structure does not fail because the maximum stress does not exceed the material ultimate tensile strength.

CDF is an important tool in terms of structures project because it allows to know the system response for a determined reliability.

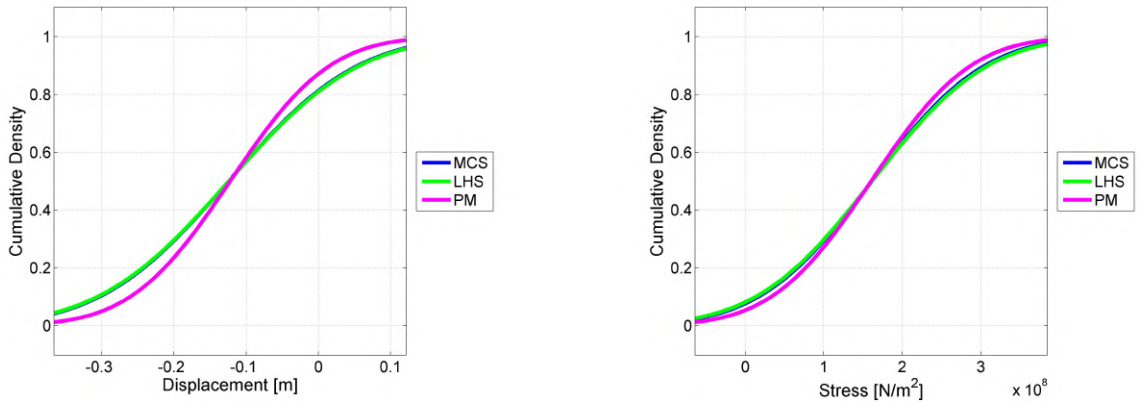

(a) Maximum displacement (b) Maximum stress

Figure 5.6: Cumulative density functions of outputs.

Like it is happened in PDF graphs, here it is also visible a little difference between PM and the other two methods, being the explanation for this the same mentioned above. A reliability of 50% corresponds to the mean value obtained. If a designer wants a different value of reliability, this graph is very important because one can know the output value for a determined reliability or the reliability for a determined input.

With a determined value of reliability, the designer could have some possible combinations for the input parameters. As an example, considering that, for a given project, it is required that the maximum displacement has 70% of reliability, then this value of reliability implies that the maximum displacement is equal to -0.05 [m]. From the UQ methods results it is possible to select some scenarios, where the objective is satisfied, as summarized in Tab. 5.5

Scenario	#1	#2	#3	#4	#5
Young Modulus [GPa]	71.74	77.85	78.38	74.96	83.8
Section length [m]	0.011	0.009	0.010	0.010	0.009
Beam length [m]	0.91	0.83	0.86	0.83	0.88
Distributed load [N/m^2]	44.6	42.7	45.0	58.8	43.7

Table 5.5: Different design scenarios for a 70% of reliability for maximum displacement.

From the Tab. 5.5, some different design scenarios can be seen that result in the same output. The differences between the results are not very high, but some of them suffered more variations in terms of the mean values defined at the beginning. For example, the Young modulus and the distributed load are the properties which suffer more fluctuations. With these results it is intended to show the influence of the uncertainty in the input parameters.

In conclusion, the results obtained for all the UQ methods studied are very close, which permits to prove that the introduction of FEM software (ANSYS®) was successful and demonstrated to be an excellent tool to study complicated structures with UQ methods.

Chapter 6

Wing Structure

The aim of this chapter is to analyze a wing structure using all the knowledge acquired in the previous chapters. For this analysis, all methods implemented are used. It starts with wing model construction in finite elements and the choice of the wing characteristics. To select the baseline load to be applied to the structure, a wing aerodynamic study is performed. Then, a deterministic analysis and an analysis using UQ methods are done. Finally, the results are compared and discussed.

6.1 Model Description

The structure selected for the final analysis is an airplane wing. The model used is as close to the reality as possible, in terms of geometry, loads and material properties.

The wing structure was built in ANSYS®, the same software that was used to build the wing spar. The model in study is a half wing, clamped at the root (Fig. 6.1). This structure has some simplifications compared to a real wing, like being composed by a wing box and a shell only. These simplifications result from a research about wing structures (Sec. 1.4.1). In the model, there are two kinds of elements, for the wing box and the shell SOLID45 [ANSYS, Inc., 2010] and SHELL63 [ANSYS, Inc., 2010] elements were selected, respectively.

Table 6.1 exhibits some of the wing geometric properties relevant to this test case.

Parameter	Value [m]
Span	5
Root Chord	1
Tip Chord	0.6
Shell thickness	2.5×10^{-3}
Wing Box thickness	1×10^{-3}

Table 6.1: Geometric properties.

The model has a NACA 0018 airfoil. Also important in the model definition is the material selection and its mechanical properties. Aluminium Al-7050-T7651 is used in the whole structure, the same

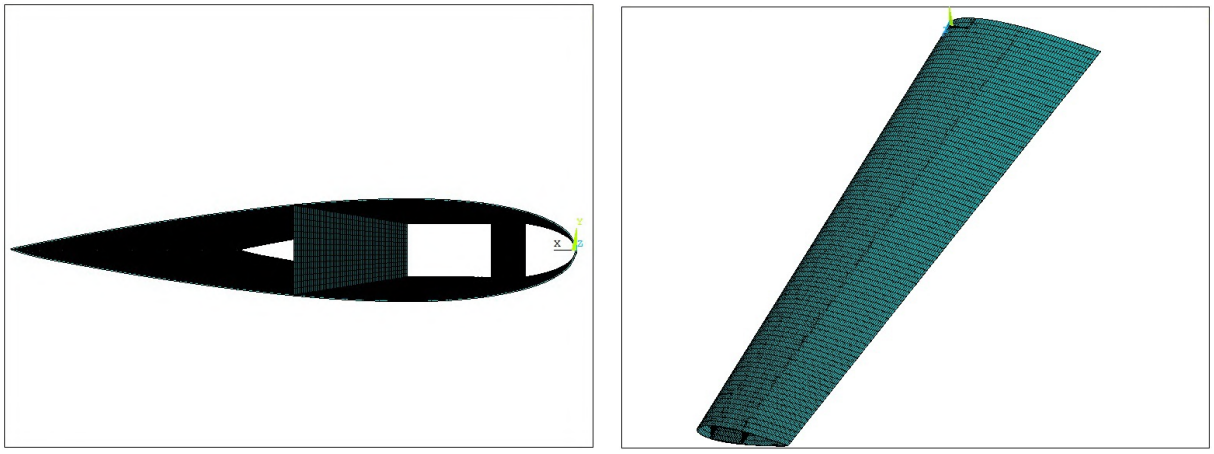

(a) Internal view (b) External view

Figure 6.1: Different views of the model.

aeronautical material used for the wing spar analysis, whose properties are presented in Tab. 5.1.

After defining the geometric properties, it is necessary to define the aerodynamic conditions for the study. This analysis was done in XFLR5® [XFLR5, 2011], which is a software used for aerodynamic analyses based on panel method. For the aerodynamic study, it was essential to define some aerodynamic characteristics, presented in Tab. 6.2.

Parameter	Value
Mach number	0.3
Velocity	103 m/s
Angle of Attack	5°
Air density	1.225 kg/m^3

Table 6.2: Aerodynamic properties.

It is also important to refer that the analysis was done considering an inviscid fluid. With these properties, it was possible to obtain the aerodynamic response of the wing. Figure 6.2 illustrates the response in terms of lift distribution and downwash velocity, generated by the wing. From the aerodynamic study, other relevant data was computed, such as the distribution of lift coefficient, the distribution of total drag coefficient and the pressure coefficient along the wing. This data is illustrated in Fig. 6.3.

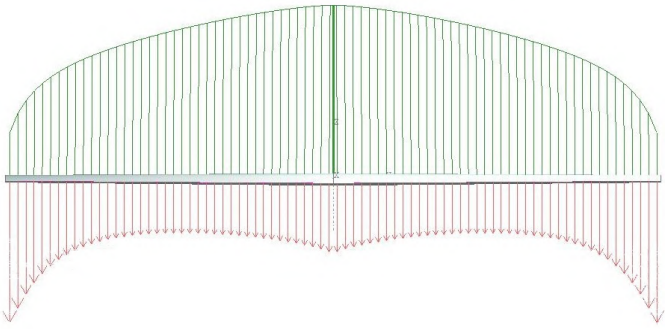

Figure 6.2: Lift and downwash distribution.

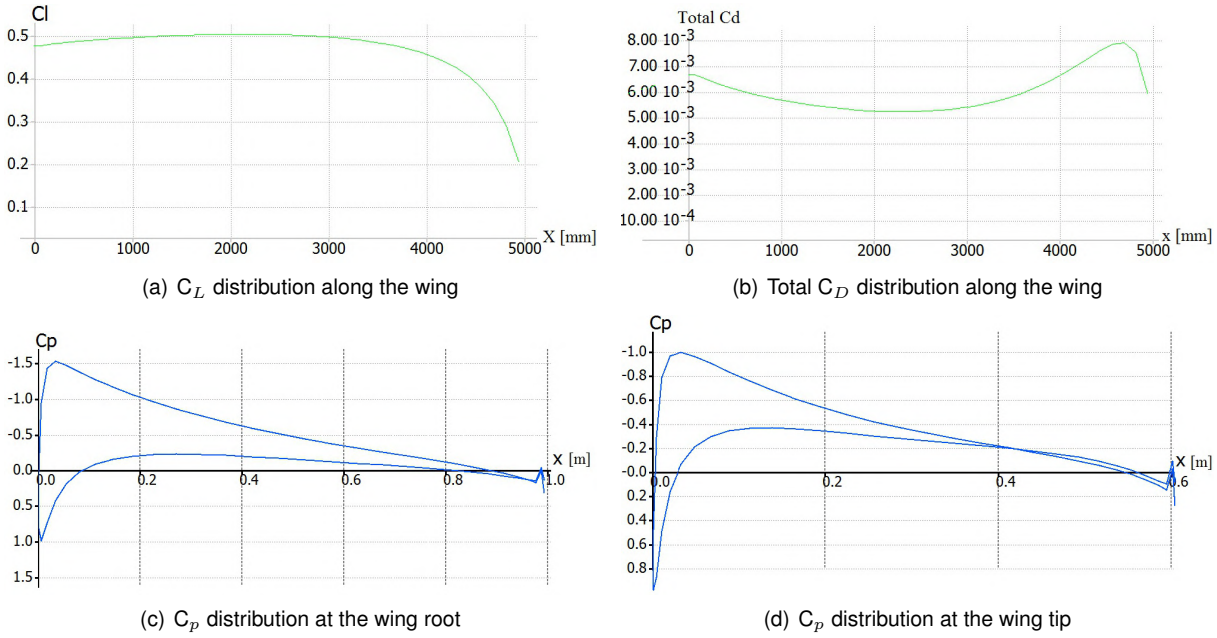

(a) C_L distribution along the wing

(b) Total C_D distribution along the wing

(c) C_p distribution at the wing root

(d) C_p distribution at the wing tip

Figure 6.3: Aerodynamic characteristics.

The aerodynamic analysis is the last study necessary to define the model completely. Now, all the variables are defined and it is possible to finish the structure model. The last data needed is the distributed load to be applied on the wing surface. The computation of this load results from the process explained in Fig. 6.4, which handles the fluid-structure interface.

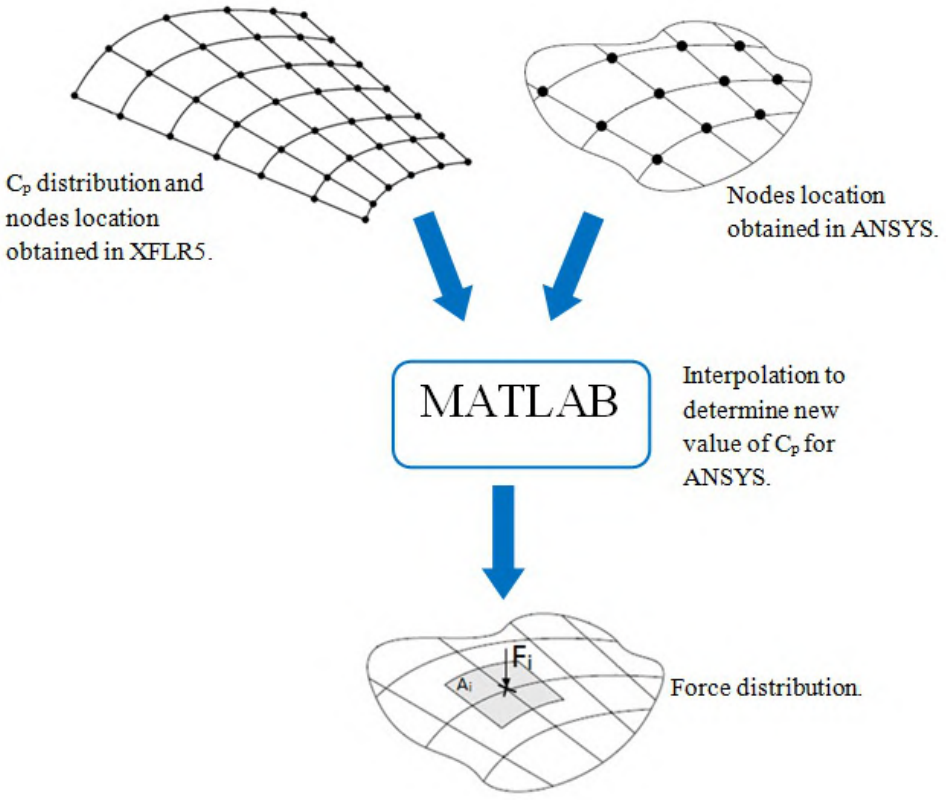

Figure 6.4: Process to obtain the pressure distribution.

From the wing analysis in XFLR5®, some relevant data is obtained, including the distribution of the pressure coefficient (C_p) on wing surfaces. Both in XFLR5® and ANSYS®, the structure is discretized in many elements, but the computacional mesh is different between the two softwares. Consequently, it is necessary to do an interpolation between the results from XFLR5® to obtain the results for the nodes location in the ANSYS® mesh. For the interpolation, MATLAB® is used, more precisely, the *griddata* function, which is a function for 2-D interpolation. After the interpolation, C_{p_i} for each node is multiplied by A_i to obtain the pressure for that node. Finally, as the pressure obtained is a normalized pressure, it is necessary to multiply each node pressure by a determined force to obtain the force for each node, F_i.

Figure 6.5 shows the model that will be analyzed both deterministically and using the UQ methods. The picture illustrates the structure, the load distribution and the wing constraints at the root.

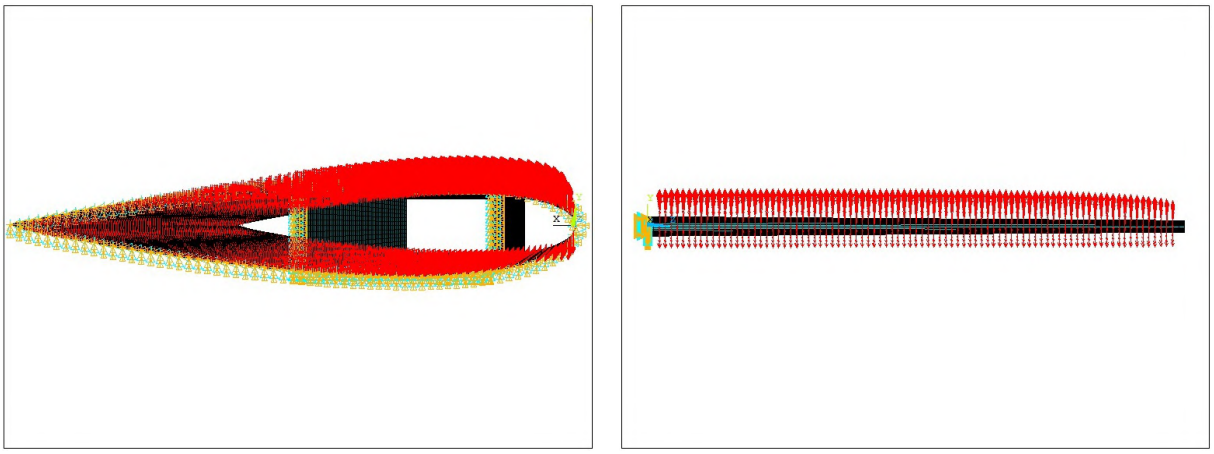

(a) Internal view (b) External view

Figure 6.5: Load distribution.

6.2 FEM Convergence Study

Before starting the analyses with UQ methods, it is essential to do a convergence study in terms of the number of elements. This study is very important to determine the number of elements required to reach accurate results. In this convergence study, the computational effort is another parameter that will be taken into account. It will be observed the maximum displacement, the maximum stress, the minimum stress and the maximum equivalent stress, using Von Mises criterion. Figure 6.6 exhibits the convergence study for each of these outputs.

Observing the results from the convergence study and comparing them to the computational effort, the case selected for future analyses is the model with nearly 20,000 elements. This case presents a good accuracy in the results at a reasonable computational effort. This is very important for this kind of study, in particular for MCS because it needs a large number of samples to ensure the convergence. By increasing the number of elements in the structure beyond 20,000, the computational time necessary to obtain the results will also increase but the difference in the output results are not significant.

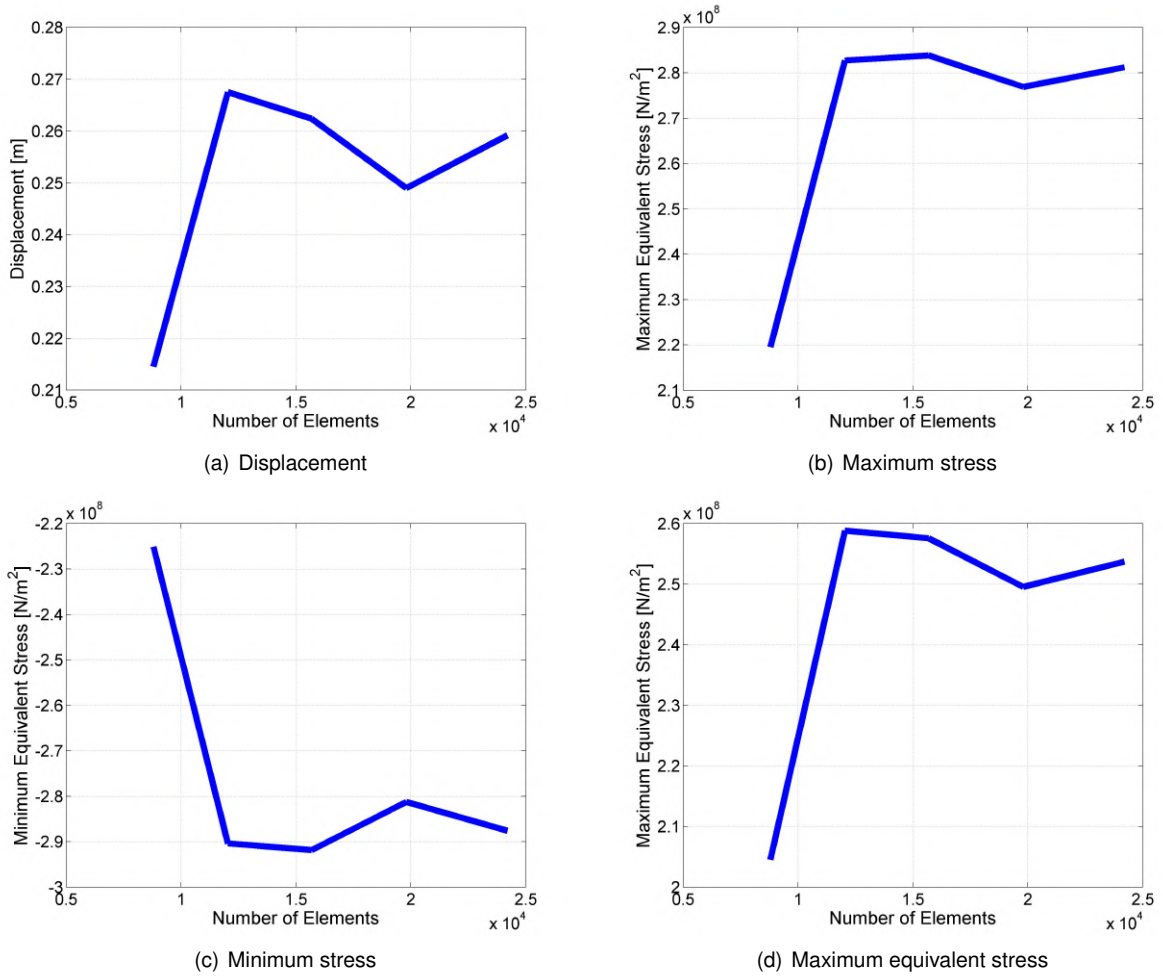

(a) Displacement

(b) Maximum stress

(c) Minimum stress

(d) Maximum equivalent stress

Figure 6.6: Convergence study in terms of the number of elements.

6.3 Deterministic Numerical Analysis

Finally, it is possible to do the deterministic analysis and obtain the results for the desired accuracy. Appendix A presents the ANSYS ® script for the wing model analysis. Table. 6.3 exhibits the deterministic results for the outputs in study.

Parameter	Value
Maximum Displacement [m]	0.249
Maximum Stress [N/m^2]	2.768$\times 10^8$
Minimum Stress [N/m^2]	-2.812$\times 10^8$
Maximum Equivalent Stress [N/m^2]	2.495$\times 10^8$

Table 6.3: Deterministic response of the structure.

Using the FEM software, it is possible to obtain the illustrations for the outputs. Figure 6.7 presents the displacement caused by the load and the stress distribution in the wing, more precisely the tension and the compression at the wing root. The last illustration presents the maximum equivalent stress using the Von Mises criterion. From the pictures, it is possible to observe that the maximum displacement is on

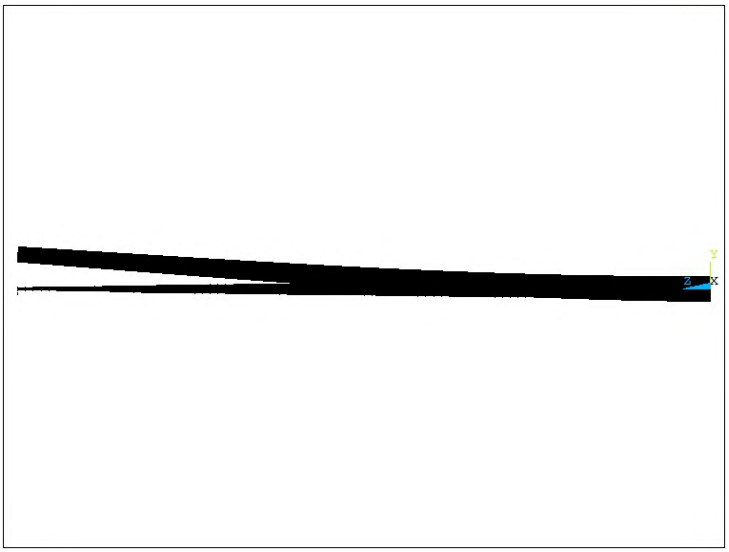

(a) Displacement

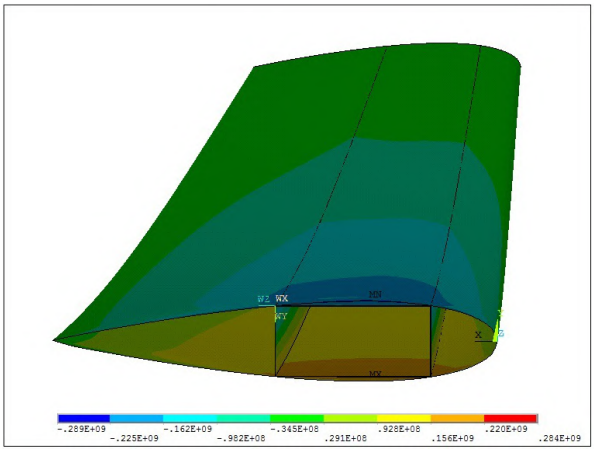

(b) Stress distribution

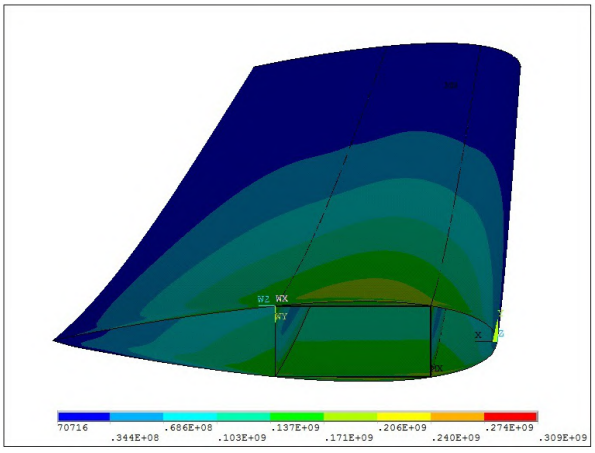

(c) Von Mises equivalent stress distribution

Figure 6.7: Deterministic output results.

the wing extremity and the maximum and minimum stress is on the wing root. Maximum stress (tension) is observed on the bottom face and the minimum (compression) is in the top face of the wing. It is important to mention that the load included both the applied aerodynamic load and the structure weight.

Analyzing the deterministic results, it is possible to observe that the structure did not suffer damage for this load because the maximum stress observed on the wing is less than the ultimate tensile strength and tensile yield strength.

6.4 Stochastic Numerical Analysis

The model in study has eight uncertainty inputs, belonging to different kind of variables such as dimensions, material properties and loads. It is considered that each variable from these groups has 3% of uncertainty. This value was chosen because in the aeronautical industry the allowable tolerances need to be extremely small. The aeronautical field works with high levels of safety, consequently the studies in this area need to know all variables and how they influence the structure response.

This structure is an academic study so it has some simplifications. Each variable has the same value of uncertainty probability and the probability distribution used is the normal distribution. In reality, there are some variables that can be expressed with different kinds of distributions. Furthermore, the percentage of uncertainty can be different for each variable. The choice of the probability distribution and the percentage of uncertainty is a difficult task because each variable has its characteristics which influence significantly the behavior of the structure.

In the wing analysis, there are three main groups of variables, the dimensions group, the mechanical properties group and the loads group.

The group of dimensions is constituted by the wing span (L), the root chord (c_r), the shell thickness (t_s), the flange thickness (t_f) and the web thickness (t_w). The following means, standard deviations and covariances were assumed:

$$\{\mu_L\} = \{5\}m \quad , \quad \{\sigma_L\} = \{0.15\}m \quad , \quad \{\gamma_L\} = \{2.25 \times 10^{-2}\},$$

$$\{\mu_{c_r}\} = \{1\}m \quad , \quad \{\sigma_{c_r}\} = \{0.03\}m \quad , \quad \{\gamma_{c_r}\} = \{9 \times 10^{-4}\},$$

$$\{\mu_{t_s}\} = \{2.5 \times 10^{-3}\}m \quad , \quad \{\sigma_{t_s}\} = \{7.5 \times 10^{-5}\}m \quad , \quad \{\gamma_{t_s}\} = \{5.625 \times 10^{-9}\},$$

$$\{\mu_{t_f}\} = \{1 \times 10^{-3}\}m \quad , \quad \{\sigma_{t_f}\} = \{3 \times 10^{-5}\}m \quad , \quad \{\gamma_{t_f}\} = \{9 \times 10^{-10}\},$$

$$\{\mu_{t_w}\} = \{1 \times 10^{-3}\}m \quad , \quad \{\sigma_{t_w}\} = \{3 \times 10^{-5}\}m \quad \text{and} \quad \{\gamma_{t_w}\} = \{9 \times 10^{-10}\}.$$

The material properties group is composed by the Young modulus (E) and the Poison coefficient (Poi). In this case, the material selected is equal for wing box and shell, having the following properties:

$$\{\mu_E\} = \{71.7 \times 10^9\}Pa \quad , \quad \{\sigma_E\} = \{2.15 \times 10^9\}Pa \quad , \quad \{\gamma_E\} = \{4.62 \times 10^{18}\},$$

$$\{\mu_{Poi}\} = \{0.33\} \quad , \quad \{\sigma_{Poi}\} = \{9.9 \times 10^{-3}\} \quad \text{and} \quad \{\gamma_{Poi}\} = \{9.8 \times 10^{-5}\}.$$

Finally, the loads group has only one variable, which is the pressure (Q) to apply on the wing surfaces. This load is applied respecting the process explained above and its properties were assumed to be

$$\{\mu_Q\} = \{-10 \times 10^3\}N \quad , \quad \{\sigma_Q\} = \{300\}N \quad \text{and} \quad \{\gamma_Q\} = \{9 \times 10^4\}.$$

Figure 6.8 shows the PDF and CDF graphs for some of the input variables. They allow to observe the variation in terms of the probability of the input parameter.

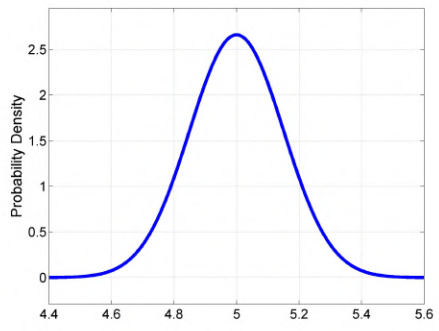

(a) PDF for wing length

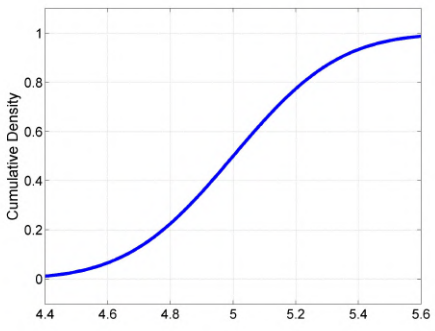

(b) CDF for wing length

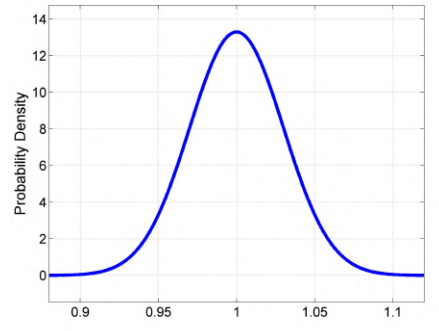

(c) PDF for root chord

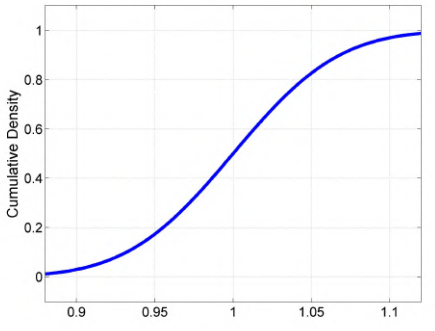

(d) CDF for root chord

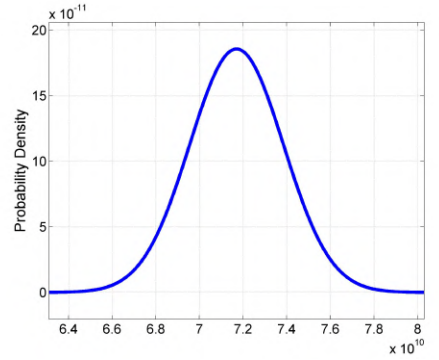

(e) PDF for Young modulus

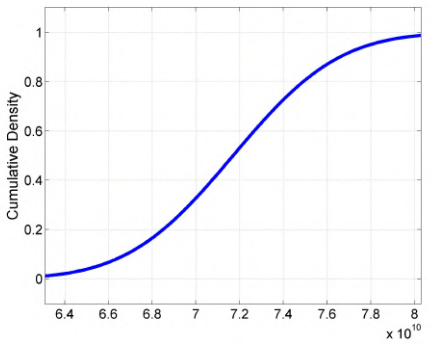

(f) CDF for Young modulus

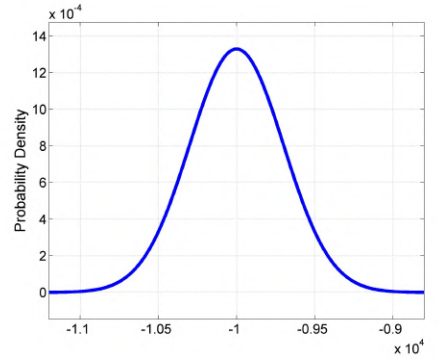

(g) PDF for pressure

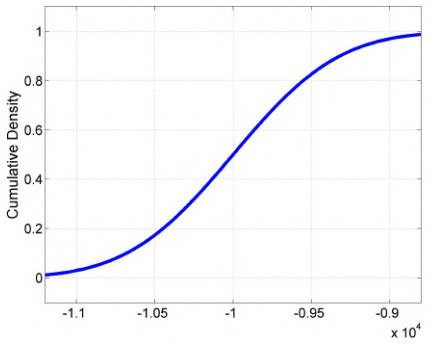

(h) CDF for pressure

Figure 6.8: PDF and CDF for some input variables.

6.5 Discussion of Results

The aim of this section is to present and discuss the results obtained from the different wing structure analyses.

As this structure is more complex than the wing spar, a convergence study for the number of samples in the sampling methods MCS and LHS is needed. Due to the computational effort of this kind of study, this will not be done because it needs a lot of tests to reach the number of samples required for good results. To deal with this situation, the selection of samples needs to be a trade-off between computational effort and results accuracy. With this in mind, 21,000 samples will be used for MCS and 2,500 samples for LHS.

The scripts for the methods MCS, LHS and PM implemented in MATLAB® are in appendix B, C and D, respectively.

Table. 6.4 presents the results for MCS, LHS and PM using the conditions presented before.

Parameter	MCS		LHS		PM	
	Mean Value	Std. dev.	Mean Value	Std. dev.	Mean Value	Std. dev.
Displacement [m]	0.253	0.037	0.252	0.034	0.252	0.033
Max. Stress [N/m^2]	2.780$\times 10^8$	1.830$\times 10^7$	2.776$\times 10^8$	1.888$\times 10^7$	2.776$\times 10^8$	1.848$\times 10^7$
Min. Stress [N/m^2]	-2.841$\times 10^8$	1.793$\times 10^7$	-2.830$\times 10^8$	1.869$\times 10^7$	-2.830$\times 10^8$	1.830$\times 10^7$
Max. Equiv. Stress [N/m^2]	2.525$\times 10^8$	1.595$\times 10^7$	2.502$\times 10^8$	1.655$\times 10^7$	2.503$\times 10^8$	1.645$\times 10^7$

Table 6.4: Finite element method analysis.

Analyzing Tab. 6.4, it is possible to conclude that both methods have very close results between them. Comparing the accuracy of the results for the wing structure analysis and the wing spar analysis, in this case the results are closer than the results in wing spar analysis. In general, the results are very close, but MCS does not present the same accuracy of the other two methods. However, the difference in MCS is not significant and the results can be considered for the study. This difference could be reduced by doing, again, the analysis with more samples.

Comparing the deterministic values and the results with uncertainty, it is observable that the deterministic values suffered an increment, which is motivated by the uncertainty in the input parameters. For the maximum displacement, it increased less than 1.5%, and for the maximum stress, minimum stress and maximum equivalent stress, it increased less than 1%. In this case, as the inputs have a small value of uncertainty, its influence in final results is also small. However, for higher values of uncertainties and more variables with uncertainty, it is expected that the difference in the output results grow.

With mean values and standard deviations from the different UQ methods, it is possible to plot their respective PDF and CDF. These graphs allow to verify the proximity between the results. The PDF graph shows the normal distribution of the results and CDF illustrates the response of the system in terms of reliability.

Figure 6.9 presents the PDF graphs for the output results: maximum displacement, maximum stress, minimum stress and maximum equivalent stress. Comparing the PDF for each methods, it is possible to verify that the results from the different methods are very close. As LHS and PM results are very close,

the LHS graph line is not possible to observe because it is under the PM graph line.

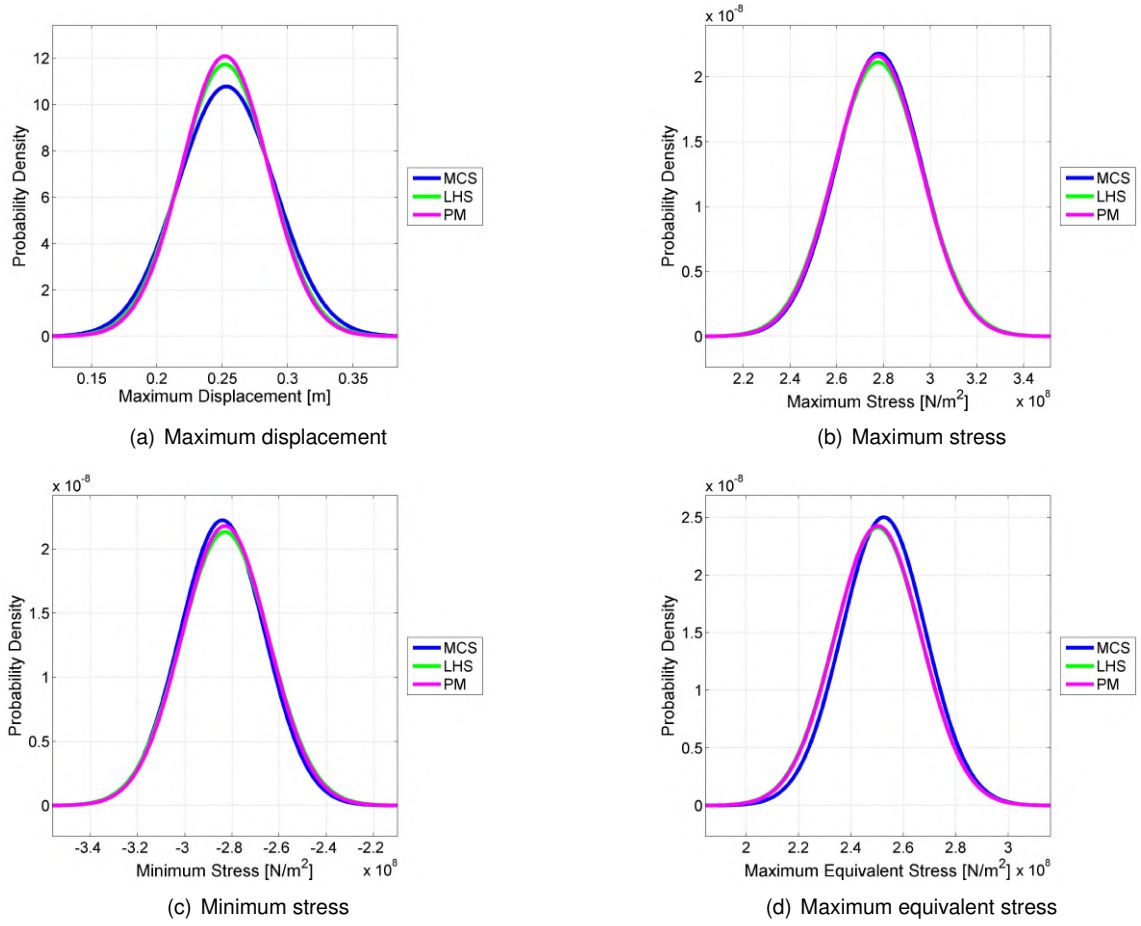

(a) Maximum displacement

(b) Maximum stress

(c) Minimum stress

(d) Maximum equivalent stress

Figure 6.9: Probability density functions of outputs.

Figure 6.10 shows the CDF graphs for each output. With them, it is also possible to see that the results are very close for each output. The CDF is a strong tool because it enables to obtain output results in terms of reliability. Mean values obtained from different methods, correspond to 50% of reliability. Designers use these graphics to collect important informations about structure behavior and use them to improve the structure. Observing these graphs, it is possible to conclude that the system resists without damage for extreme conditions. In terms of material maximum stress allowable, the structure in extreme situations presents values lower than the material maximums, which means that for situations with a reduced probability to happen, the structure maintains its performance without damages. This kind of analysis is very important because it allows to observe the response of many parameters for the extremes of the system.

Using the CDF graph, it is possible for the designer to define one value of reliability and observe the different scenarios which satisfy the premise of the project. For example, considering that the designer selects the maximum stress as the parameter of reference and determine that the reliability of the maximum stress is 70%. This value of reliability implies that the maximum stress is equal to $2.95 \times 10^8 [N/m^2]$, but for this value there are some different scenarios which can occur. These scenarios occur due to the uncertainty in the input parameters and it is possible to observe that the input parameters suffer varia-

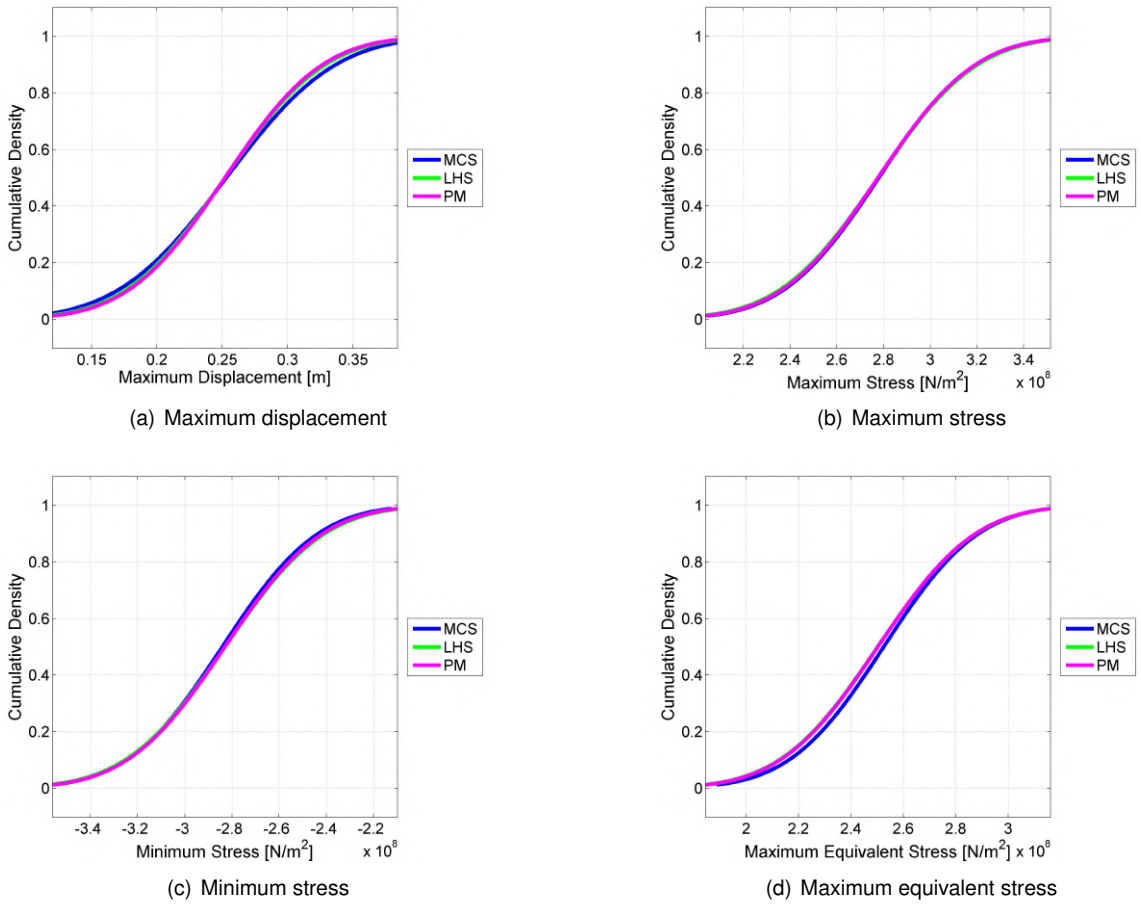

(a) Maximum displacement

(b) Maximum stress

(c) Minimum stress

(d) Maximum equivalent stress

Figure 6.10: Cumulative density functions of outputs.

tions in relation to the design values. Table 6.5 presents some scenarios for the design which satisfy the reliability for the maximum stress.

Scenario	Designer	#1	#2	#3	#4	#5
Wing span [m]	5	5.07	4.91	4.94	4.87	5.15
Root chord [m]	1	0.96	0.95	0.97	0.94	0.99
Shell thickness [m]	2.5×10^{-3}	2.6×10^{-3}	2.5×10^{-3}	2.4×10^{-3}	2.6×10^{-3}	2.4×10^{-3}
Flange thickness [m]	1×10^{-3}	0.95×10^{-3}	0.97×10^{-3}	1×10^{-3}	0.97×10^{-3}	0.99×10^{-3}
Web thickness [m]	1×10^{-3}	1×10^{-3}	1×10^{-3}	1×10^{-3}	0.98×10^{-3}	0.97×10^{-3}
Young Modulus [GPa]	71.7	70.47	72.37	70.35	70.76	72.97
Poisson coefficient	0.33	0.32	0.33	0.33	0.32	0.34
Pressure [kN]	-10	-10.02	-9.99	-9.99	-9.98	-9-98

Table 6.5: Different design scenarios for a 70% of reliability for maximum stress.

Analyzing all the results obtained, it can be concluded that all the methods implemented are working correctly and the results reached show an important accuracy.

After all analyses, it was verified that the use the FEM with UQ methods is a strong tool for study complex structures. This methodology can be applied to different kind of problems using FEM since its

implementation is generic.

6.6 Comparison of Computational Cost

As the wing structure has some complexity, it is convenient to do an analysis about the computational cost. In this case, it is used the software ANSYS® to deterministically analyze the structure and MATLAB® to compute the UQ results.

Parameter	MCS	LHS	PM
Normalized Time	598	58	1

Table 6.6: Comparison of computational cost.

Observing the computational time, MCS presents the largest computational time comparing with the other methods. The difference between the methods, in this case, is smaller than the difference exhibited in the wing spar analysis because the wing spar has only four uncertainty variables while the wing structure has eight variables. Although the normalized time is less comparing with the wing spar, the real computational time is many times more. In the wing spar, one simple analysis takes about two seconds, while in the wing structure, this analysis takes approximately sixteen seconds. These results were obtained using a laptop computer, with an Intel Pentium 4.0 GHz processor and 4 GB of RAM.

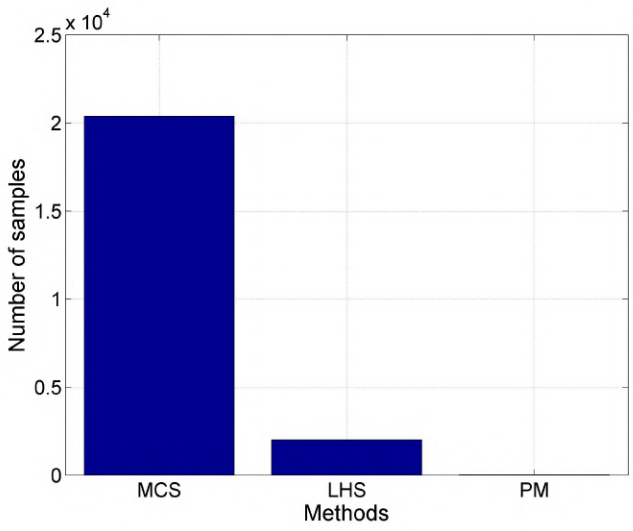

Figure 6.11: Comparison of computational cost.

Figure 6.11 shows a comparison in terms of computational effort between the three different methods. In this study, the time of a deterministic analysis is considered as reference of comparison. Normalized time, relative to the deterministic time, is the term of comparison that will be used in this study. It will be obtained the time for each analysis, in terms of the number of deterministic analyses. From the figure, it is observable that for MCS and LHS the number of times necessary are very close to the number of samples defined previously. The value is not exactly the same because they have some more samples. For example, in the script for MCS there are other tasks to do, like the sampling and the treatment of the

final results, which take some additional time. The time taken in PM corresponds, approximately, to 34 times the deterministic analysis.

From this study, it is possible to conclude, one more time, that PM has a high accuracy, but the most important issue is the computational time. In this case, comparing the time required to run the PM, it is about 600 times less then MCS and 60 times less than LHS. These results express the efficiency of PM to study complex problems with UQ. Again, this benefit comes at the expense of a more complex implementation compared to any of the sampling methods MCS and LHS.

Chapter 7

Conclusions

7.1 Achievements

The aim of this thesis was to develop knowledge in the field of Uncertainty Quantification (UQ) applied to aircraft structures, more precisely, wing structural components.

UQ is a subject in constant development, so the literature review was very important to acquire basic knowledge in this field. The review was conducted throughout the work to find new studies and reinforce the knowledge. This subject is very important in many fields, in particular to the structural aircraft industry, where it can be used in the preliminary stages of design.

From the many different methods available to quantify uncertainty, MCS, LHS and PM were selected in this study. The implementation of the methodologies was the step that took more time during the realization of this thesis. With the methodologies implemented, some tests were selected to apply them and analyze their performance. First, they were applied to a structure already studied, where the objective was to validate the methodologies using results reported in the literature. Second, with the methodologies validated, they were applied to a simple structure, which was analyzed both analytically and using a FEM software. The objective of this study was to validate the use of FEM with UQ methods. After that, a complex structure was analyzed, in this case a wing structure. This structure had some structural simplifications and a total of eight input variables with uncertainties. This wing structure did not have much complexity because the higher the structure complexity, the largest computational effort would become, and it would exceed the computational resources available.

The effort in implementation was not the same for all methods MCS and LHS were the easier, since they work with samples. In contrast, PM had a more complicated implementation because it implies the estimation of first and second derivatives.

Finally, from the results obtained, it was possible to take some important conclusions about the application of UQ, specially from the last example studied. For all methods, the results presented were very close between them, which meant that they were working correctly. As the structure analysis was done in a laptop computer, the structure complexity was conditioned in terms of simulation time and this was an important factor. From all the methods implemented, PM was the fastest method and MCS was

the slowest. MCS took much time since it needed high number of samples to reach a converged result. Comparing the deterministic and the stochastic results, it was possible to show that the uncertainty in inputs influences the outputs, being their average values increased motivated by the uncertainty.

The results obtained in the last example evidence that the thesis objective was accomplished. The methods implemented could be used to design wing structures with uncertainty in inputs and, if a workstation with strong computational capabilities is used, it will be possible to apply these methodologies to design structures more complex, closer to the reality.

Overall, the knowledge acquired in the field of UQ with this thesis can be used in future structural design projects, leading to better, more robust and reliable solutions.

7.2 Future Work

UQ is in constant development and more studies in this field are expected in the future. From all the methods implemented, PM is the one which could be used in the future because it exhibits high accuracy and low computational time. At the beginning, it could be used to study structures more complex or in a system with more input variables with uncertainty. Different kinds of distribution could be introduced in the same study, or even variables whose distribution is not known.

The UQ methodology could also be used in different fields of aeronautic, like aerodynamics, propulsion and dynamics, or any other that could be analyzed in FEM software.

Allied with the evolution of computational capabilities, new uncertainty quantification methods could be developed which need less computational time and allow to analyze more complex structures.

Other future application of the methodology implemented is in the optimization field, more precisely RDO or RBDO. This approach is a kind of optimization in which the objective is to obtain a structure with low probability of failure. RDO is based in maximization of the performance, reducing the sensitivity of the system, more exactly reducing the standard deviation. On the other hand, RBDO works to meet a reliability target. As these methods have different ways to work, the implementation of these two kinds in the same analysis is a development to consider. Other interesting development is to apply this kind of optimization to Multidisciplinary Design Optimization (MDO).

Concluding, the UQ methodologies implemented are expected to be used in future studies. If possible, they can become the basis to build a robust or a reliability-based design optimization tool.

Bibliography

M. Allen and K. Maute. Reliability-based shape optimization of structures undergoing fluid–structure interaction phenomena. *Computer Methods in Applied Mechanics and Engineering*, 194:3472–3495, 2005.

K. F. Alvin, W. L. Oberkampf, K. V. Diegert, and B. M. Rutherford. Uncertainty Quantification in Computational Structural Dynamics: A New Paradigm for Model Validation. In *16th International Modal Analysis Conference*, pages 1191–1197, Santa Barbara USA, 1999. American Institute of Aeronautics and Astronautics.

ANSYS, Inc. ANSYS Mechanical. `www.ansys.com`, 2010. Release 12.0.

Aerospace Specification Metals ASM. Aluminum 7050-T7651 - Properties. `http://asm.matweb.com/search/SpecificMaterial.asp?bassnum=MA7050T765`, Accessed in November 2012.

H. Bae. *Uncertainty Quantification and Optimization of Structural Reponse Using Evidence Theory*. PhD thesis, Wright State University, November 2004.

L. Baghdasaryan, W. Chen, T. Buranathiti, and J. Cao. Model Validation via Uncertainty Propagation Using Response Surface Models. *ASME Conference Proceedings*, 2002(36223):981–992, 2002.

A. Baker, S. Dutton, and D. Kelly. *Composite Materials for Aircraft Structures*. American Institute of Aeronautics and Astronautics, Inc, 2nd edition, 2004.

F. P. Beer, E. R. Johnston, and J. T. DeWolf. *Mechanics of Materials*. 4th edition, 2006.

P. T. Biltgen. Uncertainty Quantification for Capability-Based Systems-of-Systems Design. In *26th Congress of International Council of the Aeronautical Sciences*, Anchorage, Alaska, USA, September 2008.

J. B. Borradaile. Future Aluminium Technologies and Their Application to Aircraft Structures. In *RTO Meeting Proceedings 25*, 2000.

O. Cronvall. *Structural lifetime, reliability and risk analysis approaches for power plant components and systems*. VVT 2011, 2007.

J. Díaz, S. Hernández, L. E. Romera, and A. Baldomir. Uncertainty Quantification and Reliability Analysis Methods applied to aircraft structures. In *27th Congress of International Council of the Aeronautical Sciences*, Nice, France, September 2010.

D. M. Frangopol and Kurt Maute. Life-cycle reliability-based optimization of civil and aerospace structures. *Computers & Structures*, 81(7):397–410, 2003.

J. M. Hammersley and D. C. Handscomb. *Monte Carlo Methods*. Halsted Press, 1975.

F. M. Hemez and S. W. Doebling. Model Validation and Uncertainty Quantification. In *Proceeding of 19^{th} International Modal Analysis Conference*, Kissimmee, Florida, February 5-8 2001.

V. A. R. Henriques. Titanium Production for Aerospace Applications. *Journal of Aerospace Technology and Management*, 1(1):7–17, 2009.

D. Higdon, R. Klein, M. Anderson, M. Berliner, C. Covey, O.r Ghattas, C. Graziani, S. Habib, M. Saeger, J. Sefcik, P. Stark, and J. Stewart. Uncertainty Quantification and Error Analysis. In *Workshop on Scientific Challenges in National Security: the Role of Computing at the Extreme Scale*, pages 121–142, October 2009.

M. H. Holmes. *Introduction to Perturbation Methods*. Texts in Applied Mathematics Series. Springer, 1998.

A. Keese. A Review of Recent Developments in the Numerical Solution of Stochastic Partial Differential Equations (Stochastic Finite Elements). Technical report, Technical University Braunschweig, 2003.

Y. Lee and D. Hwang. A Study on the Techniques of Estimating the Probability of Failure. *Journal of the Chungcheong Mathematical Society*, 21(4):573–583, December 2008.

C. Lemieux and P. L'Ecuyer. On the Use of Quasi-Monte Carlo Methods in Computational Finance, booktitle=Computational Science — ICCS 2001. volume 2073 of *Lecture Notes in Computer Science*, pages 607–616. Springer Berlin Heidelberg, 2001.

R. J. LeVeque. Finite Difference Methods for Differential Equations. September 2005.

L. J. Lucas, H. Owhadi, and M. Ortiz. Rigorous verification, validation, uncertainty quantification and certification through concentration-of-measure inequalities. *Computer Methods in Applied Mechanics and Engineering - COMPUT METHOD APPL MECH ENG*, 197(51):4591–4609, 2008.

U. Maheshwaraa, C. C. Seepersad, and D. Bourell. Topology design and freeform fabrication of deployable structures with lattice skins. *Rapid Prototyping Journal*, 17:5–16, 2011.

L. Mathelin, M. Y. Hussaini, and T. A. Zang. Stochastic approaches to Uncertainty Quantification in CFD simulations. *Numerical Algorithms*, 38:209–236, 2005.

M. D. McKay, R. J. Beckman, and W. J. Conover. A Comparison of Three Methods for Selecting Values of Input Variables in the Analysis of Output from a Computer Code. *Technometrics*, 21(2):239–245, 1979.

T. H. Megson. *Aircraft Structures for Engineering Students*. Butterworth-Heinemann, 4^{th} edition, 2007.

B. Murteira, C. S. Ribeiro, J. Andrade e Silva, and C. Pimenta. *Introdução à Estatística*. 2^{th} edition, 2007.

A. M. J. Olsson and G. E. Sandberg. Latin Hypercube Sampling for Stochastic Finite Element Analysis. *Journal of Engineering Mechanics*, 128(1):121–125, 2002.

A. B. Owen. Latin Supercube Sampling for Very High Dimensional Simulations. *ACM Transactions on Modeling and Computer Simulation (TOMACS)*, 8(1):71–102, January 1998.

M. Padulo, S. A. Forth, and M. D. Guenov. Robust Aircraft Conceptual Design Using Automatic Differentiation in Matlab. In *Advances in Automatic Differentiation*, volume 64 of *Lecture Notes in Computational Science and Engineering*, pages 271–280. Springer Berlin Heidelberg, 2008.

R. M. Paiva. *A Robust and Reliability-Based Optimization Framework for Conceptual Aircraft Wing Design*. PhD thesis, University of Victoria, 2010.

S. N. Patnaik, L. Berke, and R. H. Gallagher. Integrated Force Method versus Displacement Method for Finite Element Analysis. *Computers & Structures*, 38(4):377 – 407, 1991.

S. N. Patnaik, S. S. Pai, and R. M. Coroneos. Reliability-Based Design Optimization of a Composite Airframe Component. Technical report, National Aeronautics and Space Administration, 2009.

S. N. Patnaik, S. S. Pai, and R. M. Coroneos. Reliability Based Design for a Raked Wing Tip of an Airframe. In *2^{th} International Conference on Engineering Optimization*, 2010.

J. C. Refsgaard, J. P. van der Sluijs, J. B., and P. van der Keur. A framework for dealing with uncertainty due to model structure error. *Advances in Water Resources*, 29(11):1586–1597, 2006.

S. M. Ross. *Introduction to Probability and Statistics for Engineers and Scientist*. Elsevier/Academic Press, 3^{rd} edition, 2004.

H. R. Shah. Quantifying Model Uncertainty using Measurement Uncertainty Standards. Master's thesis, Missouri University of Science and Technology, 2011.

E. A. Starke and J. T. Staley. Application of modern aluminum alloys to aircraft. *Progress in Aerospace Sciences*, 32(2):131–172, 1996.

B. Sudret and A. Der Kiureghian. Stochastic Finite Element Methods and Reliability: A State-of-the-Art Report. Technical report, Department of Civil and Environmental Engineering University of California, Berkeley, 2000.

TeachEngineering. Wing Construction. `http://www.me.utexas.edu/news/_images2009/airplane_wing_300x246.jpg`, Accessed in November 2012.

The MathWorks Inc. MATLAB 7.9 (r2009b). `http://www.ansys.com/`, 2009.

R. Wang, U. Diwekar, and C. E. G. Padró. Efficient Sampling Techniques for Uncertainties in Risk Analysis. *Environmental Progress*, 23:141–157, 2004.

X. Wei. *Stochastic Analysis and Optimization of Structures*. PhD thesis, Graduate Faculty of The University of Akron, 2006.

X. Wei and S. N. Patnaik. Application of Stochastic Sensitivity Analysis to Integrated Force Method. *International Journal of Stochastic Analysis*, 2012, 2012.

S.F. Wojtkiewicz, M. S. Eldred, Jr R.V. Field, A. Urbina, and J.R. Red-Horse. Uncertainty Quantification In Large Computational Engineering Models. Technical report, American Institute of Aeronautics and Astronautics, 2001.

G. D. Wyss and K. H. Jorgensen. A User's Guide to LHS: Sandia's Latin Hypercube Sampling Software. Technical report, Sandia National Laboratories, 1998.

XFLR5. XFLR5 v6.05 beta. `http://www.xflr5.com/xflr5.htm`, 2011.

B. D. Youn, K. K. Choi, L. Du, and D. Gorsich. Integration of Possibility-Based Optimization to Robust Design for Epistemic Uncertainty. *Journal of Mechanic Design*, 129(8):876–882, August 2007.

Appendix A

ANSYS Script for the Wing Model Analysis

```
!-----------------------------------------------------------------------------------------
!
!                                    WING MODEL SCRIPT
!
!-----------------------------------------------------------------------------------------

/CLEAR
/PREP7

tr=0.6        !Wing tip factor
NDIV=90    !Mesh factor

!-----------------------------------------------------------------------------------------
!                                    INPUT VARIABLES
!-----------------------------------------------------------------------------------------

!Read a file with property value
*DIM,LL,ARRAY,1
*CREATE,ansuitmp
*VREAD,LL(1),L,TXT,,IJK,1
(F15.8)
*END
/INPUT,ansuitmp
L=LL(1)

dens=2830
```

```
!-----------------------------------------------------------------------------------------------
!                                  MATERIAL PROPERTIES
!-----------------------------------------------------------------------------------------------
/PREP7
ET,1,SHELL63
R,1,th,th,th,th, , ,
RMORE, , , ,
MPTEMP,1,0
MPDATA,EX,1,,E
MPDATA,PRXY,1,,Poi
MPDATA,DENS,1,,dens

ET,2,SOLID45
MPTEMP,,,,,,,,
MPTEMP,1,0
MPDE,EX,1
MPDE,PRXY,1
MPDATA,EX,1,,E
MPDATA,PRXY,1,,Poi
MPDATA,DENS,1,,dens

!-----------------------------------------------------------------------------------------------
!                                    CREATE WING SHELL
!-----------------------------------------------------------------------------------------------

!Define airfoil keypoints
K,1,1.0000*w,0.00189*w,0
.
.
.
K,34,0.9500*w,-0.01210*w,0

!Create Splines using keypoints
FLST,3,12,3
.
.
.
FITEM,3,12
BSPLIN, ,P51X
```

```
!-----------------------------------------------------------------------------------------------
!                                    CREATE WING BOX
!-----------------------------------------------------------------------------------------------

!Create keypoints for the wing box

K,71,0.5000*w-t_w,0.07941*w-t_f,0
.
.
.
K,78,0.5000*w*tr-t_w*tr,-0.07941*w*tr+t_f*tr,L

!-----------------------------------------------------------------------------------------------
!                                     WING BOX MESH
!-----------------------------------------------------------------------------------------------

!Define material for the mesh
VATT,1,1,2,0

!Select entities
LSEL,S,,,9
.
.
.
LSEL,A,,,58,61,1

!Define nr of divisions
LESIZE,ALL,,,NDIV


!Generate Mesh
VMESH,1,4,3
VMESH,2,5,3
VMESH,3,9,3
VMESH,10

!-----------------------------------------------------------------------------------------------
!                                     SHELL MESH
!-----------------------------------------------------------------------------------------------
```

```
!Define material for the mesh
AATT,1,1,1,0,

LSEL,S,,,13,41,1
.
.
.
LSEL,A,,,109

!Define nr of divisions
LESIZE,ALL,,,NDIV

!Generate Mesh
AMESH,2,3,1
AMESH,37,40,1

!-----------------------------------------------------------------------------------------------
!                              MERGE SHELL AND WING BOX NODES
!-----------------------------------------------------------------------------------------------
NUMMRG,NODE,1E-4

!-----------------------------------------------------------------------------------------------
!                                    BOUNDARY CONDITIONS
!-----------------------------------------------------------------------------------------------
NSEL,S,LOC,Z,,,,
D,ALL, , , , , ,ALL, , , , ,
ALLSEL,ALL

!-----------------------------------------------------------------------------------------------
!                                      LOAD APPLICATION
!-----------------------------------------------------------------------------------------------

F,16475,FY,-0.0003321*P
.
.
.
F,28209,FY,-0.00018538*P

!-----------------------------------------------------------------------------------------------
!                                          SOLUTION
!-----------------------------------------------------------------------------------------------
```

```
/SOL
/STATUS,SOLU
SOLVE

!-----------------------------------------------------------------------------------------------
!                                          RESULTS
!-----------------------------------------------------------------------------------------------
FINISH
/POST1
PLDISP,1

!-----------------------------------------------------------------------------------------------
!                                        SAVE RESULTS
!-----------------------------------------------------------------------------------------------

!Read the outputs
NSORT,U,Y
*GET,U_MAX,SORT, ,MAX
NSORT,S,Z
*GET,S_MAX,SORT, ,MAX
NSORT,S,Z
*GET,S_MIN,SORT, ,MIN
NSORT,S,EQV
*GET,S_EQ_MAX,SORT, ,MAX

*DIM,SOL,ARRAY,1,4
SOL(1,1)=U_MAX
SOL(1,2)=S_MAX
SOL(1,3)=S_MIN
SOL(1,4)=S_EQ_MAX

!Create a file with results
*CREATE,ansuitmp
*CFOPEN,'Results','TXT',,
*DO,J,1,4,1
*VWRITE,SOL(1,J)
(E22.15)
*ENDDO
*CFCLOSE
*END
/INPUT,ansuitmp
```

Appendix B

MATLAB Script for the Monte Carlo Simulation Method

```
%*************************************************************************
%
%                          WING STRUCTURE MCS
%
%Author: Jorge Liquito
%
%Problem: Wing Struture analysis using MCS and ANSYS to obtain mean and
%         standard deviation values of displacement, maximum stress,
%         minimum stress and maximum equivalent stress
%*************************************************************************

clear all
format long
tic;

%*************************************************************************
%                            DEFINE VARIABLES
%*************************************************************************

NN=21000;   %number of samples

p=3/100;    %percentage of uncertainty

%VARIABLES WITH UNCERTAINTY
%Mean value of span
L=5;
L_STD=L*p;

%Mean value of chord on the root
w=1;
```

```
w_STD=w*p;

%Mean value of Young Modulus
E=71.7E9;
E_STD=E*p;

%Mean value of Poison Coefficient
Poi=0.33;
Poi_STD=Poi*p;

%Mean value of Load
P=-10000;
P_STD=abs(P*p);

%Mean value of shell thickness
th=2.5E-3;
th_STD=th*p;

%Mean value of wing box thickness
t_w=1E-3;                           %web
t_w_STD=t_w*p;

t_f=1E-3;                           %flange
t_f_STD=t_f*p;

%Variables Sampling
for a=1:NN

    L_MCS(a,1)=normrnd(L,L_STD);
    w_MCS(a,1)=normrnd(w,w_STD);
    E_MCS(a,1)=normrnd(E,E_STD);
    Poi_MCS(a,1)=normrnd(Poi,Poi_STD);
    P_MCS(a,1)=normrnd(P,P_STD);
    th_MCS(a,1)=normrnd(th,th_STD);
    t_w_MCS(a,1)=normrnd(t_w,t_w_STD);
    t_f_MCS(a,1)=normrnd(t_f,t_f_STD);

end


for a=1:NN

%************************************************************************
%                   CREATE FILES WITH PROPERTIES VALUES
%************************************************************************

        fid=fopen('L.txt','w');                         %Open the .txt file
        L=L_MCS(a,1);
        fprintf(fid,'%c',char(num2str(L,'%15.8f')));    % Write the variables in the file
```

```
80          fprintf(fid,'\r\n');
81          fclose(fid);                                        %Close the .txt file
82
83          .
84          .  %The same procedure for the other variables
85          .
86
87          fid=fopen('t_f.txt','w');
88          t_f=t_f_MCS(a,1);
89          fprintf(fid,'%c',char(num2str(t_f,'%15.8f')));
90          fprintf(fid,'\r\n');
91          fclose(fid);
92
93  %*************************************************************************
94  %                  DETERMINE THE OUTPUTS USING ANSYS
95  %*************************************************************************
96
97  %Open file.txt with the structure for analysis
98  entrada='Wing.txt';
99  %Open ANSYS in batch mode
100 s1='"C:\Program Files\ANSYS Inc\v120\ansys\bin\winx64\ansys120.exe" -b -i ';
101 s2=' -o out.out';
102 comando=[s1 entrada s2];
103 dos(comando);
104
105 %Read the file .txt with results
106 Results=textread('RESULTS.txt','%f');
107 U_MAX(a,1)=Results(1,1);
108 S_MAX(a,1)=Results(2,1);
109 S_MIN(a,1)=Results(3,1);
110 S_EQ_MAX(a,1)=Results(4,1);
111 end
112
113 %*************************************************************************
114 %        Determine mean values and standard variations
115 %*************************************************************************
116
117 U_MAX_MEAN=mean(U_MAX);
118 U_MAX_STD=std(U_MAX);
119
120 S_MAX_MEAN=mean(S_MAX);
121 S_MAX_STD=std(S_MAX);
122
123 S_MIN_MEAN=mean(S_MIN);
124 S_MIN_STD=std(S_MIN);
125
126 S_EQ_MAX_MEAN=mean(S_EQ_MAX);
127 S_EQ_MAX_STD=std(S_EQ_MAX);
128
```

```
%************************************************************************
%                          PLOT RESULTS
%************************************************************************

format short

disp('************************************************************************')
disp('                        COMPUTING RESULTS'                              )
disp('************************************************************************')
fprintf('Displacement [m]'                                                    )
disp(U_MAX_MEAN                                                               )
disp('Standard deviation of displacement [m]'                                 )
disp(U_MAX_STD                                                                )
disp('Maximum stress on the wing [N/m^2]'                                     )
disp(S_MAX_MEAN                                                               )
disp('Standard deviation of Maximum stress on the wing [N/m^2]'               )
disp(S_MAX_STD                                                                )
disp('Minimum stress on the wing [N/m^2]'                                     )
disp(S_MIN_MEAN                                                               )
disp('Standard deviation of Minimum stress on the wing [N/m]'                 )
disp(S_MIN_STD                                                                )
disp('Maximum Equivalent Stress on the wing [N/m^2]'                          )
disp(S_EQ_MAX_MEAN                                                            )
disp('Standard deviation of Maximum Equivalent stress on the wing [N/m^2]')
disp(S_EQ_MAX_STD                                                             )
toc
```

Appendix C

MATLAB Script for the Latin Hypercube Sampling Method

```
%*************************************************************************
%
%                          WING STRUCTURE LHS
%
%Author: Jorge Liquito
%
%Problem: Wing Struture analysis using LHS and ANSYS to obtain mean and
%         standard deviation values of displacement, maximum stress,
%         minimum stress and maximum equivalent stress
%*************************************************************************

clear all
format long
tic;

%*************************************************************************
%                            DEFINE VARIABLES
%*************************************************************************

NN=2500;   %number of samples

p=3/100;    %percentage of uncertainty

%VARIABLES WITH UNCERTAINTY
%Mean value of span
L=5;
L_STD=L*p;
L_COV=L_STD^2;

%Mean value of chord on the root
```

```
w=1;
w_STD=w*p;
w_COV=w_STD^2;

%Mean value of Young Modulus
E=71.7E9;
E_STD=E*p;
E_COV=E_STD^2;

%Mean value of Poison Coefficient
Poi=0.33;
Poi_STD=Poi*p;
Poi_COV=Poi_STD^2;

%Mean value of Load
P=-10000;
P_STD=abs(P*p);
P_COV=P_STD;

%Mean value of shell thickness
th=2.5E-3;
th_STD=th*p;
th_COV=th_STD^2;

%Mean value of wing box thickness
t_w=1E-3;                          %web
t_w_STD=t_w*p;
t_w_COV=t_w_STD^2;

t_f=1E-3;                          %flange
t_f_STD=t_f*p;
t_f_COV=t_f_STD^2;


%*************************************************************************
%                   VARIABLES SAMPLING
%*************************************************************************

L_LHS=lhsnorm(L,L_COV,NN,'off');
w_LHS=lhsnorm(w,w_COV,NN,'off');
E_LHS=lhsnorm(E,E_COV,NN,'off');
Poi_LHS=lhsnorm(Poi,Poi_COV,NN,'off');
P_LHS=lhsnorm(P,P_COV,NN,'off');
th_LHS=lhsnorm(th,th_COV,NN,'off');
t_w_LHS=lhsnorm(t_w,t_w_COV,NN,'off');
t_f_LHS=lhsnorm(t_f,t_f_COV,NN,'off');


for a=1:NN
```

```
80
81 %************************************************************************
82 %                  CREATE THE FILES WITH PROPERTIES
83 %************************************************************************
84
85
86          fid=fopen('L.txt','w');                                 %Open the .txt file
87          L=L_LHS(a,1);
88          fprintf(fid,'%c',char(num2str(L,'%15.8f')));            % Write the variables in the file
89          fprintf(fid,'\r\n');
90          fclose(fid);                                            %Close the .txt file
91
92
93          .
94          .   %The same procedure for the other variables
95          .
96
97          fid=fopen('t_f.txt','w');
98          t_f=t_f_LHS(a,1);
99          fprintf(fid,'%c',char(num2str(t_f,'%15.8f')));
100         fprintf(fid,'\r\n');
101         fclose(fid);
102
103
104 %************************************************************************
105 %                 DETERMINE THE OUTPUTS USING ANSYS
106 %************************************************************************
107
108 %Open file.txt with the structure for analysis
109 entrada='Wing.txt';
110 %Open ANSYS in batch mode
111 s1='"C:\Program Files\ANSYS Inc\v120\ansys\bin\winx64\ansys120.exe" -b -i ';
112 s2=' -o out.out';
113 comando=[s1 entrada s2];
114 dos(comando);
115
116 %Read the file .txt with results
117 Results=textread('RESULTS.txt','%f');
118 U_MAX(a,1)=Results(1,1);
119 S_MAX(a,1)=Results(2,1);
120 S_MIN(a,1)=Results(3,1);
121 S_EQ_MAX(a,1)=Results(4,1);
122 end
123
124 %************************************************************************
125 %        Determine mean values and standard variations
126 %************************************************************************
127
128 U_MAX_MEAN=mean(U_MAX);
```

```
129 U_MAX_STD=std(U_MAX);
130
131 S_MAX_MEAN=mean(S_MAX);
132 S_MAX_STD=std(S_MAX);
133
134 S_MIN_MEAN=mean(S_MIN);
135 S_MIN_STD=std(S_MIN);
136
137 S_EQ_MAX_MEAN=mean(S_EQ_MAX);
138 S_EQ_MAX_STD=std(S_EQ_MAX);
139
140 %************************************************************************
141 %                          PLOT RESULTS
142 %************************************************************************
143
144 format short
145
146 disp('************************************************************************')
147 disp('                        COMPUTING RESULTS'                             )
148 disp('************************************************************************')
149 fprintf('Displacement [m]'                                                   )
150 disp(U_MAX_MEAN                                                             )
151 disp('Standard deviation of displacement [m]'                               )
152 disp(U_MAX_STD                                                              )
153 disp('Maximum stress on the wing [N/m^2]'                                   )
154 disp(S_MAX_MEAN                                                             )
155 disp('Standard deviation of Maximum stress on the wing [N/m^2]'             )
156 disp(S_MAX_STD                                                              )
157 disp('Minimum stress on the wing [N/m^2]'                                   )
158 disp(S_MIN_MEAN                                                             )
159 disp('Standard deviation of Minimum stress on the wing [N/m]'              )
160 disp(S_MIN_STD                                                              )
161 disp('Maximum Equivalent Stress on the wing [N/m^2]'                       )
162 disp(S_EQ_MAX_MEAN                                                         )
163 disp('Standard deviation of Maximum Equivalent stress on the wing [N/m^2]')
164 disp(S_EQ_MAX_STD                                                          )
165 toc
```

Appendix D

MATLAB Script for the Perturbation Method

```
%%%%%%%%%%%%%%%%%%%%%%%%%%%%%%%%%%%%%%%%%%%%%%%%%%%%%%%%%%%%%%%%%%%%%%%%%%%%%%%
%
%                          WING STRUCTURE PM
%
%Author: Jorge Liquito
%
%Problem: Wing Struture analysis using PM and ANSYS to obtain mean and
%         standard deviation values of displacement, maximum stress,
%         minimum stress and maximum equivalent stress
%%%%%%%%%%%%%%%%%%%%%%%%%%%%%%%%%%%%%%%%%%%%%%%%%%%%%%%%%%%%%%%%%%%%%%%%%%%%%%%

clear all
format long
tic

%*************************************************************************
%                              DEFINE VARIABLES
%*************************************************************************

TV=8;       %Number of uncertainty variables

p=3/100;    %percentage of uncertainty

%VARIABLES WITH UNCERTAINTY
%Mean value of span
L=5;
L_STD=L*p;
L_COV=L_STD^2;

%Mean value of chord on the root
```

```
w=1;
w_STD=w*p;
w_COV=w_STD^2;

%Mean value of Young Modulus
E=71.7E9;
E_STD=E*p;
E_COV=E_STD^2;

%Mean value of Poison Coefficient
Poi=0.33;
Poi_STD=Poi*p;
Poi_COV=Poi_STD^2;

%Mean value of Load
P=-10000;
P_STD=abs(P*p);
P_COV=P_STD;

%Mean value of shell thickness
th=2.5E-3;
th_STD=th*p;
th_COV=th_STD^2;

%Mean value of wing box thickness
t_w=1E-3;                          %web
t_w_STD=t_w*p;
t_w_COV=t_w_STD^2;

t_f=1E-3;                          %flange
t_f_STD=t_f*p;
t_f_COV=t_f_STD^2;


rho=[L_COV/L^2 0 0 0 0 0 0 0;
     0 w_COV/w^2 0 0 0 0 0 0;
     0 0 E_COV/E^2 0 0 0 0 0;
     0 0 0 Poi_COV/Poi^2 0 0 0 0;
     0 0 0 0 P_COV/P^2 0 0 0;
     0 0 0 0 0 th_COV/th^2 0 0;
     0 0 0 0 0 0 t_w_COV/t_w^2 0;
     0 0 0 0 0 0 0 t_f_COV/t_f^2];

%************************************************************************
%                      COMPUTE DETERMINISTIC VALUES
%************************************************************************

[U_MAX_DET,S_MAX_DET,S_MIN_DET,S_EQ_MAX_DET]=DET_VALUES(L,w,E,Poi,P,th,t_w,t_f);

```

```
%************************************************************************
%                   COMPUTE FIRST AND SECOND DERIVATIVES
%************************************************************************

%Generate the first and second derivative of Wing Span
[U_MAX_L_FD,S_MAX_L_FD,S_MIN_L_FD,S_EQ_MAX_L_FD,U_MAX_L_SD,S_MAX_L_SD,S_MIN_L_SD,...
    S_EQ_MAX_L_SD] = L_DER(L,w,E,Poi,P,th,...
    t_w,t_f,U_MAX_DET,S_MAX_DET,S_MIN_DET,S_EQ_MAX_DET);

%Generate the first and second derivative of chord length
[U_MAX_w_FD,S_MAX_w_FD,S_MIN_w_FD,S_EQ_MAX_w_FD,U_MAX_w_SD,S_MAX_w_SD,S_MIN_w_SD,...
    S_EQ_MAX_w_SD] = w_DER(L,w,E,Poi,P,th,...
    t_w,t_f,U_MAX_DET,S_MAX_DET,S_MIN_DET,S_EQ_MAX_DET);

%Generate the first and second derivative of Young Modulus
[U_MAX_E_FD,S_MAX_E_FD,S_MIN_E_FD,S_EQ_MAX_E_FD,U_MAX_E_SD,S_MAX_E_SD,S_MIN_E_SD,...
    S_EQ_MAX_E_SD] = E_DER(L,w,E,Poi,P,th,...
    t_w,t_f,U_MAX_DET,S_MAX_DET,S_MIN_DET,S_EQ_MAX_DET);

%Generate the first and second derivative of Poison Coefficient
[U_MAX_Poi_FD,S_MAX_Poi_FD,S_MIN_Poi_FD,S_EQ_MAX_Poi_FD,U_MAX_Poi_SD,S_MAX_Poi_SD,...
    S_MIN_Poi_SD,S_EQ_MAX_Poi_SD] = Poi_DER(L,w,E,Poi,...
    P,th,t_w,t_f,U_MAX_DET,S_MAX_DET,S_MIN_DET,S_EQ_MAX_DET);

%Generate the first and second derivative of Pressure
[U_MAX_P_FD,S_MAX_P_FD,S_MIN_P_FD,S_EQ_MAX_P_FD,U_MAX_P_SD,S_MAX_P_SD,S_MIN_P_SD,...
    S_EQ_MAX_P_SD] = P_DER(L,w,E,Poi,P,th,t_w,t_f,...
    U_MAX_DET,S_MAX_DET,S_MIN_DET,S_EQ_MAX_DET);

%Generate the first and second derivative of Shell thickness
[U_MAX_th_FD,S_MAX_th_FD,S_MIN_th_FD,S_EQ_MAX_th_FD,U_MAX_th_SD,S_MAX_th_SD,S_MIN_th_SD,...
    S_EQ_MAX_th_SD] = th_DER(L,w,E,Poi,P,th,t_w,t_f,U_MAX_DET,...
    S_MAX_DET,S_MIN_DET,S_EQ_MAX_DET);

%Generate the first and second derivative of Web thickness
[U_MAX_t_w_FD,S_MAX_t_w_FD,S_MIN_t_w_FD,S_EQ_MAX_t_w_FD,U_MAX_t_w_SD,S_MAX_t_w_SD,S_MIN_t_w_SD,...
    S_EQ_MAX_t_w_SD] = t_w_DER(L,w,E,Poi,P,th,t_w,t_f,U_MAX_DET,...
    S_MAX_DET,S_MIN_DET,S_EQ_MAX_DET);

%Generate the first and second derivative of Flange thickness
[U_MAX_t_f_FD,S_MAX_t_f_FD,S_MIN_t_f_FD,S_EQ_MAX_t_f_FD,U_MAX_t_f_SD,S_MAX_t_f_SD,S_MIN_t_f_SD,...
    S_EQ_MAX_t_f_SD] = t_f_DER(L,w,E,Poi,P,th,t_w,t_f,U_MAX_DET,...
    S_MAX_DET,S_MIN_DET,S_EQ_MAX_DET);

%%%%%%%%%%%%%%%%%%%%%%%%%%%%%%%%%%%%%%%%%%%%%%%%%%%%%%%%%%%%%%%%%%%%%%%%%%%%
%
%                           MAXIMUM DISPLACEMENT
%
%%%%%%%%%%%%%%%%%%%%%%%%%%%%%%%%%%%%%%%%%%%%%%%%%%%%%%%%%%%%%%%%%%%%%%%%%%%%
```

```
129
130 %*************************************************************************
131 %             CALCULATE MEAN VALUE OF MAXIMUM DISPLACEMENT
132 %*************************************************************************
133
134 %Build the second derivative matrix
135
136 for i=1:TV
137     for j=1:TV
138
139         if i==1 & j==1
140
141             U_MAX_SD(i,j)=U_MAX_L_SD;
142
143         elseif i==2 & j==2
144
145             U_MAX_SD(i,j)=U_MAX_w_SD;
146
147         elseif i==3 & j==3
148
149             U_MAX_SD(i,j)=U_MAX_E_SD;
150
151         elseif i==4 & j==4
152
153             U_MAX_SD(i,j)=U_MAX_Poi_SD;
154
155         elseif i==5 & j==5
156
157             U_MAX_SD(i,j)=U_MAX_P_SD;
158
159         elseif i==6 & j==6
160
161             U_MAX_SD(i,j)=U_MAX_th_SD;
162
163         elseif i==7 & j==7
164
165             U_MAX_SD(i,j)=U_MAX_t_w_SD;
166
167         elseif i==8 & j==8
168
169             U_MAX_SD(i,j)=U_MAX_t_f_SD;
170         end
171     end
172 end
173
174 %Calculate mean value
175 U_MAX=0;
176 for i=1:TV
177     for j=1:TV
```

```
178
179      U_MAX=U_MAX_SD(i,j)*rho(i,j)+U_MAX;
180
181      end
182  end
183
184  U_MAX_MEAN=U_MAX_DET+0.5*U_MAX;
185
186  % ************************************************************************
187  %            Calculate standard deviation of maximum displacement
188  % ************************************************************************
189
190  %Build first derivative matrix
191
192  for i=1:TV
193
194          if i==1
195
196              U_MAX_FD(1,i)=U_MAX_L_FD;
197
198          elseif i==2
199
200              U_MAX_FD(1,i)=U_MAX_w_FD;
201
202          elseif i==3
203
204              U_MAX_FD(1,i)=U_MAX_E_FD;
205
206          elseif i==4
207
208              U_MAX_FD(1,i)=U_MAX_Poi_FD;
209
210          elseif i==5
211
212              U_MAX_FD(1,i)=U_MAX_P_FD;
213
214          elseif i==6
215
216              U_MAX_FD(1,i)=U_MAX_th_FD;
217
218          elseif i==7
219
220              U_MAX_FD(1,i)=U_MAX_t_w_FD;
221
222          elseif i==8
223
224              U_MAX_FD(1,i)=U_MAX_t_f_FD;
225          end
226  end
```

```
227
228 %Calculate standard deviation
229 COV=0;
230 COV_U_MAX=0;
231 for i=1:TV
232     for j=1:TV
233
234         COV=(U_MAX_FD(1,i))*(U_MAX_FD(1,i)')*rho(i,j);
235         COV_U_MAX=COV_U_MAX+COV;
236
237     end
238 end
239
240 U_MAX_STD=sqrt(COV_U_MAX);
241
242 .
243 .  %The same methodology to determine the values for the other
244 .  %properties
245
246
247 %%%%%%%%%%%%%%%%%%%%%%%%%%%%%%%%%%%%%%%%%%%%%%%%%%%%%%%%%%%%%%%%%%%%%%%%%%%%
248 %
249 %                            RESULTS
250 %
251 %%%%%%%%%%%%%%%%%%%%%%%%%%%%%%%%%%%%%%%%%%%%%%%%%%%%%%%%%%%%%%%%%%%%%%%%%%%%
252
253 %************************************************************************
254 %                          PLOT RESULTS
255 %************************************************************************
256
257 format short
258
259 disp('************************************************************************')
260 disp('                        COMPUTING RESULTS'                             )
261 disp('************************************************************************')
262 fprintf('Displacement [m]'                                                   )
263 disp(U_MAX_MEAN                                                             )
264 disp('Standard deviation of displacement [m]'                               )
265 disp(U_MAX_STD                                                              )
266 disp('Maximum stress on the wing [N/m^2]'                                   )
267 disp(S_MAX_MEAN                                                             )
268 disp('Standard deviation of Maximum stress on the wing [N/m^2]'             )
269 disp(S_MAX_STD                                                              )
270 disp('Minimum stress on the wing [N/m^2]'                                   )
271 disp(S_MIN_MEAN                                                             )
272 disp('Standard deviation of Minimum stress on the wing [N/m]'              )
273 disp(S_MIN_STD                                                              )
274 disp('Maximum Equivalent Stress on the wing [N/m^2]'                       )
275 disp(S_EQ_MAX_MEAN                                                         )
```

```
276 disp('Standard deviation of Maximum Equivalent stress on the wing [N/m^2]')
277 disp(S_EQ_MAX_STD                                                          )
278 toc
```